Combining transmitter beamforming and space-time block codes in slow rayleigh flat fading channels

Liu, Jin

2006

Liu, J. (2006). Combining transmitter beamforming and space-time block codes in slow rayleigh flat fading channels. Doctoral thesis, Nanyang Technological University, Singapore.

https://hdl.handle.net/10356/39109

https://doi.org/10.32657/10356/39109

Combining Transmitter Beamforming and Space-Time Block Codes in Slow Rayleigh Flat Fading Channels

Liu Jin

School of Electrical & Electronic Engineering

A thesis submitted to the Nanyang Technological University
in fulfillment of the requirement for the degree of
Doctor of Philosophy

2006

Statement of Originality

I hereby certify that the work embodied in this thesis is the result of original research and has not been submitted for a higher degree to any other University or Institution.

11 – Sep. – 2006
Date

刘瑾
Liu Jin

Acknowledgements

There are lots of people I would like to thank for a huge variety of reasons.

Firstly, I would like to express my sincere gratitude and appreciation to my supervisor, Associate Professor, **Erry Gunawan** for his wisdom, friendship, understanding, and for teaching me how to be a good researcher. I could not have imagined having a better advisor and mentor for my PhD, and without his many insightful conversations, patient guidance, invaluable advice and helpful comments on the text I would never have finished this work.

I would like to thank Nanyang Technological University for the research scholarship and the study facilities that it has provided.

Many thanks to my many friends and student colleagues in Communications Laboratory IV for providing a stimulating and fun environment in which to discuss, learn and help with each other.

Most importantly, I am forever indebted to my parents, Liu Cheng and Dong Changcui. They bore me, raised me, supported me, taught me, and loved me with endless patience.

Finally, I am grateful to my husband, Zhang Feng, for his persistent encouragement, support and helping me get through the difficult times. I am also grateful

to my newborn son, Zhang Haoxiang, who brings me a lot of joy and infinite hope.

To them I dedicate this thesis.

List of Abbreviations and Symbols

Abbreviations

3G	third generation
4G	fourth generation
AWGN	additive white Gaussian noise
BER	bit error rate
BLER	codeword/block error probability
BPS	bits per symbol
BPSK	binary phase shift keying
CSI	channel state information
EVD	eigenvalue decomposition
EDGE	enhanced data rates for GSM evolution
FEC	forward error correcting
GSM	global system for mobile communications
iff	if and only if
i.i.d.	independent and identically distributed
ISI	inter-symbol interference

LOS	line-of-sight
LST	layered space-time
MGF	moment generating function
MIMO	multiple-input and multiple-output
MISO	multiple-input and single-output
ML	maximum likelihood
M-ASK	M-ary amplitude shift keying
M-PSK	M-ary phase shift keying
MRC	maximum ratio combining
OFDM	orthogonal frequency division multiplexing
OSTBC	orthogonal space-time block code/codes/coding
PDF	probability density function
PEP	pairwise error probability
PAM	pulse amplitude modulation
QPSK	quadrature phase shift keying
SER	symbol error rate
SGA	simple genetic algorithm
SIMO	single-input multiple-output
SNR	signal-to-noise ratio
STBC	space-time block code/codes/coding
STD	selective transmitting diversity
STTC	space-time trellis code/codes/coding
WCDMA	wideband code division multiple access

Symbols

M_t	number of transmitting antennas
M_r	number of receiving antennas
P_o	total average transmitted power
P_r	average power at each receiving antenna
E_s	the total transmitted energy per symbol time instant
N_0	noise power per receiving antenna
γ	average SNR at each receiving antenna
$\mathbf{H}$	channel matrix
$\mathbf{h}$	row vector of channel coefficients
$\hat{\mathbf{H}}$	CSI matrix at the transmitter
$\hat{\mathbf{h}}$	row vector of CSI at the transmitter
$\mathbf{Y}$	received data matrix
$\mathbf{y}$	vector of received signals
$\mathbf{E}$	received noise matrix
$\mathbf{e}$	vector of received noise
σ_h^2	channel variance
σ^2	noise variance
N	number of symbols per block codeword
K	number of codewords in the constellation
L	length of the block codeword

R	code rate
η_{se}	spectral efficiency
B	bandwidth
$\mathcal{C}$	constellation for transmitted codewords
$\mathbf{C}$	transmission matrix
$\mathbf{W}$	beamforming matrix
$\mathbf{S}$	transmission matrix of STBC
$\mathbf{m}$	mean vector
$\mathbf{R}$	covariance matrix
$\mathbf{I}$	identity matrix
δ	squared Euclidean distance between the codeword pair
ρ	normalized correlation coefficient
α	conditional variance of channel coefficients
$\mathbf{\Lambda}$	diagonal eigenvalue matrix
λ	eigenvalues
$\mathbf{V}$	eigenvector matrix
$\mathbf{v}$	eigenvectors
μ	Lagrange multiplier
$\mathbf{\Delta}$	codeword difference matrix
p	quantized CSI at the transmitter
ζ	row vector of initial channel information at the receiver
r	rank of the matrix
P_2	BER

n_f	degrees of freedom for chi-square distribution
$(\cdot)^T$	transpose operator of a vector or matrix
$(\cdot)^*$	complex conjugate operator
$(\cdot)^{\mathcal{H}}$	Hermitian transpose (complex conjugate and transpose) operator
$(\cdot)^{1/2}$	matrix square root with Hermitian symmetry
$E[\cdot]$	expectation operator
$\|\cdot\|_{\mathrm{F}}$	Frobenius norm
$\|\cdot\|$	vector norm
$\otimes$	Kronecker product
$\det(\cdot)$	determinant operator of a matrix
$\mathrm{rvec}(\cdot)$	row vectorization operator
$tr(\cdot)$	trace operator
$\mathsf{Re}(\cdot)$	real part
$\mathsf{Im}(\cdot)$	imaginary part
$\mathrm{diag}(\cdot)$	diagonal matrix generating operator
$Q(\cdot)$	Gaussian Q function
$\exp(\cdot)$	exponent function
$\Gamma(\cdot)$	Gamma function
$\Phi_{\xi_w}(s)$	moment generating function of random variable ξ_w
$J_\nu(\cdot)$	Bessel function of the first kind for the νth order
$I_\nu(\cdot)$	modified Bessel function of the first kind for the νth order
${}_1F_1(\cdot;\cdot;\cdot)$	confluent Hypergeometric function

Contents

List of Figures

List of Tables

Summary

In this thesis, we consider the design of two types of closed-loop combined systems of beamforming and space-time block codes (STBC) taking the degree of the feedback channel state information (CSI) at the transmitter into account. The first type is the combined system of beamforming and predetermined Alamouti's STBC, where only the beamforming matrix is the free parameter that can be adjusted according to the feedback. Different from the existing combined system of beamforming and orthogonal STBC (OSTBC) where different OSTBC is used for different number of transmitting antennas, our combined system uses fixed Alamouti's STBC regardless of the number of the transmitting antennas. Thus, the application of Alamouti's STBC for two transmitting antennas is extended to more than two by using the beamforming technique. Typical simulation results are presented and performance analysis is also conducted. It is shown that the new combined system has a significant performance improvement over Alamouti's STBC while still maintaining high bandwidth efficiency. Furthermore, it achieves a tradeoff between system complexity and performance compared with the existing combined system of beamforming and OSTBC. Following that, in the second type of combined systems, we are motivated to jointly design the beamforming and

STBC from a performance point of view. The existing jointly-designed unstructured STBC has been known to give an excellent performance, but at the expense of high design and decoding complexity. Hence, we propose a jointly-designed linearly-structured STBC to reduce the computational complexity of the joint design. Although the linear structure generally limits the degrees of freedom in the design, simulation results show that the proposed system can provide better performance than the unstructured code. This is because the jointly-designed linear STBC is based on a more efficient design criterion developed in this thesis than the one applied by the unstructured STBC. In addition, the gradient search techniques used in the existing unstructured code is a local numerical optimization procedure, which requires repeating the searches with different initializations. Therefore, a simple genetic algorithm (SGA) which is a global optimization method is adopted to further reduce the complexity of the system in this thesis.

Chapter 1

Introduction

1.1 Background Information

The demand for capacity in cellular and wireless local area networks, as well as information throughput in the wireless internet access and multimedia applications has grown in a literally explosive manner during the last decade. One major technological breakthrough of improving the capacity, data rate, and reliability of a wireless communication link is the use of multiple antennas at the transmitter and receivers in the system. A system with multiple transmitting and receiving antennas is often called a multiple-input multiple-output (MIMO) system. With multiple antennas at the base station, and one antenna at the mobile, the uplink is a single-input multiple-output (SIMO) radio channel, whereas the downlink is multiple-input single-output (MISO). Current research efforts demonstrate the great potential of MIMO technology in third- and fourth-generation (3G,4G) cellular systems, fixed wireless access, wireless local area networks and ad hoc wireless battlefield networks.

The attractive characteristic of a MIMO channel is that it may be used to

increase the data rate by transmitting multiple streams simultaneously using different spatial channels. Thus, in a sense, the MIMO channel increases the effective bandwidth of a wireless channel [37]. This challenges the conventional idea that extremely high data rates either require extremely wide frequency bandwidth and/or extremely high transmission power. Nevertheless, since the MIMO techniques require heavy signal processing to gain access to the projected spatial bandwidth, the complexity of the terminals and network elements will increase compared to the traditional models offering similar data rates with a larger bandwidth. Despite the implementation complexity, the MIMO techniques are attractive especially for those systems which have no bandwidth in abundance while require high data rates. Furthermore, even if extremely high data rates are not necessary, the increased fading resistance inherently arising from diversity of many MIMO systems can be used to increase system capacity or coverage.

The calculations of the information-theoretic capacity assuming a flat Rayleigh fading environment are developed in [16, 90]. Such capacity results are important because they express bounds on the maximal achievable data rate. The fundamental capacity limits for transmission over MIMO channels are derived and discussed in [52, 94], which can be used for the analysis of different transmission schemes. The capacity limits highlight the potential spectral efficiency of MIMO channels, which grows approximately linearly with the minimum number of antennas, assuming ideal propagation [16, 90].

To evaluate various techniques adopted by the MIMO systems, it is worth introducing and defining three important performance measurement parameters

involving coding gain, diversity gain and array gain.

- *Coding gain* refers to the increase in efficiency that a coded signal provides over an uncoded signal. Expressed in decibels (dB), the coding gain indicates a level of power reduction that can be achieved for the same bit error rate (BER).

- *Diversity gain* refers to the number of independent fading signal branches between the transmitter and the receiver. Wireless links are impaired by the random fluctuations in signal level across space, time and frequency known as fading. Diversity is used in wireless channels to combat fading. Diversity provides the receiver with multiple (ideally independent) looks at the same transmitted signal. Each look constitutes a diversity branch. With an increase in the number of independent diversity branches, the probability that all branches are in a fade at the same time reduces sharply. Thus diversity techniques stabilize the wireless link leading to an improvement in link reliability or error rate.

- *Array gain* refers to the average increase in the signal-to-noise ratio (SNR) at the receiver that arises from the coherent combining effect of multiple antennas at the receiver or transmitter or both. For example, in a SIMO channel, signals arriving at the receiving antennas have different amplitudes and phases. The receiver can combine the signals coherently so that the resultant signal is enhanced. The average increase in signal power at the receiver is proportional to the number of receiving antennas. In the MISO

or MIMO channels, array gain exploitation requires the channel state information (CSI) at the transmitter.

The diversity gain and coding gain affect the performance curves in different ways. Diversity gain affects the slope of the error rate versus SNR curve on a log-log scale — the greater the diversity, the more negative the slope. Coding gain affects the horizontal shift of the curve — the greater the coding gain, the greater the shift to the left. The effect of array gain is similar to that of coding gain (i.e., it causes a left parallel shift in the curves) and is strictly independent of SNR.

1.2 Literature Review and Motivations

The increased interest in MIMO model for future evolutions of wireless systems arises from its benefits and potentials such as improved fading resistance, interference mitigation, reduced transmitter power levels per transmitting antenna path (which simplifies power amplifier design problems), a new dimension provided for rate and power allocation problems and theoretically higher system capacity, etc [37].

The MIMO communication system is usually equipped by implementing antenna diversity involving receiving diversity and transmitting diversity techniques, where one exploits the fact that the channel fading is (at least partially) independent between different points in space. The *receiving diversity* is widely recognized and employed as an effective means to improve the quality of the uplink. It leads to a considerable performance gain, both in terms of a better link budget and in terms of tolerance to co-channel interference. The signals from the multiple receiving an-

tennas are typically combined in digital hardware, and the so-obtained performance gain is related to the diversity effect obtained from the independence of the fading of the signal paths corresponding to the different antennas. Maximum-ratio combining (MRC) [4, 26, 41, 78] is a classical combining technique used for receiving diversity, where the signals from the receiving antennas are weighted such that the SNR of their sum is maximized.

However, equipment size, cost and power consumption limitations hamper the deployment of receiving diversity at the mobile, hence, it makes the use of *transmitting diversity* in the downlink a powerful and promising method for increasing the performance. It has been realized that many of the benefits as well as a substantial amount of the performance gain of receiving diversity can be reproduced by transmitting diversity. The development of transmitting diversity techniques began from the early 1990's and since then the interest in the topic has grown in a rapid fashion. Owing to transmitting diversity, a performance increase is possible without adding extra antennas, power consumption or significant complexity to the mobile. Furthermore, the cost of the extra transmitting antenna at the base station can be shared among all users, consequently the use of transmitting diversity at the base station has attracted a special interest in a cellular or wireless local area network. In this thesis, our attention is thereby concentrated mainly on the MISO system equipped by using transmitting diversity.

Perhaps one of the first forms of transmitting diversity was antenna hopping. It attracted some attention during the early 1990's as a comparatively inexpensive way of achieving a transmitting diversity gain in systems such as GSM. More re-

cently there has been a strong interest in systematic transmission techniques that can use multiple transmitting antennas in an optimal manner. Thus, space-time coding finds its applications in cellular communications as well as in wireless local area networks. Space-time coding is a means of enhancing the level of diversity presented to a receiver in a wireless link. Since it can separate the problem of combating fades from that of channel equalization, the design criteria are generally derived from the case of a narrowband modulation and a flat fading. In 1998, Tarokh *et al.* proposed space-time trellis codes (STTC) in [87]. By jointly designing the forward error correcting (FEC) code, modulation, transmitting diversity and optional receiving diversity scheme, they increased the throughput of band-limited wireless channels. The drawback of STTC is that the decoding complexity increases exponentially with the transmission rate.

In addressing the issue of decoding complexity, Alamouti [4] proposed a much less complex scheme with two transmitting antennas than STTC, namely space-time block codes (STBC), but there is a loss in performance. Despite of the performance penalty, STBC is still appealing in terms of simplicity and performance. This motivates Tarokh *et al.* to generalize the Alamouti's transmission scheme to STBC with an arbitrary number of transmitting antennas by applying the theory of orthogonal designs. These codes, called orthogonal space-time block codes (OSTBC), are able to achieve the full diversity promised by the transmitting and receiving antennas and retain the property of having a very simple maximum-likelihood (ML) decoding algorithm based only on linear processing at the receiver. However, the orthogonal design prevents OSTBC from achieving full code rate for

systems with more than two antennas in the case of using complex constellations.

Recently, linear STBC represents an interesting class of codes that has received much attention in the literature [27, 31]. The well-known class of OSTBC is an important type of linear STBC. However, linear STBC deliberately relax the requirement of orthogonal designs and break the rate limitations associated with OSTBC. Thus a full diversity gain or/and the simple ML decoding algorithm based on linear processing at the receiver are not guaranteed. An automatic procedure for designing linear STBC is proposed in [47], based on a performance measure which is obtained by upper bounding the union bound expression of the codeword/block error probability (BLER).

In general, STBC are open-loop solutions for transmitting diversity in MIMO/MISO systems, which are designed to operate without CSI at the transmitter. The system performance may be further improved if the information of channel realization is available at the transmitter. The closed-loop concepts exploit CSI that is provided to the transmitter using closed-loop signalling. The CSI can be used to weigh the signals transmitted from the base station antennas so as to achieve constructive signal combining, producing additional array gain, and therefore link capacity increases. The non-coded transmitting diversity techniques with a feedback channel have been around for some time [20, 21, 95]. Currently, the closed-loop transmitting diversity without STBC is explicitly supported by the wideband code division multiple access (WCDMA) wireless standard, which illustrates the practical significance of such schemes [14]. The WCDMA Release'99 and Release 4 specifications include two transmission closed-loop modes [2, 3], where different channel

quantization and feedback signalling strategies are considered. But the WCDMA transmitting diversity solutions explicitly support only two transmitting antennas.

The traditional way of exploiting CSI at the transmitter is via transmitter beamforming techniques that essentially steer the transmission in the direction of the receiver so as to improve the SNR. Generally, under the ideal conditions of infinite precision instantaneous feedback, purely (without STBC) closed-loop schemes with feedback offer a substantial performance advantage over schemes without feedback in the slow flat fading scenario, and can achieve full diversity [45, 56, 60]. However, several issues arise in the practical implementation of these schemes, including channel variations during the feedback delay, bit errors induced by the feedback link, quantization errors of the CSI, channel estimation errors at the receiver, etc. Although we may generally assume that the channel estimation at the receiver is perfect [45, 48, 69, 93], the feedback delay and feedback channel bit errors are known to severely impair the system performance and the asymptotic diversity gain of the purely closed-loop schemes is equal to unity [37]. This drawback of purely closed-loop schemes makes their applicability depend on the operation point of the system.

To mitigate the detrimental consequences of errors in the channel information, the performance of hybrid open-loop and closed-loop MISO systems with partial CSI has been addressed from a capacity point of view in [38, 50, 69, 93], from a pairwise error probability (PEP) point of view in [45, 48, 49] and from a BER point of view in [97, 98]. From these studies, it is suggested that the hybrid closed-loop and open-loop transceiver concepts are able to maintain a high diversity order,

even in the presence of imperfect CSI at the transmitter.

Among those hybrid transmission methods [38, 45, 48–50, 69, 93, 97, 98], the combined system of beamforming and STBC [45, 48, 49] relying on the degree of CSI at the transmitter becomes remarkably attractive. It is obvious that when perfect channel feedback is assumed, beamforming is the optimal strategy entailing transmission in a single direction specified by the feedback [69]. On the other hand, with no channel feedback, coded diversity is the optimum strategy to transmit equal power signal in orthogonal independent directions [70, 90]. The combined transmission scheme combines the two extremes according to the degree of the available CSI at the transmitter, which can balance the array gain (due to the CSI feedback) and the diversity gain (due to open-loop modulation concepts). In this way, the combined transmission scheme continues to work well even when the quality of the feedback CSI is low, since it holds purely open-loop concept in the absence of feedback CSI.

The feedback CSI in the aforementioned combined system [45, 48, 49] is modelled using a purely statistical approach, known as mean feedback. Even though a similar model for the CSI was utilized in [69, 96] for determining suitable transmitter beamformers in the presence of channel estimation errors, those papers do not consider space-time codes. Another possibility for modelling partial CSI is to take on a physical perspective where the signals are assumed to propagate along a finite number of directions, known at the transmitter, before entering a rich local scattering environment near the receiver. This is the approach used in [71] for adapting a predetermined space-time code to the particular channel.

The seamless combination of beamforming and OSTBC in [45] is referred to as weighted OSTBC, where the feedback CSI at the transmitter taken into account is assumed to be noisy and outdated but unquantized. In order to achieve full diversity, the dimensions of OSTBC and beamforming matrix are enlarged as the number of antenna increases, resulting in the system to become significantly complex in the case of a large number of transmitting antennas. A tradeoff between system complexity and performance is, therefore, an important issue for the design of the combined system and has motivated us to do further study in this thesis. Furthermore, the pioneering work on weighted OSTBC present only simulation results, leaving the analytical performance evaluation of this type of combined system as an open problem. Therefore, this also motivates us to develop effective tools for investigating the error probability performance of the combined system under study.

In the above weighted OSTBC system, OSTBC is predetermined and only beamforming matrix is the free parameter that can be adjusted. From a performance point of view, STBC and beamforming should be defined jointly. The CSI-dependent unstructured STBC in [48], on the other hand, is a jointly-designed transmission method based on quantized CSI obtained via a dedicated feedback link. In addition to noisy feedback channel and feedback delay induced errors mentioned previously, the system in [48] is assumed to suffer from errors in the channel information due to CSI quantization. The adopted design criterion is obtained by upper bounding the BLER conditioned on the CSI through the use of union bound principle as well as an upper bound on the PEP. Due to the non-linear unstruc-

tured nature of the codewords, the system in [48] has the cost of a higher decoding complexity over the closed-loop linear structured STBC system, albeit it should potentially have better performance. Motivated by the excellent performance of the existing jointly-designed system and the need of finding a less complex system, a study is made in this thesis that uses linear structured STBC, rather than the unstructured STBC, in the design process to reduce the complexity of the joint-design. However, the linear structure generally limits the degrees of freedom in the design, which incurs performance penalty. This further motives us to investigate more efficient design criterion than the one applied by [48] to improve the system performance. In addition, the gradient search techniques used for finding suitable CSI-dependent unstructured STBC in [48] is a local numerical optimization procedure, which requires repeating the searches with different initializations to come to the possible global optimum solution. Therefore in our study, a global numerical optimization method will be adopted to further reduce the complexity of the system.

1.3 Objectives

The major objective of this thesis is to investigate and develop some typical and efficient combined systems of beamforming and STBC in slow Rayleigh flat fading channels. Specifically, we aim to:

(i) Study a simple combined system of beamforming and Alamouti's STBC to improve the performance of the Alamouti's STBC system while still keeping the system simple.

(ii) Theoretically analyze the PEP and BER performance of the new combined system of beamforming and Alamouti's STBC, and demonstrate its effectiveness from the BER performance point of view.

(iii) Investigate the design criterion of the CSI dependent unstructured STBC [48] to develop a more efficient performance criterion for the jointly-designed beamforming and linear STBC.

(iv) Propose a CSI dependent linear STBC design which is based on the new performance criterion.

1.4 Major Contributions of the Thesis

Several contributions are made in this thesis to the body of closed-loop communication systems engineering. The major contributions of this research include the following:

(i) We extended the application of Alamouti's STBC for two transmitting antennas to more than two by using the existing combined beamforming and OSTBC technique. This proposal was motivated by the fact that Alamouti's STBC has the simplest form of STBC and is the unique OSTBC that can achieve full code rate and full diversity gain simultaneously for complex constellation, but designed only for two transmitting antennas system. The new combined system has a significant performance improvement over Alamouti's STBC due to the array gain growing as the number of transmitting antennas increases, while still maintaining the full code rate. When compared with the

existing combined scheme, the proposed combined beamforming and Alamouti's STBC system requires no new design of OSTBC of different dimension every time when the number of antennas is changed. Hence, the proposed system has a simple design and decoding. It has also a better bandwidth efficiency than the existing combined system of the same number of transmitting antennas because it has a full code rate. More importantly, the new combined system has a comparative performance with the existing combined system at low to moderate SNR, especially for a large number of antennas and good feedback quality. Generally speaking, the new combined system can achieve the tradeoff between complexity and performance.

(ii) We developed some effective tools for calculating the error probabilities of the combined system of beamforming and Alamouti's STBC, and evaluated the system performance analytically. The analytical results can be further used to confirm the simulation results. Under perfect feedback CSI at the transmitter, we derived the exact PEP using the moment-generating function (MGF) approach and Guass-Chebyshev quadrature rule [86]. Then we demonstrated the diversity property of the ideal combined system and provided a tight union bound on the BER based on the derived exact PEP. Furthermore, a more efficient method, the conditional probability method, was employed to derive the closed-form expressions for the upper bound of PEP and the BER. In addition, an analysis of the system diversity gain and coding gain derived from the upper bound of PEP was carried out. Under

imperfect CSI at the transmitter, the closed-form upper bound of PEP was also derived for the purpose to analyze the diversity gain, coding gain and array gain. Moveover, we presented the exact BER of the non-ideal combined system that involves only double integrals. With the exact BER, the new combined system BER performance can be obtained much faster than the simulation, especially at high SNR.

(iii) We proposed a new performance criterion endeavoring to minimize the BER performance for the linear STBC, which is derived from the weighted sum of the associated PEP with respect to the current transmitted codeword.

(iv) Based on the new performance criterion, we proposed to jointly design beamforming and linear structured STBC dependent on the noisy and outdated feedback CSI at the transmitter which was considered under two different and fairly general models of unquantized and quantized measurement. The jointly-designed code was optimized and searched by means of a simple genetic algorithm (SGA), which is a global optimization algorithm. Although the linear structure of the proposed code limits the freedom of design compared with the unstructured code in [48], the simulation results demonstrate that the jointly-designed code still has better BLER and BER performance than the existing CSI dependent unstructured STBC.

1.5 Organization of the Thesis

The thesis is organized as follows. In Chapter 2, an overview of STBC is provided. The MIMO model and the classical MRC technique are briefly introduced as the background knowledge or the comparison benchmark. Following that, some typical STBC forms and their properties are presented in detail.

In Chapter 3, we review two representative closed-loop combined systems of beamforming and STBC. We discuss their benefits and disadvantages and study their performance criteria and optimization algorithms. We first describe how to adaptively design the beamforming matrix based on the predetermined OSTBC by utilizing the unquantized but noisy and outdated feedback CSI at the transmitter. Then we describe how to incorporate the quantized and outdated feedback CSI into the adaptive joint-design of unstructured STBC.

In Chapter 4, we develop a new combined system of beamforming and Alamouti's STBC dependent on the unquantized but noisy and outdated CSI at the transmitter. The analytical expressions of the upper bound on PEP and the exact BER for the ideal combined system and the non-ideal combined system are given, respectively. The numerical results are presented to illustrate the reliability of aforementioned performance analysis and to show the significant gains of the new combined system over the conventional OSTBC at a particular BER. The new combined system is also compared with the existing combined system of beamforming and OSTBC to demonstrate the low complexity and high throughput efficiency of the former, while retaining the desired BER performance.

The discussion in Chapter 4 is mainly limited to separately design the beamforming matrix based on the predetermined Alamouti's STBC. In Chapter 5, we focus on the joint design of beamforming and linear STBC dependent on the noisy and outdated CSI at the transmitter. The two different CSI models in forms of unquantized and quantized measurement are described one by one. The new performance criteria and the resulting optimization problems for two CSI models are developed, respectively. A brief introduction of the SGA numerical technique used for solving the optimization problem is provided. Some representative simulation examples to show the performance advantage of the jointly-designed linear STBC over the existing jointly-designed unstructured STBC technique are given in detail.

Finally, Chapter 6 summarizes the most important conclusions of this thesis and gives some recommendations for future work.

Chapter 2

Space-Time Block Codes

2.1 Introduction

It is well-known that space-time coding proposed in [87] is an effective and practical way to approach the capacity of MIMO wireless channels. Space-time coding is a coding technique designed for use with multiple transmitting antennas. Coding is performed in both spatial and temporal domains to introduce correlation between signals transmitted from various antennas at various time instants. The spatial-temporal correlation is used for exploiting the MIMO channel fading and minimizing transmission errors at the receiver. Hence, space-time coding can achieve transmitting diversity and power gain over spatially uncoded systems without sacrificing the bandwidth. Among the large body of literature on space-time coding by employing extra transmitting antennas, such as [4, 25, 26, 54, 59, 67, 68, 75–77, 79, 87–89], some of the work focused on explicitly improving the performance of existing systems in terms of the probability of incorrectly detected data packets, and other research capitalizes on the promises of information theory to increase the throughput. Generally speaking, the design of space-time codes amounts to

finding a constellation of matrices that satisfy certain optimality criteria discussed in [87]. In particular, the construction of space-time coding schemes is to a large extent a tradeoff between the three conflicting goals of maintaining a simple decoding, maximizing the error performance, and maximizing the information rate as described in [52].

There are various approaches in coding structures, including STBC [4, 89], STTC [67, 87] space-time turbo trellis codes [94] and layered space-time (LST) codes [94]. A central issue in all these schemes is the exploitation of multipath effects in order to achieve high spectral efficiencies and performance gains.

Compared with the other coding structures of space-time coding, STBC is an appealing transmitting diversity technique, which has the significantly low structure complexity and low decoding complexity, albeit the cost of a loss in performance. Moreover, the concatenated system of STBC based on orthogonal design and standard additive white Gaussian noise (AWGN) codes can outperform some of the best-known STTC (with the same transmission power and transmission rate) in terms of error performance [81]. A remarkable transmission scheme of STBC by using two transmitting antennas is first discovered in [4]. The key feature of the scheme is that it achieves a full diversity gain with a simple ML decoding algorithm. Then it is generalized to an arbitrary number of transmitting antennas based on the theory of orthogonal designs [89], leading to the concept of OSTBC. Subsequently, freer designs of STBC are developed without the limit of orthogonality, including linear STBC [52], such as higher rate quasi-orthogonal STBC proposed in [40, 74, 83], and nonlinear STBC [52, 82].

In this chapter, a brief overview of STBC by considering MIMO system model and the classical MRC technique is presented. The introduction of the system model and the classical technique is important, since it will assist us in highlighting the philosophy of STBC at a later stage.

2.2 MIMO System Model

As illustrated in Fig. 2.1, a wireless point-to-point MIMO communication system with M_t transmitting antennas and M_r receiving antennas is considered. The

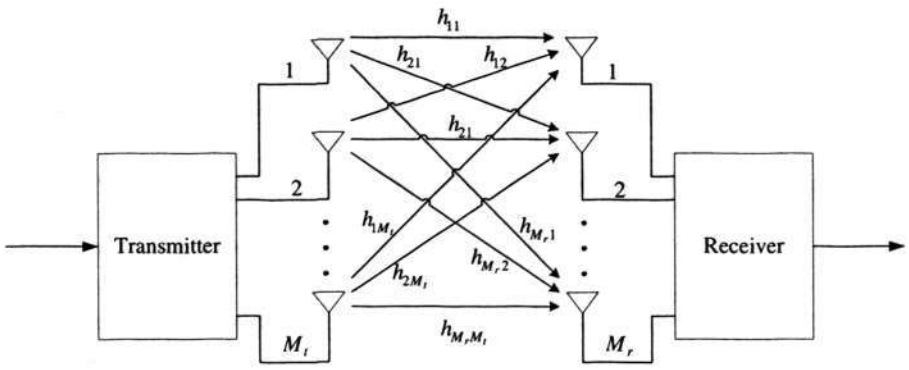

Figure 2.1: Block diagram of a MIMO system [94]

transmitted signals in each time instant are represented by an $M_t \times 1$ column vector $\mathbf{x}$, where the ith component x_i, refers to the transmitted signal from the ith transmitting antenna. The total average transmitted power is constrained to P_o, regardless of the number of transmitting antennas M_t. If the channel is unknown at the transmitter, it is assumed that the signals transmitted from individual antenna elements have equal powers of P_o/M_t.

The MIMO channel is described by an $M_r \times M_t$ complex matrix, denoted by

$\mathbf{H}$.

$$\mathbf{H} = \begin{bmatrix} h_{11} & h_{12} & \cdots & h_{1M_t} \\ h_{21} & h_{22} & \cdots & h_{2M_t} \\ \vdots & \vdots & \ddots & \vdots \\ h_{M_r1} & h_{M_r2} & \cdots & h_{M_rM_t} \end{bmatrix} \tag{2.1}$$

where the ijth component of the matrix $\mathbf{H}$, denoted by h_{ij}, represents the channel fading coefficient from the jth transmitting antenna to the ith receiving antenna. The information carrying signals are transmitted over the wireless fading channels.

In this thesis, we limit the analysis to the case of narrowband channels, so that they can be modeled as frequency-nonselective or flat. In other words, we assume that the channels are memoryless. In addition, Rayleigh fading which is frequently used to model environments with a large number of scatterers without line-of-sight (LOS) radio propagation is assumed. We define the channels as *independent Rayleigh fading* when a signal transmitted from every individual transmitting antenna appears uncorrelated at each of the receiving antennas. As a result, the signal corresponding to every transmitting antenna has a distinct spatial signature at a receiving antenna.

The independent Rayleigh fading model can be approximated in MIMO channels where the spacing of antenna elements is considerably larger than the carrier wavelength or the incoming wave incidence angle spread is relatively large (larger than 30°). For example, in the uplink of a cellular radio, at the base stations which are located high above the ground, the receiving antenna signals get correlated due to a small angular spread of the incoming waves. In order to obtain independent signals between adjacent receiving antenna elements, much higher antenna separations are needed if the incoming wave incidence angle spread is large.

Many measurements and experiment results indicate that if two receiving antennas are used to provide diversity at the base station receiver, they must be on the order of ten wavelengths apart to provide sufficient de-correlation, while it is sufficient to separate the antennas by about three wavelengths at remote handsets to get the same diversity improvements. Due to the reciprocity principle, the same results are appropriate to the downlink scenario also.

The received power for each of M_r receiving antennas is assumed equal to the total average transmitted power for normalization purpose. Physically, it means that we ignore signal losses and amplifications in the propagation process, including shadowing, antenna gains, etc. Thus we obtain the normalization constraint for the elements of the channel matrix $\mathbf{H}$, on a channel with random coefficients, as

$$\sum_{j=1}^{M_t} E[|h_{ij}|^2] = M_t, \quad i = 1, 2, \ldots, M_r \tag{2.2}$$

where $E[\cdot]$ denotes the expectation.

The channel matrix can be estimated at the receiver by transmitting a training sequence. We assume that the channel matrix is known to the receiver throughout the thesis, i.e., the receiver can get perfect channel estimates. But the channel matrix is not always known at the transmitter. The CSI can be communicated from the receiver to the transmitter via a reliable feedback link or estimated by using reciprocity in duplexing schemes.

The noise term at the receiver is described by an $M_r \times 1$ column vector, denoted by $\mathbf{e}$. Its components are statistically independent zero-mean, temporally and spatially white, complex Gaussian random variable with the variance $\sigma^2 = N_0/2$

per dimension.

The received signals at each time instant are represented by an $M_r \times 1$ column vector, denoted by $\mathbf{y}$, where each complex component refers to a receiving antenna. The average power at each receiving antenna is denoted by P_r. The average SNR at each receiving antenna is defined as

$$\gamma = \frac{P_r}{N_0} \tag{2.3}$$

Since it has been assumed that the total average received power per antenna is equal to the total average transmitted power, the SNR is also equal to the ratio of the total average transmitted power and the noise power per receiving antenna as follows,

$$\gamma = \frac{P_o}{N_0} \tag{2.4}$$

Clearly, it is independent of the number of transmitting antennas M_t.

By collecting the filtered and symbol sampled complex baseband equivalent outputs from the receiving antenna array, the received signal at each time instant can be written as

$$\mathbf{y} = \mathbf{H}\mathbf{x} + \mathbf{e} \tag{2.5}$$

Throughout the thesis, we also assume that the MIMO channel is a *slow* or *quasi-static fading*, i.e., its entries vary randomly but are fixed at the start of a transmission block and kept constant during the transmission block, which means that the symbol duration is small compared to the channel coherence time.

2.3 Maximum Ratio Combining

In most scattering environments, the transmitted symbols experience severe magnitude fluctuation and phase rotation, namely the effect of multipath fading. In order to address the issue of multipath, antenna diversity is a practical, effective and hence, a widely applied technique [41]. The classical approach is to use multiple antennas at the receiver. The replicas of the same transmitted symbol through independent fading paths are received and combining or selection and switching are performed. Even if a particular path is severely faded, we may still be able to recover a reliable estimate of the transmitted symbols through other propagation paths. Therein, one of the classical methods that performs combining replicas of the transmitted symbol is referred to as the MRC technique [4, 26, 41, 78].

Fig. 2.2 shows the baseband representation of the classical MRC technique for two receiving antennas. At a particular time instant, a signal s is sent from the transmitter. The transmitted signal s propagates via two different channels, namely h_1 and h_2, which are modelled as complex multiplicative distortion. Noise is added at the two receiver. The resulting received baseband signals y_1 and y_2 are given as follows,

$$y_1 = h_1 s + e_1 \tag{2.6}$$

$$y_2 = h_2 s + e_2 \tag{2.7}$$

where e_1 and e_2 are the complex AWGN samples. Consistent with Section 2.2, the channel estimators at the receiver are assumed to be perfect, i.e., we can get perfect channel information at the receiver. In order to remove the channel's effects, the

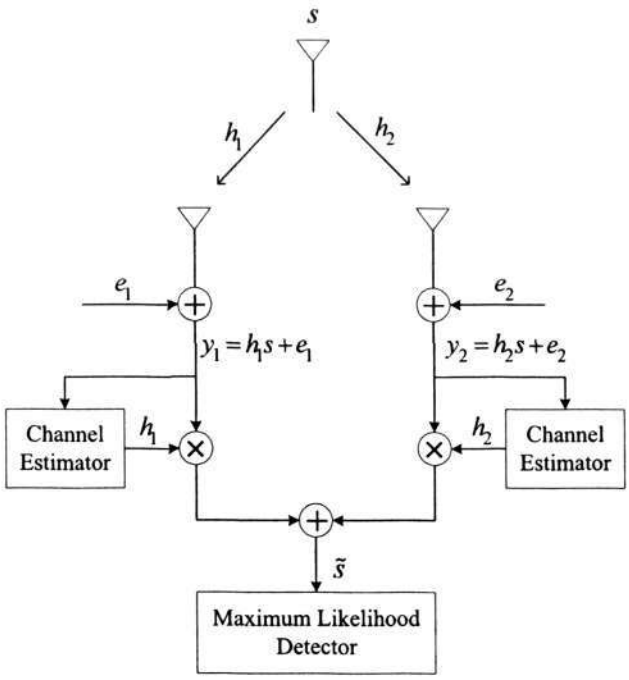

Figure 2.2: Baseband representation of two-branch MRC [94]

received signals y_1 and y_2 are multiplied by the conjugate of the complex channel transfer function h_1^* and h_2^*, respectively, where $(\cdot)^*$ denotes the complex conjugate operator. Then the receiver combining scheme for two-branch MRC is as follows,

$$\begin{aligned} \tilde{s} &= h_1^* y_1 + h_2^* y_2 \\ &= \left(|h_1|^2 + |h_2|^2\right) s + h_1^* e_1 + h_2^* e_2. \end{aligned} \tag{2.8}$$

The combined signal $\tilde{s}$ is passed to the ML detector. The ML decision rule at the receiver for these received signals is to choose signal s_i if and only if (iff)

$$dist(\tilde{s}, s_i) \leq dist(\tilde{s}, s_k), \quad \forall i \neq k \tag{2.9}$$

where $dist(a, b)$ is the Euclidean distance between signals a and b, and the index k spans all possible transmitted signals. As seen from (2.9) that the ML estimate s_i of the transmitted symbol is the one having the minimum Euclidean distance

from the combined signal $\tilde{s}$.

Since the total transmitted energy is $E_s = E[|s|^2]$ per time interval, the average SNR before the ML detector is given by

$$\gamma_{MRC} = \left(|h_1|^2 + |h_2|^2\right) \frac{E[|s|^2]}{N_0} = \left(|h_1|^2 + |h_2|^2\right) \frac{E_s}{N_0} \tag{2.10}$$

which is taken as a benchmark to compare with that of the Alamouti's STBC in the following section.

2.4 Principles and Structures of STBC

In the previous sections, we have briefly introduced the well-known MIMO system model and the classic MRC technique. In this section, some basic principles and structures of STBC will be presented. We first introduce the Alamouti scheme [4], which is the simplest form of STBC, designed only for use with two transmitting antennas. The key feature of this scheme is that it can achieve a full diversity gain and a full code rate simultaneously for arbitrary constellation with a simple ML decoding algorithm. Following a rudimentary introduction of Alamouti scheme, we also present the generalized STBC with a large number of transmitting antennas based on orthogonal designs [89]. Then the linear STBC with more degrees of freedom in the design is discussed.

2.4.1 Alamouti Scheme

One of the first STBC was proposed by Alamouti in 1998 [4]. He studied the case of two transmitting antennas ($M_t = 2$) and suggested to simultaneously transmit $N = 2$ complex symbols s_1 and s_2 and their conjugates during $L = 2$ time instants.

The transmission matrix is defined as follows,

$$\mathbf{G}_2 = \begin{bmatrix} s_1 & -s_2^* \\ s_2 & s_1^* \end{bmatrix} \tag{2.11}$$

In the time instant $l = 1$, signal s_1 is transmitted from the first antenna and simultaneously signal s_2 is transmitted from the second antenna. In the next time instant $l = 2$, signal $-s_2^*$ and s_1^* are simultaneously transmitted from two transmitting antennas, respectively.

For the moment, we ignore any scaling factor needed to normalize the transmission power. Note that the transmission matrix of Alamouti's STBC has the following property

$$\mathbf{G}_2 \cdot \mathbf{G}_2^{\mathcal{H}} = \left(|s_1|^2 + |s_2|^2\right) \mathbf{I}_2 \tag{2.12}$$

where $(\cdot)^{\mathcal{H}}$ denotes the Hermitian operator, i.e., the complex conjugate and transpose operator, and $\mathbf{I}_2$ denotes the 2×2 dimensional identity matrix. The code rate of Alamouti's STBC is given by

$$R = \frac{N}{L} = 1. \tag{2.13}$$

Let us now consider an example of encoding and decoding the Alamouti's STBC of $\mathbf{G}_2$ in (2.11) employing a single receiving antenna. However, it can be easily extended to an arbitrary number of receiving antennas as in [94]. The baseband representation of the Alamouti scheme for one receiving antenna is shown in Fig. 2.3. As mentioned earlier, the channel is assumed to be constant across the corresponding two consecutive time instants due to quasi-static fading. The independent AWGN samples are added at the receiver at two consecutive time instants. The received

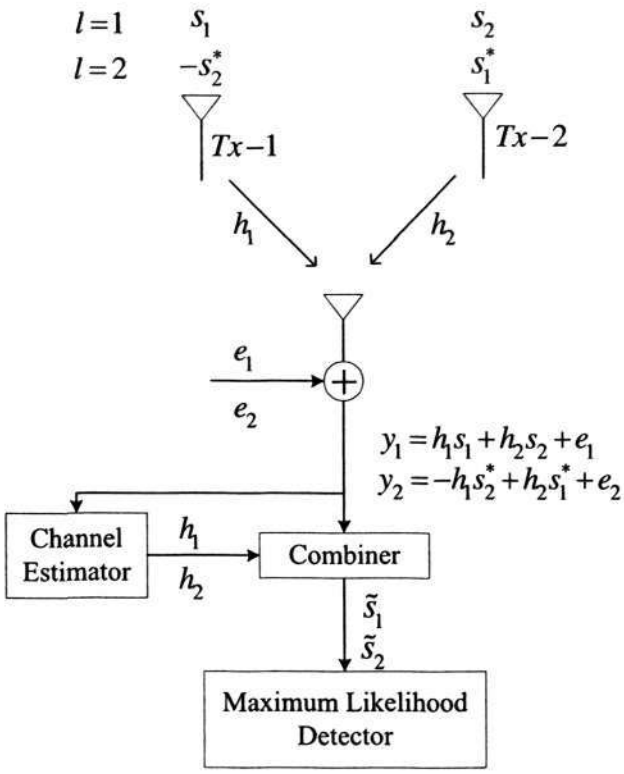

Figure 2.3: Baseband representation of Alamouti's STBC for one receiving antenna [26]

signals can, then, be expressed by,

$$y_1 = h_1 s_1 + h_2 s_2 + e_1 \tag{2.14}$$

$$y_2 = -h_1 s_2^* + h_2 s_1^* + e_2 \tag{2.15}$$

where y_1 is the first received signal and y_2 is the second. Note that y_1 consists of the transmitted signals s_1 and s_2, while y_2 consists of their conjugates. For decision of the transmitted symbols, we have to extract the signals s_1 and s_2 from the received signals y_1 and y_2. Hence, both signals y_1 and y_2 are passed to the combiner, as shown in Fig. 2.3. Consistently, the channel estimator is assumed to provide perfect estimation of the diversity channels. After performing a simple

signal processing, the transmitted signals s_1 and s_2 are separated completely.

In order to extract the signal s_1, y_1 and y_2 are combined as follows,

$$\begin{aligned}\tilde{s}_1 &= h_1^* y_1 + h_2 y_2^* \\ &= \left(|h_1|^2 + |h_2|^2\right) s_1 + h_1^* e_1 + h_2 e_2^*.\end{aligned} \tag{2.16}$$

Similarly, for signal s_2, we generate

$$\begin{aligned}\tilde{s}_2 &= h_2^* y_1 - h_1 y_2^* \\ &= \left(|h_1|^2 + |h_2|^2\right) s_2 + h_2^* e_1 - h_1 e_2^*.\end{aligned} \tag{2.17}$$

It is clear that the signals s_1 and s_2 are separated by simple multiplications and additions. Due to the orthogonal nature of $\mathbf{G}_2$, the unwanted signal s_2 is removed from (2.16) and vice versa, s_1 is cancelled out in (2.17). Both combined signals $\tilde{s}_1$ and $\tilde{s}_2$ are then passed to the ML detector in Fig. 2.3. According to the ML decision rule in (2.9), the most likely transmitted symbols are chosen based on the Euclidean distances between $\tilde{s}_i (i = 1, 2)$ and all possible transmitted symbols.

If the total transmitted power is normalized so that the total transmitted energy per time interval is E_s, and the transmitted power is equally distributed between two transmitting antennas, i.e., $E[|s_1|^2] = E[|s_2|^2] = E_s/2$, the average SNR for each signal $s_i (i = 1, 2)$ before the ML detector is given by

$$\gamma_{Alamouti} = \left(|h_1|^2 + |h_2|^2\right) \frac{E[|s_i|^2]}{N_0} = \left(|h_1|^2 + |h_2|^2\right) \frac{E_s}{2N_0} \tag{2.18}$$

By comparing (2.18) to the average SNR in (2.10) for MRC technique, we find that Alamouti scheme can achieve full transmitting diversity equal to the diversity of a two-branch MRC, which is 2. However, it has a 3dB power loss relative to the latter. The 3dB performance penalty is due to the assumption that the

energy radiated from each transmitting antenna in Alamouti scheme is half of that radiated from the single antenna in MRC in order that Alamouti scheme and MRC diversity have the same total transmission power.

2.4.2 Orthogonal STBC

Motivated by the appealing feature of Alamouti's STBC in terms of simplicity and performance, in 1999, Tarokh *et al.* [89] generalized Alamouti's STBC to some similar schemes by using an arbitrary number of transmitting antennas based on the theory of orthogonal designs. The generalized schemes are referred to as OSTBC. For two transmitting antennas, OSTBC along with its various extensions to inter-symbol interference (ISI) channels, such as space-time orthogonal frequency division multiplexing (OFDM) and time-reversal OSTBC, is currently being considered as a means for improving the performance of wireless local area networks [59], GSM [55], and enhanced data rates for GSM evolution (EDGE) [12]. Also, the simplest form of OSTBC, Alamouti's STBC described in Section 2.4.1, has been adopted in the third generation cellular standard, WCDMA [14]. The OSTBC can achieve the full transmitting diversity specified by the number of transmitting antennas M_t, while allowing a very simple ML decoding algorithm, based only on linear processing of the received signals [89]. The complexity of this decoder is linearly proportional to the number of antennas and the transmission rate. The performance evaluation of the resulting generalized code is given in [88].

OSTBC describes the relationship between the original transmitted signal s and the signal replicas artificially created at the transmitter for transmission over

various diversity channels. In general, it is defined by an $M_t \times L$ dimensional transmission matrix $\mathbf{G}$ as follows,

$$\mathbf{G} = \begin{bmatrix} g_{11} & g_{12} & \cdots & g_{1L} \\ g_{21} & g_{22} & \cdots & g_{2L} \\ \vdots & \vdots & \ddots & \vdots \\ g_{M_t1} & g_{M_t2} & \cdots & g_{M_tL} \end{bmatrix} \tag{2.19}$$

where M_t denotes the number of transmitting antennas and L denotes the number of time instants for transmission of one block of symbols. The entries g_{ij} $(i = 1, \ldots, M_t; j = 1, \ldots, L)$ of this matrix are linear combination of the N modulated symbols $s_1, s_2, \ldots, s_N$ and their conjugates.

In order to achieve full transmitting diversity of M_t, the transmission matrix $\mathbf{G}$ is constructed based on orthogonal designs as follows,

$$\mathbf{G} \cdot \mathbf{G}^{\mathcal{H}} = \left(|s_1|^2 + |s_2|^2 + \cdots + |s_N|^2\right) \mathbf{I}_{M_t} \tag{2.20}$$

where $\mathbf{I}_{M_t}$ is the $M_t \times M_t$ dimensional identity matrix. The orthogonal nature enables to achieve the full transmitting diversity for any number of transmitting antennas. Moreover, it allows the receiver to decouple the different transmitted signals. As a result, a simple ML decoding algorithm can be applied, based only on linear processing of the received signals as shown in [88].

The code rate of OSTBC is defined as the ratio between the number of symbols the encoder takes as its input and the number of transmission time instants, given by

$$R = \frac{N}{L} \tag{2.21}$$

If it is assumed that the signal constellation consists of 2^m points, then the spectral

efficiency of OSTBC is given by [94]

$$\eta_{se} = \frac{r_b}{B} = \frac{r_s m R}{r_s} = \frac{mN}{L} \text{ bits/s/Hz} \tag{2.22}$$

where r_b and r_s are the bit and symbol rates, respectively, and B is the bandwidth. It is known from [89, 94] that the code rate of OSTBC with full transmitting diversity is less than or equal to one, i.e., $R \leq 1$. Hence, the full code rate of $R = 1$ corresponds to no bandwidth expansion, while the code rate of $R < 1$ corresponds to a bandwidth expansion of $1/R$. From the bandwidth efficiency point of view, it is desirable to construct the transmission schemes with the full code rate for any number of transmitting antennas.

According to the type of the signal constellation, OSTBC can be classified into OSTBC with real signals and OSTBC with complex signals.

(i) For arbitrary real constellation such as PAM and M-ASK, OSTBC based on square transmission matrices can be constructed to achieve full code rate for only $M_t = 2, 4$, or 8, while the generalized OSTBC without the limitations of square transmission matrices can be constructed to achieve full code rate for any number M_t of transmitting antennas [89]. The minimum length L of codeword to achieve $R = 1$ for M_t is given by [89]

$$L_{min} = \min(2^{4c+d}) \tag{2.23}$$

subject to the constraint of

$$\{c, d | \ 0 \leq c, 0 \leq d < 4 \text{ and } 8c + 2^d \geq M_t\}. \tag{2.24}$$

From the above orthogonal design theory, when $c = 0$, $L_{min} = 2$ for $M_t = 2$, $L_{min} = 4$ for $M_t = 3, 4$, and $L_{min} = 8$ for $5 \leq M_t \leq 8$; while when $c > 0$, $L_{min} \geq 16$, and $8c + 2^d < 2^{4c+d}$ leads to non-square transmission matrix $\mathbf{G}$ with $M_t < L_{min}$. Hence, OSTBC with $M_t \times M_t$ square transmission matrix $\mathbf{G}$ (i.e., $M_t = L_{min}$) which achieve full code rate exist iff $M_t = 2, 4, 8$ [89]. This provides a proof to the above statement.

(ii) For any complex constellation such as M-PSK, OSTBC based on square transmission matrices exists iff $M_t = 2$, i.e., the Alamouti's STBC, while the generalized OSTBC without the limitations of square transmission matrices can be constructed to achieve code rate of $1/2$ for any number M_t of transmitting antennas. For example, OSTBC with complex constellation and $R = 1/2$ for $M_t = 3$ and $M_t = 4$ are constructed in [89] respectively as

$$\mathbf{G}_3 = \begin{bmatrix} s_1 & -s_2 & -s_3 & -s_4 & s_1^* & -s_2^* & -s_3^* & -s_4^* \\ s_2 & s_1 & s_4 & -s_3 & s_2^* & s_1^* & s_4^* & -s_3^* \\ s_3 & -s_4 & s_1 & s_2 & s_3^* & -s_4^* & s_1^* & s_2^* \end{bmatrix} \tag{2.25}$$

$$\mathbf{G}_4 = \begin{bmatrix} s_1 & -s_2 & -s_3 & -s_4 & s_1^* & -s_2^* & -s_3^* & -s_4^* \\ s_2 & s_1 & s_4 & -s_3 & s_2^* & s_1^* & s_4^* & -s_3^* \\ s_3 & -s_4 & s_1 & s_2 & s_3^* & -s_4^* & s_1^* & s_2^* \\ s_4 & s_3 & -s_2 & s_1 & s_4^* & s_3^* & -s_2^* & s_1^* \end{bmatrix} \tag{2.26}$$

To provide higher code rate of OSTBC with a complex constellation and more than two antennas, Tarokh *et al.* in [89] constructed two OSTBC $\mathbf{G}_3^h$ and $\mathbf{G}_4^h$ with $R = 3/4$ for $M_t = 3$ and $M_t = 4$, respectively, as follows,

$$\mathbf{G}_3^h = \begin{bmatrix} s_1 & -s_2^* & \frac{s_3^*}{\sqrt{2}} & \frac{s_3^*}{\sqrt{2}} \\ s_2 & s_1^* & \frac{s_3^*}{\sqrt{2}} & -\frac{s_3^*}{\sqrt{2}} \\ \frac{s_3}{\sqrt{2}} & \frac{s_3}{\sqrt{2}} & \frac{-s_1 - s_1^* + s_2 - s_2^*}{2} & \frac{s_2 + s_2^* + s_1 - s_1^*}{2} \end{bmatrix} \tag{2.27}$$

$$\mathbf{G}_4^h = \begin{bmatrix} s_1 & -s_2 & \frac{s_3^*}{\sqrt{2}} & \frac{s_3^*}{\sqrt{2}} \\ s_2 & s_1 & \frac{s_3^*}{\sqrt{2}} & -\frac{s_3^*}{\sqrt{2}} \\ \frac{s_3}{\sqrt{2}} & \frac{s_3}{\sqrt{2}} & \frac{-s_1 - s_1^* + s_2 - s_2^*}{2} & \frac{s_2 + s_2^* + s_1 - s_1^*}{2} \\ \frac{s_3}{\sqrt{2}} & -\frac{s_3}{\sqrt{2}} & \frac{-s_2 - s_2^* + s_1 - s_1^*}{2} & -\frac{s_1 + s_1^* + s_2 - s_2^*}{2} \end{bmatrix} \tag{2.28}$$

Another two OSTBC $\widetilde{\mathbf{G}}_3^h$ [32] and $\widetilde{\mathbf{G}}_4^h$ [18, 91] with complex constellations and $R = 3/4$ for $M_t = 3$ and $M_t = 4$, respectively, are given by

$$\widetilde{\mathbf{G}}_3^h = \begin{bmatrix} s_1 & s_2^* & s_3^* & 0 \\ -s_2 & s_1^* & 0 & -s_3^* \\ -s_3 & 0 & s_1^* & s_2^* \end{bmatrix} \tag{2.29}$$

$$\widetilde{\mathbf{G}}_4^h = \begin{bmatrix} s_1 & s_2^* & s_3^* & 0 \\ -s_2 & s_1^* & 0 & -s_3^* \\ -s_3 & 0 & s_1^* & s_2^* \\ 0 & s_3 & -s_2 & s_1 \end{bmatrix} \tag{2.30}$$

We can conclude that the Alamouti's STBC is unique in that it is the only OSTBC with square transmission matrix to achieve the full code rate for complex constellation.

2.4.3 Linear STBC

In principle, all instances of the OSTBC discussed in Section 2.4.2 are an important subclass of linear STBC, which is not a new different code family. Linear STBC has the general linear structure without necessarily requiring the orthogonal designs. Linear STBC is a particular interesting technique attracting much attention recently in the literature [27, 31, 47, 52]. The codeword matrices in such linear STBC are formed as linear combinations of some information carrying signals, each weighted by a corresponding matrix that spreads the information both in time and space. According to [52], the linear STBC chooses the linear mapping

from a set of N symbols onto a matrix $\mathbf{C}$ of dimension $M_t \times L$ as follows,

$$\mathbf{C} = \sum_{n=1}^{N} (s_n \mathbf{A}_n + s_n^* \mathbf{B}_n) \tag{2.31}$$

where s_n $(n = 1, 2, \ldots, N)$ represents the modulated information carrying signal. Here, $\{\mathbf{A}_n, \mathbf{B}_n\}_{n=1}^{N}$ are $M_t \times L$ dimensional weighting matrices used for spreading the information both in time and space. According to the definition in (2.21), the code rate of linear STBC is given by

$$R = \frac{N}{L} \tag{2.32}$$

By an appropriate choice of these weighting matrices, linear STBC can achieve appealing properties from both performance and implementation points of views regardless of transmitting antenna array size and code rate [47]. The Alamouti's STBC and the generalized OSTBC discussed in the previous sections are the well-known types of linear STBC, where the weighting matrices are taken to satisfy the orthogonal conditions [89] that ensure optimally low complexity decoding while providing full spatial diversity. If we rewrite the Alamouti's STBC $\mathbf{G}_2$ with $R = 1$ [4] and the generalized OSTBC $\mathbf{G}_3$, $\mathbf{G}_4$ with $R = 1/2$ [89] as well as $\widetilde{\mathbf{G}}_3^h$ [32], $\widetilde{\mathbf{G}}_4^h$ [18, 91] with $R = 3/4$ by using the form in (2.31), it is clear that each entry of the weighting matrices $\{\mathbf{A}_n, \mathbf{B}_n\}_{n=1}^{N}$ of these codes are drawn from $\{1, 0, -1\}$.

2.5 Summary

In this chapter, as the background knowledge of STBC, the MIMO system model and the classical MRC technique are rudimentarily introduced. After that, the

structures and properties of some typical and well-known STBC including Alamouti's STBC, generalized OSTBC and linear STBC are described, respectively. The definition of independent Rayleigh fading and slow or quasi-static fading is provided, which is assumed throughout the thesis. A few important terms such ML decision rule, orthogonal property, code rate, spectral efficiency and average SNR are presented mathematically. Particularly, for the two-branch MRC technique and Alamouti's STBC, the simple linear processing at the receiver used for ML decoding is illustrated, and their average SNRs are compared. It is found that Alamouti's STBC can obtain the MRC-like diversity, but has a 3dB performance penalty relative to the two-branch MRC.

Chapter 3

Combining Beamforming and STBC

3.1 Introduction

STBC introduced in Chapter 2 is a transmitting diversity technique that relies on coding across space (transmitting antennas) to extract MRC-like diversity in the absence of CSI at the transmitter. In addition to diversity gain, array gain can also be incorporated through CSI feedback. It has been noticed earlier in the 3G WCDMA standardization that even crude feedback signalling of the CSI can be extremely useful in improving the downlink performance. The CSI can be fed back from the receiver to the transmitter through a dedicated feedback link or estimated by using reciprocity in duplexing schemes. This leads to the categorization of transmitting diversity into *open-loop mode* and *closed-loop mode*.

As stated in [61], the MIMO communication networks in the closed-loop mode can help customize the transmitted waveforms to provide higher link capacity and throughput, improve system capacity by sharing the spatial channel with multiple users simultaneously, enable channel-aware scheduling for multiple users,

simplify multi-user receivers through interference avoidance, and provide a simple and general means to exploit spatial diversity. Essentially, CSI makes it easier to obtain the benefits of MIMO technology while lessening the complexity impact incurred through MIMO transmission and reception.

The selective transmitting diversity (STD) [35, 72] is the first closed-loop mode introduced to 3G systems, where only one additional feedback bit is used to select the desired transmitting antennas. The WCDMA Release '99 and Release 4 specifications include two closed-loop transmitting diversity concepts as described in [14, 36], where the CSI is used to control the weights at different transmitting antenna elements in order to maximize the SNR at the receiver. The weighted signals should arrive co-phased at the receiver. The received signal power is increased through constructive signal combining, and therefore link capacity is also increased. But the WCDMA transmitting diversity solutions explicitly support only two transmitting antennas.

This weights adaptation operation in the closed-loop transmitting diversity is sometimes called *beamforming*, although it may not have the physical interpretation of forming or steering the directional beam patterns towards the desired user as the smart antenna. As we know, spatial diversity requires large antenna spacing (on the order of several carrier wavelengths) to ensure uncorrelated fading, but, on the other hand, beamforming methods in the smart antenna systems utilize antenna spacing of less than a carrier wavelength (typically half the wavelength) [14] depending on the antenna configuration. It seems that the closed-loop transmitting diversity inducing spatial diversity and the beamforming for smart antenna

inducing directionality are two different techniques which have no relationship with each other. However, the problem formulation for calculating the antenna weights remains the same if one recognizes the fact that the knowledge of the different channel coefficients in the case of closed-loop transmitting diversity is equivalent to that of the steering vector in the case of beamforming for smart antenna. Therefore, "beamforming" has become a popular notion of weights adaptation operation in the closed-loop transmitting diversity as in [43, 45, 97, 98]. From now on, the term "beamforming" used in the thesis indicates the weight adaptation operation for the closed-loop transmitting diversity.

Usually the performance of transmitting diversity via open-loop STBC is inferior to that of beamforming with perfect feedback CSI by a factor of *array gain*. Loosely speaking, the absence of array gain is due to the STBC methods spreading power uniformly in all directions in space, while beamforming distributes the transmission power across different transmitting antennas according to the feedback CSI. In [29, 69, 96], the design of transmitter beamforming considering the imperfect feedback CSI was addressed. The feedback errors destroy the diversity property of pure beamforming without combining with STBC system. It means that the open-loop STBC may outperform the pure beamforming system at high SNR as shown in [45] resulted from the diversity loss in the pure beamforming system due to imperfect CSI. Since STBC is proposed and designed for the open-loop systems, i.e., no feedback CSI at all, the feedback errors in general can not destroy the diversity property of a STBC system. Motivated by this fact, recently, many researchers have suggested to improve the performance of STBC by using a feed-

back of CSI in the literature [7, 39, 45, 65, 66, 69, 80, 84, 93, 97, 98], which provides additional array gain while keeping the diversity property due to STBC.

In view of the fact that the perfect CSI at the transmitter is in practice not always possible, particularly in environments where the parameters of the channel are rapidly time-varying, a combined system of beamforming and OSTBC proposed by Jongren *et al.* in [45] is attractive since it incorporates the degree of the feedback CSI into the design. The CSI is modelled using a purely statistical approach, which is called channel mean feedback in [93, 97]. The OSTBC is predetermined and the beamforming matrix is adapted to the available CSI at the transmitter by means of a linear transformation. Therefore, the combined system possesses simultaneously the benefits of transmitter beamforming due to array gain and OSTBC resulted from diversity gain. To maximize the performance gain of the combined system, a performance criterion based on the worst-case pairwise error probability (PEP) is derived, which takes the available CSI at the transmitter into account. A semi-closed-form solution of the optimization problem resulted from the worst-case PEP performance criterion is obtained under the consideration of a specific simplified fading scenario as described in [45, 48].

Subsequently, the design of unstructured STBC that uses the imperfect quantized CSI at the transmitter from the receiver via a dedicated feedback link is proposed and investigated by Jongren *et al.* in [48]. The quantized CSI is incorporated into the code-construction process by using a performance criterion based on the codeword/block error probability (BLER) conditioned on the CSI at the transmitter. The efficient codes are found by optimizing the performance criterion

using a simple gradient search algorithm. Due to the unstructured nature of the codewords, the degrees of freedom in the code-construction process is maximized, at the cost of a high decoding complexity. From the analysis in [87], we can deduce that as long as the rank of the codeword difference matrix of the unstructured STBC is sustained, the imperfect quantized CSI at the transmitter cannot destroy the full diversity property of the unstructured code constructed.

Although we mainly concentrate on developing and investigating the MISO systems, the reviewed systems in the following Sections 3.2 and 3.3 are for the MIMO schemes.

3.2 Review of Combining Beamforming and OSTBC

In this section, we embark on describing the combined system of beamforming and OSTBC proposed in [45] in more detail.

3.2.1 System Model

Fig. 3.1 shows the combined system of beamforming and OSTBC, employing M_t transmitting antennas and M_r receiving antennas. It is assumed that some, but not necessarily perfect, CSI is available at the transmitter, although the receiver is assumed to get perfect CSI. The transmitter consists of an orthogonal space-time block encoder followed by a beamforming $\mathbf{W}$. The information data are mapped into the OSTBC $\mathbf{S}$ by the space-time block encoder. Then the OSTBC is linearly transformed by using the beamforming technique to adapt the code to the available CSI at the transmitter. As a result, a set of parallel and generally different symbol

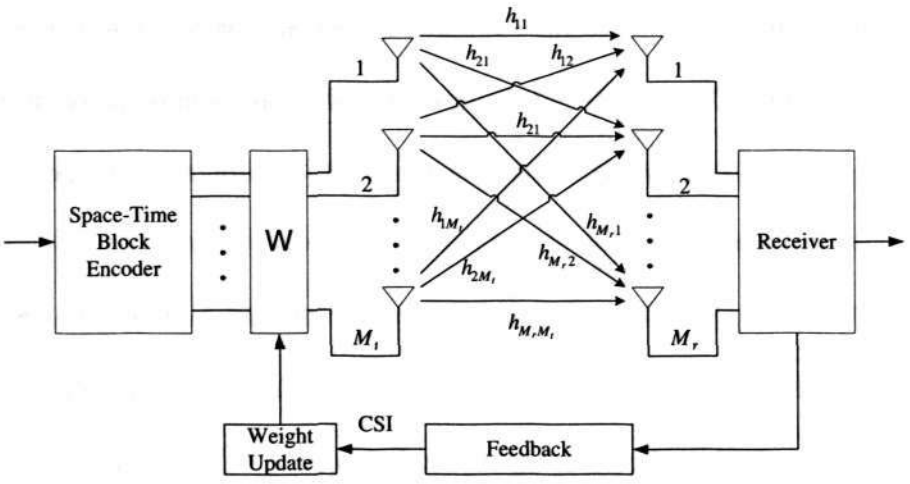

Figure 3.1: Block diagram of the combined system model

sequences for transmitting from the M_t antennas is formed by,

$$\mathbf{C} = \mathbf{WS} \tag{3.1}$$

where $\mathbf{W}$ is an $M_t \times M_t$ square matrix, $\mathbf{C}$ is an $M_t \times L$ dimensional matrix and L represents the length of the transmitted codeword.

The output signals from the beamforming are transmitted over a wireless MIMO fading channel, denoted by a $M_r \times M_t$ dimensional matix $\mathbf{H}$, as described in (2.1). For describing purpose, the MIMO channel is also represented by the $1 \times M_t M_r$ row vector

$$\mathbf{h} = \text{rvec}(\mathbf{H}) \tag{3.2}$$

where rvec$(\cdot)$ denotes the row vectorization operator which serializes the rows of its argument into a row vector. It is assumed that the channels are statistically identical, space-independent, time-correlated and satisfy quasi-static flat fading, i.e., the channel is constant during the transmission of a burst of codewords but

may vary from one burst to another in a statistically stationary fashion. The individual channel between each transmitting and receiving antenna is assumed to obey a complex Gaussian distribution with mean vector $\mathbf{m_h}$ and covariance matrix $\mathbf{R_{hh}}$.

At the receiver, the signal output from each receiving antenna is a weighted superposition of the M_t transmitted signals, corrupted by additive noise. It is assumed that the ML decoding algorithm, based on the perfect channel estimate at the receiver, is employed to recover the information data. The system data model can be expressed by

$$\mathbf{Y} = \mathbf{HWS} + \mathbf{E} \tag{3.3}$$

where $\mathbf{Y}$ is a $M_r \times L$ dimensional matrix denoting the received signals and the noise matrix $\mathbf{E}$ is assumed to be a temporally and spatially white, complex Gaussian random variable with zero-mean and variance $\sigma^2 = N_0/2$ per dimension.

In general, the CSI available at the transmitter is fed back from the receiver through a dedicated feedback link or estimated by using reciprocity in duplex schemes. It is not only noisy but also outdated due to feedback delay or duplex time. In this section, the development is exemplified by, but not limited to, systems where the CSI at the transmitter is obtained through a dedicated feedback channel. To denote the CSI at the transmitter, a $M_r \times M_t$ dimensional matrix $\hat{\mathbf{H}}$ is introduced, and $\hat{\mathbf{h}}$ represents its row vectorized counterpart. Motivated by the well-known Jakes model [41], the CSI $\hat{\mathbf{h}}$ at the transmitter is assumed to be correlated with the true channel $\mathbf{h}$ and the amount of such correlation is determined by

the time it takes to feed back the CSI. It is reasonable to assume that the CSI $\hat{\mathbf{h}}$ at the transmitter and the true channel $\mathbf{h}$ are jointly complex Gaussian distributed since they are the samples of the same Gaussian random process. The statistics of $\hat{\mathbf{h}}$ and the relationship between $\hat{\mathbf{h}}$ and $\mathbf{h}$ are described by the mean vector $\mathbf{m}_{\hat{\mathbf{h}}}$, the covariance matrix $\mathbf{R}_{\hat{\mathbf{h}}\hat{\mathbf{h}}}$ and the cross-covariance matrix $\mathbf{R}_{\mathbf{h}\hat{\mathbf{h}}}$.

3.2.2 Performance Criterion for the Beamforming Matrix Design

In order to obtain the optimal beamforming matrix, a performance criterion is described for the combined transmission scheme which takes the available CSI at the transmitter into account. As shown in [45], the performance criterion is based on the union bound on the BLER.

Let $\mathcal{C} = \{\mathbf{C}_1, \ldots, \mathbf{C}_K\}$ denotes the set of the transmitted codewords, where K represents the number of codewords and $\mathbf{C}_k$ $(k = 1, \ldots, K)$ is the kth linearly transformed codeword from the beamforming with the dimension of $M_t \times L$. The BLER is denoted by $P_{bl}(\mathbf{C}' \neq \mathbf{C})$, i.e., the probability that $\mathbf{C}'$ is different from $\mathbf{C}$. Under the assumption that the codewords are transmitted with equal likelihood, the union bound on BLER is expressed by

$$P_{bl}(\mathbf{C}' \neq \mathbf{C}) \leq \frac{1}{K} \sum_{k \neq l} P(\mathbf{C}_k \rightarrow \mathbf{C}_l) = P_{union} \tag{3.4}$$

where $P(\mathbf{C}_k \rightarrow \mathbf{C}_l)$ represents the PEP, i.e., the probability that the ML decoding metric for codeword $\mathbf{C}_l$ is smaller than the metric for $\mathbf{C}_k$, where $k, l \in 1, \ldots, K$ and $k \neq l$. The largest PEP, $P(\mathbf{C}_{\bar{k}} \rightarrow \mathbf{C}_{\bar{l}})$, is the dominating term in the union bound, where $\{\mathbf{C}_{\bar{k}}, \mathbf{C}_{\bar{l}}\}$ $(\bar{k}, \bar{l} \in 1, \ldots, K;\ \bar{k} \neq \bar{l})$ is the worst-case codeword pair

[45]. Thus the overall design goal is to minimize $P(\mathbf{C}_{\bar{k}} \rightarrow \mathbf{C}_{\bar{l}})$. Since the CSI $\hat{\mathbf{h}}$ at the transmitter is available, conditioning on $\hat{\mathbf{h}}$ leads to the following relation,

$$P(\mathbf{C}_{\bar{k}} \rightarrow \mathbf{C}_{\bar{l}}) = \int P\left(\mathbf{C}_{\bar{k}} \rightarrow \mathbf{C}_{\bar{l}}|\hat{\mathbf{h}}\right) p_{\hat{\mathbf{h}}}\left(\hat{\mathbf{h}}\right) d\hat{\mathbf{h}} \tag{3.5}$$

where $P\left(\mathbf{C}_{\bar{k}} \rightarrow \mathbf{C}_{\bar{l}}|\hat{\mathbf{h}}\right)$ is the largest PEP, conditioned on the CSI at the transmitter, and $p_{\hat{\mathbf{h}}}\left(\hat{\mathbf{h}}\right)$ is the probability density function (PDF) of $\hat{\mathbf{h}}$. Clearly, minimizing $P(\mathbf{C}_{\bar{k}} \rightarrow \mathbf{C}_{\bar{l}})$ is equal to minimizing $P\left(\mathbf{C}_{\bar{k}} \rightarrow \mathbf{C}_{\bar{l}}|\hat{\mathbf{h}}\right)$ due to $p_{\hat{\mathbf{h}}}\left(\hat{\mathbf{h}}\right) > 0$.

In order to derive a closed-form expression for the performance criterion, we start from the upper bound of PEP of transmitting $\mathbf{C}_{\bar{k}}$ and deciding in favor of $\mathbf{C}_{\bar{l}}$ at the decoder, conditioned on the true channel $\mathbf{h}$ and the CSI $\hat{\mathbf{h}}$, which is given by [45]

$$\begin{aligned} P\left(\mathbf{C}_{\bar{k}} \rightarrow \mathbf{C}_{\bar{l}}|\mathbf{h}, \hat{\mathbf{h}}\right) &= Q\left(\sqrt{d^2(\mathbf{C}_{\bar{k}}, \mathbf{C}_{\bar{l}}) \frac{1}{2N_0}}\right) \\ &\leq \frac{1}{2} \exp\left(-d^2(\mathbf{C}_{\bar{k}}, \mathbf{C}_{\bar{l}}) \frac{1}{4N_0}\right) \end{aligned} \tag{3.6}$$

where $Q(\cdot)$ is the Gaussian Q function and $d^2(\mathbf{C}_{\bar{k}}, \mathbf{C}_{\bar{l}})$ is the modified Euclidean distance between the two transformed codeword matrices $\mathbf{C}_{\bar{k}}$ and $\mathbf{C}_{\bar{l}}$, given by

$$\begin{aligned} d^2(\mathbf{C}_{\bar{k}}, \mathbf{C}_{\bar{l}}) &= \|\mathbf{H}(\mathbf{C}_{\bar{k}} - \mathbf{C}_{\bar{l}})\|_{\mathrm{F}}^2 \\ &= \mathbf{h}\left(\mathbf{I}_{M_r} \otimes \mathbf{A}(\mathbf{C}_{\bar{k}}, \mathbf{C}_{\bar{l}})\right) \mathbf{h}^{\mathcal{H}} \end{aligned} \tag{3.7}$$

where $\|\cdot\|_{\mathrm{F}}$ denotes the Frobenius norm [33], $\otimes$ denotes the Kronecker product [34] and $\mathbf{I}_{M_r}$ is the $M_r \times M_r$ dimensional identity matrix. The $M_t \times M_t$ codeword distance matrix $\mathbf{A}(\mathbf{C}_{\bar{k}}, \mathbf{C}_{\bar{l}})$ is constructed and defined by [45, 87]

$$\mathbf{A}(\mathbf{C}_{\bar{k}}, \mathbf{C}_{\bar{l}}) = (\mathbf{C}_{\bar{k}} - \mathbf{C}_{\bar{l}})(\mathbf{C}_{\bar{k}} - \mathbf{C}_{\bar{l}})^{\mathcal{H}} \tag{3.8}$$

It has been mentioned in Section 3.2.1 that the true channel and the CSI at the transmitter are jointly complex Gaussian distributed, hence the PDF of $\mathbf{h}$

conditioned on $\hat{\mathbf{h}}$ is also complex Gaussian, given in [45] as follows,

$$p_{\mathbf{h}|\hat{\mathbf{h}}}\left(\mathbf{h}|\hat{\mathbf{h}}\right) = \frac{\exp\left[-(\mathbf{h}-\mathbf{m}_{\mathbf{h}|\hat{\mathbf{h}}})\mathbf{R}^{-1}_{\mathbf{hh}|\hat{\mathbf{h}}}(\mathbf{h}-\mathbf{m}_{\mathbf{h}|\hat{\mathbf{h}}})^{\mathcal{H}}\right]}{\pi^{M_t M_r}\det\left(\mathbf{R}_{\mathbf{hh}|\hat{\mathbf{h}}}\right)} \tag{3.9}$$

where $\det(\cdot)$ denotes the determinant operator, $\mathbf{m}_{\mathbf{h}|\hat{\mathbf{h}}}$ and $\mathbf{R}_{\mathbf{hh}|\hat{\mathbf{h}}}$ are the mean and covariance matrix of $\mathbf{h}$ conditioned on $\hat{\mathbf{h}}$, respectively. The upper bound $V(\mathbf{C}_{\bar{k}} \to \mathbf{C}_{\bar{l}}|\hat{\mathbf{h}})$ on the PEP, conditioned on the CSI $\hat{\mathbf{h}}$, is formed by averaging both sides of (3.6) over the distribution in (3.9),

$$\begin{aligned} P\left(\mathbf{C}_{\bar{k}} \to \mathbf{C}_{\bar{l}}|\hat{\mathbf{h}}\right) &\le \frac{1}{2}\int \exp\left(-\frac{d^2(\mathbf{C}_{\bar{k}},\mathbf{C}_{\bar{l}})}{4N_0}\right) p_{\mathbf{h}|\hat{\mathbf{h}}}\left(\mathbf{h}|\hat{\mathbf{h}}\right) d\mathbf{h} \\ &= V(\mathbf{C}_{\bar{k}} \to \mathbf{C}_{\bar{l}}|\hat{\mathbf{h}}) \end{aligned} \tag{3.10}$$

After following simple manipulations [45], we have

$$V(\mathbf{C}_{\bar{k}} \to \mathbf{C}_{\bar{l}}|\hat{\mathbf{h}}) = \frac{\exp\left[\mathbf{m}_{\mathbf{h}|\hat{\mathbf{h}}}\mathbf{R}^{-1}_{\mathbf{hh}|\hat{\mathbf{h}}}(\boldsymbol{\Psi}^{-1}_{\bar{k}\bar{l}} - \mathbf{R}_{\mathbf{hh}|\hat{\mathbf{h}}})\mathbf{R}^{-1}_{\mathbf{hh}|\hat{\mathbf{h}}}\mathbf{m}^{\mathcal{H}}_{\mathbf{h}|\hat{\mathbf{h}}}\right]}{2\det\left(\mathbf{R}_{\mathbf{hh}|\hat{\mathbf{h}}}\right)\det(\boldsymbol{\Psi}_{\bar{k}\bar{l}})} \tag{3.11}$$

where

$$\boldsymbol{\Psi}_{\bar{k}\bar{l}} = \left(\mathbf{I}_{M_r} \otimes \mathbf{A}(\mathbf{C}_{\bar{k}},\mathbf{C}_{\bar{l}})\right)/4N_0 + \mathbf{R}^{-1}_{\mathbf{hh}|\hat{\mathbf{h}}}. \tag{3.12}$$

Taking the logarithm, neglecting parameter-independent terms and reformulating the exponent in (3.11) lead to the desired logarithmic form of the so-called *codeword pair criterion* used in [45] as

$$\ell(\mathbf{C}_{\bar{k}} \to \mathbf{C}_{\bar{l}}|\hat{\mathbf{h}}) = \mathbf{m}_{\mathbf{h}|\hat{\mathbf{h}}}\mathbf{R}^{-1}_{\mathbf{hh}|\hat{\mathbf{h}}}\boldsymbol{\Psi}^{-1}_{\bar{k}\bar{l}}\mathbf{R}^{-1}_{\mathbf{hh}|\hat{\mathbf{h}}}\mathbf{m}^{\mathcal{H}}_{\mathbf{h}|\hat{\mathbf{h}}} - \log\det(\boldsymbol{\Psi}_{\bar{k}\bar{l}}). \tag{3.13}$$

Corresponding to the worst-case codeword pair $\{\mathbf{C}_{\bar{k}},\mathbf{C}_{\bar{l}}\}$, $\ell(\mathbf{C}_{\bar{k}} \to \mathbf{C}_{\bar{l}}|\hat{\mathbf{h}})$ is the maximum of $\ell(\mathbf{C}_k \to \mathbf{C}_l|\hat{\mathbf{h}})$, taken over all codeword pairs. Conditioned on the available CSI at the transmitter, we can design the beamforming matrix $\mathbf{W}$ from the mapping of $\mathbf{C} = \mathbf{WS}$ by minimizing $\ell(\mathbf{C}_{\bar{k}} \to \mathbf{C}_{\bar{l}}|\hat{\mathbf{h}})$, since the OSTBC, $\mathbf{S}$,

is predetermined. Note that the first term in the performance criterion of (3.13) mainly deals with the CSI at the transmitter, while the second term strives for a code design with no CSI at the transmitter, suitable for an open-loop mode. Therefore, in the case of perfect CSI at the transmitter, the first term is dominating and, on the other hand, in the case of no CSI at the transmitter, the second term is dominating.

3.2.3 Optimization of the Beamforming Matrix

Although the optimal beamforming matrix can be constructed based on the performance criterion described in Section 3.2.2 by using a conventional exhaustive search over all possible codewords, in this section, a semi-closed-form optimization solution [45] in a simplified fading scenario is adopted for its feasibility.

It is assumed that the codewords are equally probable and the average energy per symbol is normalized to E_s. Hence, we have the power constraint as

$$E[\|\mathbf{C}\|_{\mathrm{F}}^2] = \frac{1}{K}\sum_{k=1}^{K}\|\mathbf{C}_k\|_{\mathrm{F}}^2 = NE_s \tag{3.14}$$

where N denotes the number of symbols per block codeword. In view of the mapping of $\mathbf{C} = \mathbf{WS}$ and the appealing orthogonal nature of OSTBC, i.e.,

$$\mathbf{S}\mathbf{S}^{\mathcal{H}} = \left(\sum_{n=1}^{N}|s_n|^2\right)\mathbf{I}_{M_t} = NE_s\mathbf{I}_{M_t} \tag{3.15}$$

the constraint

$$\|\mathbf{W}\|_{\mathrm{F}}^2 = 1 \tag{3.16}$$

is imposed and the codeword distance matrix $\mathbf{A}(\mathbf{C}_k, \mathbf{C}_l)$ becomes

$$\begin{aligned}\mathbf{A}(\mathbf{C}_k, \mathbf{C}_l) &= \mathbf{W}(\mathbf{S}_k - \mathbf{S}_l)(\mathbf{S}_k - \mathbf{S}_l)^{\mathcal{H}}\mathbf{W}^{\mathcal{H}} \\ &= \delta_{kl}\mathbf{W}\mathbf{W}^{\mathcal{H}}, \qquad \forall k \neq l\end{aligned} \tag{3.17}$$

where $\delta_{kl} = \sum_{n=1}^{N} |s_n^{(k)} - s_n^{(l)}|^2$ is the squared Euclidean distance between the OSTBC codeword pair of $\mathbf{S}_k$ and $\mathbf{S}_l$. Here, $s_n^{(k)}$ $(n = 1, 2, \ldots, N)$ is the modulated information symbol of the kth codeword. Subsequently, $\mathbf{\Psi}_{kl}$ of (3.12) is rewritten as

$$\mathbf{\Psi}_{kl}\left(\mathbf{W}\mathbf{W}^{\mathcal{H}}, \delta_{kl}\right) = \frac{\delta_{kl}}{4N_0}\left(\mathbf{I}_{M_r} \otimes \mathbf{W}\mathbf{W}^{\mathcal{H}}\right) + \mathbf{R}^{-1}_{\mathbf{hh}|\hat{\mathbf{h}}} \tag{3.18}$$

Substituting (3.18) into (3.13) leads to the modified performance criterion involving δ_{kl} and $\mathbf{W}\mathbf{W}^{\mathcal{H}}$ as follows,

$$\begin{aligned}\ell(\mathbf{W}\mathbf{W}^{\mathcal{H}}, \delta_{kl}|\hat{\mathbf{h}}) = \mathbf{m}_{\mathbf{h}|\hat{\mathbf{h}}}\mathbf{R}^{-1}_{\mathbf{hh}|\hat{\mathbf{h}}}\left[\mathbf{\Psi}_{kl}\left(\mathbf{W}\mathbf{W}^{\mathcal{H}}, \delta_{kl}\right)\right]^{-1}\mathbf{R}^{-1}_{\mathbf{hh}|\hat{\mathbf{h}}}\mathbf{m}^{\mathcal{H}}_{\mathbf{h}|\hat{\mathbf{h}}} \\ - \log\det\left[\mathbf{\Psi}_{kl}\left(\mathbf{W}\mathbf{W}^{\mathcal{H}}, \delta_{kl}\right)\right].\end{aligned} \tag{3.19}$$

It is clear that (3.19) is a decreasing function with respect to δ_{kl}. The maximum of $\ell(\mathbf{W}\mathbf{W}^{\mathcal{H}}, \delta_{kl}|\hat{\mathbf{h}})$ is corresponding to the minimum of δ_{kl}, i.e., $\delta_{\bar{k}\bar{l}}$, which is the squared Euclidean distance between the worst-case OSTBC codeword pair $\{\mathbf{S}_{\bar{k}}, \mathbf{S}_{\bar{l}}\}$, which corresponds to the Euclidean distance of the codeword pair $\{\mathbf{C}_{\bar{k}}, \mathbf{C}_{\bar{l}}\}$.

Introducing $\eta = \delta_{\bar{k}\bar{l}}/4N_0$ and $\mathbf{Z} = \mathbf{W}\mathbf{W}^{\mathcal{H}}$, the optimization problem is formed as

$$\mathbf{Z} = \arg \min_{\mathbf{Z}\succeq 0,\ tr(\mathbf{Z})=1} \ell(\mathbf{Z}|\hat{\mathbf{h}}) \tag{3.20}$$

where $\mathbf{Z} \succeq 0$ means that $\mathbf{Z}$ is a positive semidefinite matrix, i.e., Hermitian matrix all of whose eigenvalues are nonnegative. The power constraint of $tr(\mathbf{Z}) = 1$ is resulted from (3.16), where $tr(\cdot)$ denotes the trace operator. The performance criterion involving the new parameter $\mathbf{Z}$ is given by

$$\begin{aligned}\ell(\mathbf{Z}|\hat{\mathbf{h}}) = \mathbf{m}_{\mathbf{h}|\hat{\mathbf{h}}}\mathbf{R}^{-1}_{\mathbf{hh}|\hat{\mathbf{h}}}\left[\eta\left(\mathbf{I}_{M_r} \otimes \mathbf{Z}\right) + \mathbf{R}^{-1}_{\mathbf{hh}|\hat{\mathbf{h}}}\right]^{-1}\mathbf{R}^{-1}_{\mathbf{hh}|\hat{\mathbf{h}}}\mathbf{m}^{\mathcal{H}}_{\mathbf{h}|\hat{\mathbf{h}}} \\ - \log\det\left[\eta\left(\mathbf{I}_{M_r} \otimes \mathbf{Z}\right) + \mathbf{R}^{-1}_{\mathbf{hh}|\hat{\mathbf{h}}}\right].\end{aligned} \tag{3.21}$$

The optimization problem as well as the constraint in (3.20) is convex, which is proved in [45]. It means that the local minimum is also global minimum.

For illustrative purpose, we consider a so-called *simplified fading scenario* as in [45, 48, 69], i.e.,

(i) the channels obey independent Rayleigh fading,

(ii) the channel coefficient h_{ij} as well as the coefficient $\hat{h}_{ij}$ of the CSI at the transmitter is modelled as circularly independent and identically distributed (i.i.d) complex Gaussian with zero-mean and variance of $\sigma_h^2 = E[|h_{ij}|^2]$,

(iii) each $\hat{h}_{ij}$ is correlated with the corresponding h_{ij} and uncorrelated with all others.

The normalized correlation coefficient ρ is introduced to describe the degree of correlation, where $\rho = E\left[h_i \hat{h}_i^*\right] / \sigma_h^2$, which is a measure of the feedback CSI quality ($0 \leq |\rho| \leq 1$). This model is completely characterized by the mean vectors $\mathbf{m_h} = \mathbf{m_{\hat{h}}} = \mathbf{0}$, the covariance matrices $\mathbf{R_{hh}} = \mathbf{R_{\hat{h}\hat{h}}} = \sigma_h^2 \mathbf{I}_{M_t M_r}$ and the cross-covariance matrix $\mathbf{R_{h\hat{h}}} = \sigma_h^2 \rho \mathbf{I}_{M_t M_r}$. According to [51], the mean and covariance matrix of $\mathbf{h}$ conditioned on $\hat{\mathbf{h}}$ are described by

$$\mathbf{m_{h|\hat{h}}} = \rho \hat{\mathbf{h}} \tag{3.22}$$

$$\mathbf{R_{hh|\hat{h}}} = \sigma_h^2 (1 - |\rho|^2) \mathbf{I}_{M_t M_r} = \alpha \mathbf{I}_{M_t M_r} \tag{3.23}$$

where

$$\alpha = \sigma_h^2 (1 - |\rho|^2) \tag{3.24}$$

represents the conditional variance of the channel coefficients. Let $\mathbf{\Omega}_i$ denote the ith block of size $M_t \times M_t$ on the diagonal of $\mathbf{m}_{\mathbf{h}|\hat{\mathbf{h}}}^{\mathcal{H}} \mathbf{m}_{\mathbf{h}|\hat{\mathbf{h}}}$. By using the eigenvalue decomposition (EVD) method, we have the descriptions as follows,

$$\mathbf{Z} = \mathbf{W}\mathbf{W}^{\mathcal{H}} = \mathbf{V}\mathbf{\Lambda}\mathbf{V}^{\mathcal{H}} \tag{3.25}$$

$$\frac{1}{\alpha}\sum_{i=1}^{M_r} \mathbf{\Omega}_i = \hat{\mathbf{V}}\hat{\mathbf{\Lambda}}\hat{\mathbf{V}}^{\mathcal{H}} \tag{3.26}$$

where $\mathbf{\Lambda}$ and $\hat{\mathbf{\Lambda}}$ are the diagonal matrices with the corresponding eigenvalues $\{\lambda_i\}_{i=1}^{M_t}$ and $\{\hat{\lambda}_i\}_{i=1}^{M_t}$ on the diagonal and they are assumed to be sorted in ascending order. Here, $\mathbf{V}$ and $\hat{\mathbf{V}}$ are the matrices of eigenvectors which are assumed to be unitary.

The performance criterion in (3.21) is further simplified by substituting (3.25) and (3.26) into the equation and neglecting the parameter independent terms as

$$\begin{aligned}
\ell(\{\lambda_i\}_{i=1}^{M_t}, \mathbf{V}|\hat{\mathbf{h}}) &= \frac{1}{\alpha}\mathbf{m}_{\mathbf{h}|\hat{\mathbf{h}}} \left[\mathbf{I}_{M_r} \otimes (\alpha\eta\mathbf{Z}) + \mathbf{I}_{M_t M_r}\right]^{-1} \mathbf{m}_{\mathbf{h}|\hat{\mathbf{h}}}^{\mathcal{H}} \\
&\quad - \log\det\left[\mathbf{I}_{M_r} \otimes (\alpha\eta\mathbf{Z}) + \mathbf{I}_{M_t M_r}\right] \\
&= \frac{1}{\alpha} tr\left\{\left[\mathbf{I}_{M_r} \otimes (\alpha\eta\mathbf{Z} + \mathbf{I}_{M_t})\right]^{-1} \mathbf{m}_{\mathbf{h}|\hat{\mathbf{h}}}^{\mathcal{H}} \mathbf{m}_{\mathbf{h}|\hat{\mathbf{h}}}\right\} \\
&\quad - \log\det\left[\mathbf{I}_{M_r} \otimes (\alpha\eta\mathbf{Z} + \mathbf{I}_{M_t})\right] \\
&= tr\left[(\alpha\eta\mathbf{\Lambda} + \mathbf{I}_{M_t})^{-1}\mathbf{V}^{\mathcal{H}}\hat{\mathbf{V}}\hat{\mathbf{\Lambda}}\hat{\mathbf{V}}^{\mathcal{H}}\mathbf{V}\right] - M_r \log\det\left(\alpha\eta\mathbf{\Lambda} + \mathbf{I}_{M_t}\right)
\end{aligned} \tag{3.27}$$

subject to the following constraints

$$\begin{cases} \sum_{i=1}^{M_t} \lambda_i = 1, \\ \lambda_i \geq 0, & i = 1, \ldots, M_t \\ \lambda_1 \leq \lambda_2 \leq \cdots \leq \lambda_{M_t}. \end{cases} \tag{3.28}$$

According to [5], the optimum $\mathbf{V}$ can be chosen as $\mathbf{V} = \hat{\mathbf{V}}$, and the optimum $\mathbf{\Lambda}$ can be obtained by means of the Karush-Kuhn-Tucker (KKT) conditions [5].

The detailed procedure of determining the optimum eigenvalues $\{\lambda_i\}_{i=1}^{M_t}$ for general cases is described in [45].

Since our attention is focused on MISO systems in this thesis, we only show the procedure of calculating the optimum eigenvalues for the special case. For a MISO system in the simplified fading scenario, (3.26) can be rewritten as

$$\frac{1}{\alpha}\sum_{i=1}^{M_r}\mathbf{\Omega}_i = \frac{1}{\alpha}\mathbf{\Omega}_1 = \frac{|\rho|^2}{\alpha}\hat{\mathbf{h}}^{\mathcal{H}}\hat{\mathbf{h}} = \hat{\mathbf{V}}\hat{\mathbf{\Lambda}}\hat{\mathbf{V}}^{\mathcal{H}} \tag{3.29}$$

It can be found that the eigenvalues $\{\hat{\lambda}_i\}_{i=1}^{M_t}$ are given by

$$\begin{cases} \hat{\lambda}_i = 0, & i = 1, \ldots, M_t - 1; \\ \hat{\lambda}_i = \dfrac{|\rho|^2}{\alpha}\|\hat{\mathbf{h}}\|^2, & i = M_t, \end{cases} \tag{3.30}$$

where $\|\cdot\|$ denotes the vector norm. The eigenvector located at the last column of $\hat{\mathbf{V}}$ corresponds to the largest eigenvalue and is given by

$$\hat{\mathbf{v}}_{M_t} = \frac{\hat{\mathbf{h}}^{\mathcal{H}}}{\|\hat{\mathbf{h}}\|} \tag{3.31}$$

where $\|\hat{\mathbf{h}}\|$ is used to normalize the total transmission power to E_s, i.e.,

$$\|\hat{\mathbf{h}}\| = \sqrt{|\hat{h}_1|^2 + |\hat{h}_2|^2 + \cdots + |\hat{h}_{M_t}|^2}, \tag{3.32}$$

and the remaining eigenvectors are orthogonal to $\hat{\mathbf{v}}_{M_t}$. Then the optimum eigenvalues $\{\lambda_i\}_{i=1}^{M_t}$ are given by

$$\begin{aligned} \lambda_i &= \max\left\{0, \frac{\alpha\eta + \sqrt{\alpha^2\eta^2 + 4\alpha\eta\mu\hat{\lambda}_i}}{2\alpha\eta\mu} - \frac{1}{\alpha\eta}\right\} \\ &= \max\left\{0, \frac{1}{\mu} - \frac{1}{\alpha\eta}\right\}, \qquad i = 1, \ldots, M_t - 1 \end{aligned} \tag{3.33}$$

and

$$\lambda_{M_t} = 1 - \lambda_1 - \ldots - \lambda_{M_t - 1} \tag{3.34}$$

Here, μ is the Lagrange multiplier of the performance criterion in (3.27) subject to the power constraint in (3.28), and it is given by

$$\mu = \frac{\eta\left(\kappa(2M_t-1)+|\rho|^2\|\hat{\mathbf{h}}\|^2+\sqrt{2\kappa(2M_t-1)|\rho|^2\|\hat{\mathbf{h}}\|^2+|\rho|^4\|\hat{\mathbf{h}}\|^4+\kappa^2}\right)}{2(M_t+\alpha\eta)^2} \tag{3.35}$$

where $\kappa = \alpha(M_t + \alpha\eta)$. Therefore, the optimal beamforming matrix is obtained by

$$\mathbf{W}_{opt} = \hat{\mathbf{V}}\mathbf{\Lambda}^{1/2} \tag{3.36}$$

where $(\cdot)^{1/2}$ denotes a matrix square root with Hermitian symmetry, i.e., $\mathbf{\Lambda}^{1/2}$ can be computed simply by taking the square root of each element of the diagonal matrix $\mathbf{\Lambda}$. It is clear that $\mathbf{W}_{opt}$ is a square matrix with dimension $M_t \times M_t$.

3.3 Review of Designing Unstructured STBC Based on Quantized CSI

In Section 3.2, a rudimentary introduction to the closed-loop combined system of beamforming and OSTBC is provided. The feedback CSI at the transmitter is assumed to be noisy and outdated due to the feedback delay but unquantized. It is employed to design the beamforming matrix to adapt the predetermined OSTBC to the channel characteristics. In this section, we introduce a general strategy for incorporating imperfect quantized CSI at the transmitter into the design of unstructured STBC as described in [48]. Although the dedicated feedback link is assumed to have an ideal feedback channel, which does not lead to any bit errors, both quantization errors as well as feedback delay are assumed to plague the CSI

at the transmitter. The code-construction process is based on the BLER union bound technique conditioned on the CSI at the transmitter. The codeword pair criterion derived in Section 3.2 plays an important role in the design process of this section. Due to no structure is imposed on the codewords, the degrees of freedom in the code-construction process is maximized.

3.3.1 System Model

Fig. 3.2 shows a closed-loop MIMO wireless communication system making use of unstructured STBC based on the quantized feedback CSI at the transmitter. The feedback integer p represents the quantized CSI at the transmitter, which is

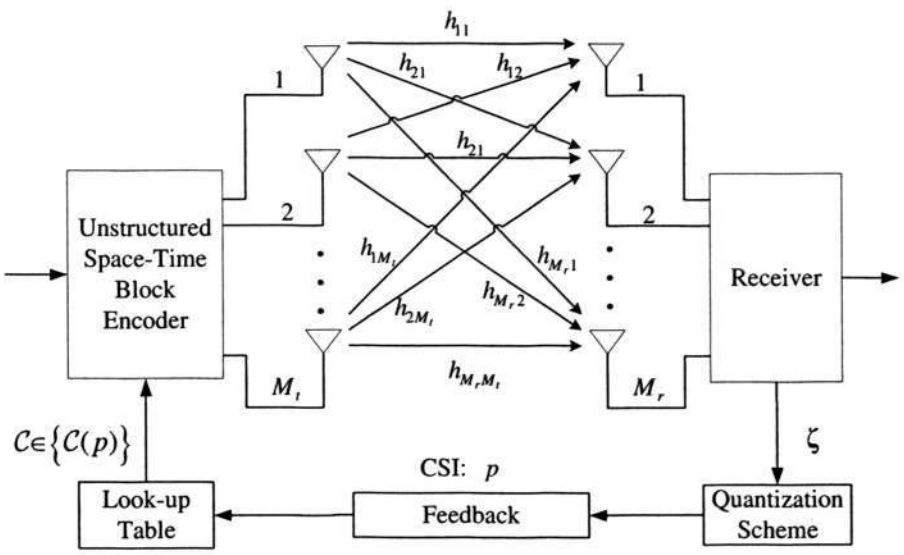

Figure 3.2: Block diagram of the system model

utilized to determine the unstructured STBC $\mathcal{C}$ currently from a set of codes $\{\mathcal{C}(p)\}$ from the look-up table. Each code is designed so as to increase the performance by using a design criterion based on the BLER union bound conditioned on the

CSI at the transmitter.

Consistent with the description in Section 3.2, the information carrying signals are transmitted over a wireless MIMO fading channel, denoted by a complex matrix $\mathbf{H}$ with dimension $M_r \times M_t$. Alternatively, the MIMO channel is represented by a $1 \times M_t M_r$ row vector $\mathbf{h} = \text{rvec}(\mathbf{H})$. The channels are also assumed to be statistically identical, space-independent, time-correlated and satisfy the quasi-static flat fading.

At the receiver, the channel estimate is assumed to be obtained perfectly and the ML decoding algorithm is used to recover the transmitted codeword. The received signals $\mathbf{Y}$ are the weighted superposition of the transmitted signals corrupted by additive noise, which is expressed by

$$\mathbf{Y} = \mathbf{HC} + \mathbf{E} \tag{3.37}$$

where the noise vector $\mathbf{E}$ is assumed to be a temporally and spatially white complex Gaussian random variable with zero-mean and variance $\sigma^2 = N_0/2$ per dimension. The unstructured STBC is the transmitted matrix denoted by $\mathbf{C}$ with dimension $M_t \times L$, where L is the length of the transmitted codewords. Each codeword of the unstructured STBC is taken from the currently used code $\mathcal{C} = \{\mathbf{C}_k\}_{k=1}^{K}$, where K represents the number of codewords in each code $\mathcal{C}$. For the signal constellation consisting of $M = 2^m$ points,

$$K = M^N = 2^{mN} \tag{3.38}$$

where N is the number of modulated symbols in the codeword. According to the definition in (2.22), the code rate is $R = N/L$ and the spectral efficiency of the

unstructured STBC is given by

$$\eta_{se} = \frac{mN}{L} = \frac{\log_2 K}{L} \text{ bits/s/Hz.} \tag{3.39}$$

The choice of L and K allows an appropriate tradeoff between data rate and time redundancy.

3.3.2 Feedback Model and Quantization Scheme

Let a $1 \times M_t M_r$ dimensional row vector $\boldsymbol{\zeta}$, with elements $\{\zeta_i\}$, be used to represent the *initial channel information* at the receiver, which is assumed to be the outdated version of the current true channel $\mathbf{h}$ due to the feedback delay in conjunction with the common scenario of a time-varying channel. As explained in Section 3.2, the initial channel information $\boldsymbol{\zeta}$ is correlated, to an arbitrary degree, with the true channel $\mathbf{h}$. Moreover, it is reasonable to assume that they are jointly complex Gaussian distributed, which can be completely characterized by their mean vector $\mathbf{m}_{\boldsymbol{\zeta}}$ and $\mathbf{m}_{\mathbf{h}}$, covariance matrices $\mathbf{R}_{\boldsymbol{\zeta}\boldsymbol{\zeta}}$ and $\mathbf{R}_{\mathbf{hh}}$, and cross-covariance matrix $\mathbf{R}_{\mathbf{h}\boldsymbol{\zeta}}$. According to [48, 51], the conditional mean and covariance matrix of $\mathbf{h}$ based on $\boldsymbol{\zeta}$ are given by

$$\mathbf{m}_{\mathbf{h}|\boldsymbol{\zeta}} = \mathbf{m}_{\mathbf{h}} + (\boldsymbol{\zeta} - \mathbf{m}_{\boldsymbol{\zeta}})\mathbf{R}_{\boldsymbol{\zeta}\boldsymbol{\zeta}}^{-1}\mathbf{R}_{\mathbf{h}\boldsymbol{\zeta}} \tag{3.40}$$

$$\mathbf{R}_{\mathbf{hh}|\boldsymbol{\zeta}} = \mathbf{R}_{\mathbf{hh}} - \mathbf{R}_{\mathbf{h}\boldsymbol{\zeta}}^{\mathcal{H}}\mathbf{R}_{\boldsymbol{\zeta}\boldsymbol{\zeta}}^{-1}\mathbf{R}_{\mathbf{h}\boldsymbol{\zeta}} \tag{3.41}$$

respectively. To indicate the quality of the initial channel information, the normalized correlation coefficient ρ is introduced to describe the correlation between $\mathbf{h}$ and $\boldsymbol{\zeta}$, which is expressed by [48]

$$|\rho| = \sqrt{\frac{tr\left(\mathbf{R}_{\mathbf{h}\boldsymbol{\zeta}}^{\mathcal{H}}\mathbf{R}_{\boldsymbol{\zeta}\boldsymbol{\zeta}}^{-1}\mathbf{R}_{\mathbf{h}\boldsymbol{\zeta}}\mathbf{R}_{\mathbf{hh}}^{-1}\right)}{M_t M_r}} \tag{3.42}$$

As ρ increases, the quality of $\boldsymbol{\zeta}$ improves, and vice versa. In general, $0 \leq |\rho| \leq 1$, where $|\rho| = 0$ corresponds to no correlation, while $|\rho| = 1$ corresponds to full correlation.

As illustrated in Fig. 3.2, the initial channel information is quantized into a b-bit integer $p = f_n(\boldsymbol{\zeta}) \in \{0, 1, \ldots, 2^b - 1\}$, which is transported to the transmitter via an ideal dedicated feedback channel. Consequently, the integer p represents the quantized CSI available at the transmitter. It is used to choose the unstructured STBC $\mathcal{C}$ from a set of look-up table $\mathcal{C}(p)$ with 2^b different codes. In [48], the *uniform phase-quantization* scheme is implemented for the quantization function $f_n(\boldsymbol{\zeta})$. It is similar to the so called partial-phase-combining scheme in [29] and also closely related to the feedback scheme in the closed-loop mode of the WCDMA system [1].

The uniform phase-quantization scheme is named from the b-bit uniform scalar quantization of the phases of ζ_i/ζ_1, $i = 2, \ldots, M_t M_r$. The quantizer $f_n(\boldsymbol{\zeta})$ divides the space of the initial channel information vector $\boldsymbol{\zeta}$ into 2^b encoder regions $\{O_p\}_{p=0}^{2^b-1}$, based on the mapping $\boldsymbol{\zeta} \in O_p \Rightarrow f_n(\boldsymbol{\zeta}) = p$. The codebook vectors $\{\hat{\boldsymbol{\zeta}}(p)\}_{p=0}^{2^b-1}$ is given by

$$\hat{\boldsymbol{\zeta}}(p) = \begin{bmatrix} 1 & e^{j\phi_{\tau_0(p)}} & \cdots & e^{j\phi_{\tau_{M_t M_r - 2}(p)}} \end{bmatrix} \tag{3.43}$$

where $\phi_{\tau_\nu(p)} = 2\pi\tau_\nu(p)/2^{\bar{b}}, \nu = 0, \ldots, M_t M_r - 2$, $\bar{b} = b/(M_t M_r - 1)$ represents the number of bits per complex-valued dimension and $\tau_\nu(p) \in \{0, 1, \ldots, 2^{\bar{b}} - 1\}$ is implicitly defined via the relation of $p = \sum_{\nu=0}^{M_t M_r - 2} \tau_\nu(p) 2^{\bar{b}\nu}$. Thus, the specific

quantization function is defined by

$$p = f_n(\boldsymbol{\zeta}) = \arg \min_{p \in \{0,1,\ldots,2^b-1\}} \left\| \frac{\boldsymbol{\zeta}}{\zeta_1} - \hat{\boldsymbol{\zeta}}(p) \right\|^2 \tag{3.44}$$

For the purpose of illustration, we describe the associated quantization process in the case of $\bar{b} = 2$, i.e., 2π is partitioned into $2^{\bar{b}} = 4$ regions and each region is $\pi/2$, as shown in Fig. 3.3. Then, we have $\tau_\nu(p) \in \{0, 1, 2, 3\}$ and $\phi_{\tau_\nu(p)} = \frac{\pi}{2}\tau_\nu(p) \in$

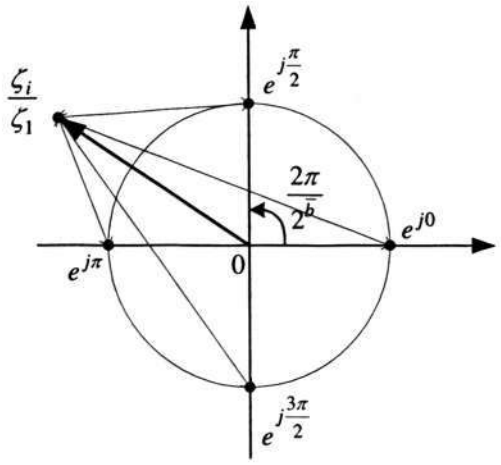

Figure 3.3: Diagram of uniform phase-quantization

$\left\{0, \frac{\pi}{2}, \pi, \frac{3\pi}{2}\right\}$. From (3.43), it is known that the element of the pth codebook vector is given by $\hat{\zeta}_i(p) = e^{j\phi_{\tau_\nu(p)}} \in \left\{e^{j0}, e^{j\pi/2}, e^{j\pi}, e^{j3\pi/2}\right\}$, $i = 2, \ldots, M_t M_r$. It means that there are four quantization points $e^{j0}, e^{j\pi/2}, e^{j\pi}, e^{j3\pi/2}$. As shown in Fig. 3.3, $\tau_\nu(p)$ is obtained by normalizing ζ_i/ζ_1 to the closest quantization point, and expressed by

$$\tau_\nu(p) = \arg \min_{\tau_\nu(p) \in \{0,1,2,3\}} \left| \frac{\zeta_i}{\zeta_1} - \hat{\zeta}_i(p) \right|^2, \quad \nu = i - 2 \tag{3.45}$$

In the end, p is obtained through $p = \sum_{\nu=0}^{M_t M_r - 2} \tau_\nu(p) 2^{\bar{b}\nu}$.

Besides this scalar quantization, the vector quantization also can be used, such as in [44, 46, 61, 69]. However, it goes beyond the discussion range of our thesis.

3.3.3 Performance Criterion and Optimization for Design of CSI Dependent Unstructured STBC

To systematically take the quantized and outdated CSI at the transmitter into account in the code-construction process, a performance criterion based on the BLER union bound technique is derived and shown in [48]. We start from exploiting the BLER union bound conditioned on the CSI at the transmitter p and the true channel $\mathbf{h}$. Under the assumption that the codewords are transmitted with equal likelihood, the conditional BLER union bound is expressed by

$$\begin{aligned} P_{bl}(\mathbf{C}' \neq \mathbf{C}|\, p, \mathbf{h}) &\leq \frac{1}{K}\sum_{k\neq l} P(\mathbf{C}_k^{(p)} \rightarrow \mathbf{C}_l^{(p)} \mid p, \mathbf{h}) \\ &= \frac{1}{K}\sum_{k\neq l} Q\left(\sqrt{\frac{\|\mathbf{H}(\mathbf{C}_k^{(p)} - \mathbf{C}_l^{(p)}\|_{\mathrm{F}}^2}{2N_0}}\right) \\ &\leq \frac{1}{K}\sum_{k<l} \exp\left(-\frac{\|\mathbf{H}(\mathbf{C}_k^{(p)} - \mathbf{C}_l^{(p)}\|_{\mathrm{F}}^2}{4N_0}\right) \end{aligned} \tag{3.46}$$

An upper bound P_{upb} on the BLER is obtained by averaging over p and $\mathbf{h}$ in (3.46) to arrive at

$$\begin{aligned} P_{bl}(\mathbf{C}' \neq \mathbf{C}) &\leq \frac{1}{K}\sum_{k<l} E_{p,\mathbf{h}}\left[\exp\left(-\frac{\|\mathbf{H}(\mathbf{C}_k^{(p)} - \mathbf{C}_l^{(p)}\|_{\mathrm{F}}^2}{4N_0}\right)\right] \\ &= \frac{1}{K}\sum_{k<l} E_{p,\boldsymbol{\zeta}}\left[V(\mathbf{C}_k^{(p)} \rightarrow \mathbf{C}_l^{(p)} \mid \boldsymbol{\zeta})\right] \\ &= \frac{1}{K}\sum_{p=0}^{2^b-1} P_p \sum_{k<l} E_{\boldsymbol{\zeta}}\left[V(\mathbf{C}_k^{(p)} \rightarrow \mathbf{C}_l^{(p)} \mid \boldsymbol{\zeta})|p\right] \\ &= P_{upb} \end{aligned} \tag{3.47}$$

where P_p is the probability that the quantization function outputs an integer value p and the notation $E_{p,\mathbf{h}}[\cdot]$ is used to emphasize that the subscripted parameters are

the only random quantities within the brackets. Following the derivation in [45], the so-called codeword pair criterion is given by

$$\begin{aligned} V(\mathbf{C}_k^{(p)} \rightarrow \mathbf{C}_l^{(p)} \mid \boldsymbol{\zeta}) &= E\left[\exp\left(-\|\mathbf{H}(\mathbf{C}_k^{(p)} - \mathbf{C}_l^{(p)}\|_{\mathrm{F}}^2/(4N_0)\right) \mid p, \boldsymbol{\zeta}\right] \\ &= \frac{\exp\left[\mathbf{m}_{\mathbf{h}|\boldsymbol{\zeta}}\mathbf{R}_{\mathbf{hh}|\boldsymbol{\zeta}}^{-1}\left((\boldsymbol{\Psi}_{kl}^{(p)})^{-1} - \mathbf{R}_{\mathbf{hh}|\boldsymbol{\zeta}}\right)\mathbf{R}_{\mathbf{hh}|\boldsymbol{\zeta}}^{-1}\mathbf{m}_{\mathbf{h}|\boldsymbol{\zeta}}^{\mathcal{H}}\right]}{\det(\mathbf{R}_{\mathbf{hh}|\boldsymbol{\zeta}})\det(\boldsymbol{\Psi}_{kl}^{(p)})} \end{aligned} \tag{3.48}$$

where

$$\boldsymbol{\Psi}_{kl}^{(p)} = \mathbf{I}_{M_r} \otimes \frac{(\mathbf{C}_k^{(p)} - \mathbf{C}_l^{(p)})(\mathbf{C}_k^{(p)} - \mathbf{C}_l^{(p)})^{\mathcal{H}}}{4N_0} + \mathbf{R}_{\mathbf{hh}|\boldsymbol{\zeta}}^{-1} \tag{3.49}$$

Although the optimal set of codewords can be constructed by minimizing P_{upb} with respect to the codewords, while subject to the output power constraint, as suggested in [46], this approach is very challenging from a computational point of view.

By introducing

$$\begin{aligned} \ell(\mathbf{C}_k^{(p)} \rightarrow \mathbf{C}_l^{(p)} \mid \boldsymbol{\zeta}) = \mathbf{m}_{\mathbf{h}|\boldsymbol{\zeta}}\mathbf{R}_{\mathbf{hh}|\boldsymbol{\zeta}}^{-1}(\boldsymbol{\Psi}_{kl}^{(p)})^{-1}\mathbf{R}_{\mathbf{hh}|\boldsymbol{\zeta}}^{-1}\mathbf{m}_{\mathbf{h}|\boldsymbol{\zeta}}^{\mathcal{H}} - \mathbf{m}_{\mathbf{h}|\boldsymbol{\zeta}}\mathbf{R}_{\mathbf{hh}|\boldsymbol{\zeta}}^{-1}\mathbf{m}_{\mathbf{h}|\boldsymbol{\zeta}}^{\mathcal{H}} \\ - \log\det(\boldsymbol{\Psi}_{kl}^{(p)}), \end{aligned} \tag{3.50}$$

and using the convexity of e^x and Jensen's inequality [24] to address the computational complexity of the upper bound P_{upb} in (3.47), we have

$$\begin{aligned} P_{upb} &\geq \frac{1}{K\det(\mathbf{R}_{\mathbf{hh}|\boldsymbol{\zeta}})}\sum_{p=0}^{2^b-1} P_p \sum_{k<l} \exp\left\{E\left[\ell(\mathbf{C}_k^{(p)} \rightarrow \mathbf{C}_l^{(p)} \mid \boldsymbol{\zeta}) \mid p\right]\right\} \\ &= P_{LBupb} \end{aligned} \tag{3.51}$$

with equality if $\ell(\mathbf{C}_k^{(p)} \rightarrow \mathbf{C}_l^{(p)} \mid \boldsymbol{\zeta})$ is a constant for a fixed p. Here, P_{LBupb} is used to denote the right hand side of the inequality. With (3.41), the exponent of (3.51) can be rewritten as

$$\begin{aligned} E\left[\ell(\mathbf{C}_k^{(p)} \rightarrow \mathbf{C}_l^{(p)} \mid \boldsymbol{\zeta}) \mid p\right] = tr\left((\boldsymbol{\Psi}_{kl}^{(p)})^{-1}\mathbf{R}_{\mathbf{hh}|\boldsymbol{\zeta}}^{-1}E\left[\mathbf{m}_{\mathbf{h}|\boldsymbol{\zeta}}^{\mathcal{H}}\mathbf{m}_{\mathbf{h}|\boldsymbol{\zeta}} \mid p\right]\mathbf{R}_{\mathbf{hh}|\boldsymbol{\zeta}}^{-1}\right) \\ - tr\left(\mathbf{R}_{\mathbf{hh}|\boldsymbol{\zeta}}^{-1}E\left[\mathbf{m}_{\mathbf{h}|\boldsymbol{\zeta}}^{\mathcal{H}}\mathbf{m}_{\mathbf{h}|\boldsymbol{\zeta}} \mid p\right]\right) - \log\det(\boldsymbol{\Psi}_{kl}^{(p)}) \end{aligned} \tag{3.52}$$

From (3.40), it is known that $E\left[\mathbf{m}_{\mathbf{h}|\boldsymbol{\zeta}}^{\mathcal{H}}\mathbf{m}_{\mathbf{h}|\boldsymbol{\zeta}} \mid p\right]$ can be expressed in terms of $E[\boldsymbol{\zeta} \mid p]$ and $E\left[\boldsymbol{\zeta}^{\mathcal{H}}\boldsymbol{\zeta} \mid p\right]$, which can be obtained from the corresponding sample estimates by using a Monte Carlo simulation of the quantization function in the feedback link. Since they do not depend on the codewords, they can be evaluated prior to the code search, so as to reduce the computational complexity. As stated in [48], in certain cases that the quantization is dense, the noise variance σ^2 per dimension at the receiver is low, and/or the correlation between $\boldsymbol{\zeta}$ and $\mathbf{h}$ is small, i.e., the variance of $\ell(\mathbf{C}_k^{(p)} \rightarrow \mathbf{C}_l^{(p)} \mid \boldsymbol{\zeta})$ is small, P_{LBupb} approximates P_{upb} well. Therefore, the goal of an alternative optimization approach is to minimize the lower bound P_{LBupb}. Neglecting the parameter independent terms in (3.52) and taking the exponent, the modified codeword pair criterion is reformulated as

$$\widetilde{V}(\mathbf{C}_k^{(p)} \rightarrow \mathbf{C}_l^{(p)} \mid \boldsymbol{\zeta}) = \frac{\exp\left\{tr\left((\boldsymbol{\Psi}_{kl}^{(p)})^{-1}\mathbf{R}_{\mathbf{hh}|\boldsymbol{\zeta}}^{-1}E\left[\mathbf{m}_{\mathbf{h}|\boldsymbol{\zeta}}^{\mathcal{H}}\mathbf{m}_{\mathbf{h}|\boldsymbol{\zeta}} \mid p\right]\mathbf{R}_{\mathbf{hh}|\boldsymbol{\zeta}}^{-1}\right)\right\}}{\det(\boldsymbol{\Psi}_{kl}^{(p)})} \tag{3.53}$$

From (3.51), the final performance criterion adopted is defined by

$$W(\mathcal{C} \mid p) = \sum_{k<l} \widetilde{V}(\mathbf{C}_k^{(p)} \rightarrow \mathbf{C}_l^{(p)} \mid \boldsymbol{\zeta}) \tag{3.54}$$

It is known from [48] that both the uniform phase-quantization method described in this section and the feedback method in the closed-loop mode of the WCDMA system [1] exhibit certain symmetries, i.e., the quantized regions are rotated copies of each other. In view of the fact that a unitary matrix may correspond to a rotation, the feedback scenario is regarded to be symmetric if $E\left[\mathbf{m}_{\mathbf{h}|\boldsymbol{\zeta}}^{\mathcal{H}}\mathbf{m}_{\mathbf{h}|\boldsymbol{\zeta}} \mid p\right]$ and $\mathbf{R}_{\mathbf{hh}|\boldsymbol{\zeta}}$ have the following forms,

$$E\left[\mathbf{m}_{\mathbf{h}|\boldsymbol{\zeta}}^{\mathcal{H}}\mathbf{m}_{\mathbf{h}|\boldsymbol{\zeta}} \mid p\right] = \widetilde{\mathbf{D}} \otimes \boldsymbol{\Theta}_p \mathbf{U} \boldsymbol{\Theta}_p^{\mathcal{H}} \tag{3.55}$$

$$\mathbf{R}_{\mathbf{hh}|\boldsymbol{\zeta}} = \mathbf{D} \otimes \mathbf{I}_{M_t} \tag{3.56}$$

where $\boldsymbol{\Theta}_p$ is a $M_t \times M_t$ dimensional unitary rotation matrix depending on p, $\mathbf{U}$ is a constant matrix with dimension $M_t \times M_t$, and

$$\tilde{\mathbf{D}} = \text{diag}(\tilde{d}_1, \tilde{d}_2, \ldots, \tilde{d}_{M_r}) \tag{3.57}$$

$$\mathbf{D} = \text{diag}(d_1, d_2, \ldots, d_{M_r}) \tag{3.58}$$

where diag$(\cdot)$ denotes the diagonal matrix generating operator. The values of the elements $\tilde{d}_1, \tilde{d}_2, \ldots, \tilde{d}_{M_r}$ and $d_1, d_2, \ldots, d_{M_r}$ are obtained from (3.55) and (3.56), respectively. For example, in a simplified fading scenario,

$$\mathbf{R}_{\mathbf{hh}|\boldsymbol{\zeta}} = \alpha \mathbf{I}_{M_t M_r} = \alpha \mathbf{I}_{M_r} \otimes \mathbf{I}_{M_t}. \tag{3.59}$$

Thus, $\mathbf{D} = \alpha \mathbf{I}_{M_r}$ and $d_1 = d_2 = \cdots = d_{M_r} = \alpha$.

By introducing $\tilde{\mathcal{C}} = \boldsymbol{\Theta}_p^{\mathcal{H}} \mathcal{C}$ and substituting (3.55) and (3.56) into (3.54), we can get

$$W(\tilde{\mathcal{C}} \mid p) = \sum_{k<l} \frac{\exp\left\{tr\left[\tilde{\boldsymbol{\Psi}}_{kl}^{-1}(\tilde{\mathbf{D}}\mathbf{D}^{-2} \otimes \mathbf{U})\right]\right\}}{\det(\tilde{\boldsymbol{\Psi}}_{kl})} \tag{3.60}$$

where

$$\tilde{\boldsymbol{\Psi}}_{kl} = \mathbf{I}_{M_r} \otimes \frac{(\tilde{\mathbf{C}}_k - \tilde{\mathbf{C}}_l)(\tilde{\mathbf{C}}_k - \tilde{\mathbf{C}}_l)^{\mathcal{H}}}{4N_0} + \mathbf{D}^{-1} \otimes \mathbf{I}_{M_t} \tag{3.61}$$

It is obvious that (3.60) is independent of p. Therefore, we can design the specific unstructured STBC $\tilde{\mathcal{C}} = \{\tilde{\mathbf{C}}_k\}_{k=1}^K$ by minimizing the re-parameterized performance criterion (3.60) while subjecting it to the corresponding transformed power constraint in (3.14) to arrive at

$$\tilde{\mathcal{C}} = \arg \min_{\|\tilde{\mathcal{C}}\|_{\mathrm{F}}^2 = NKE_s} W(\tilde{\mathcal{C}} \mid p) \tag{3.62}$$

The unstructured STBC $\mathcal{C}(p)$ corresponding to the quantized CSI of p can be constructed through the linear mapping $\mathbf{C}_k^{(p)} = \mathbf{\Theta}_p \tilde{\mathbf{C}}_k$. The whole set of look-up table $\{\mathcal{C}(p)\}$ is formed by collecting the 2^b unstructured STBC corresponding to the different quantized CSI of p. Hence, the design process is substantially expedited and the memory required to store the code is drastically reduced.

The optimization problem in (3.62) is non-convex and generally difficult to solve analytically unlike the one described in Section 3.2. Consequently, numerical optimization techniques are required to implement the design procedure. In [48], a simple gradient search algorithm is used, but the resulting solutions can only be expected to be locally optimal. This algorithm must be remedied by repeating the gradient search several times using different initial guesses. Thus, the codeword search by exploiting the simple gradient search algorithm requires substantial computing power. Therefore, the decoding complexity of the unstructured STBC due to the exhaustive search over all codewords prevents its application for high data rate scenarios.

When certain structure is imposed on the code, the number of parameters needed to be optimized is drastically reduced. However, this typically comes at the price of lower performance based on the same performance criterion, since structure generally limits the degrees of freedom in the design.

3.4 Summary

In this chapter, two important closed-loop wireless communication systems making use of STBC based on the CSI at the transmitter are reviewed. In the combined

system of beamforming and OSTBC, the predetermined OSTBC is adapted to the channel characteristics by using the beamforming technique according to the noisy and outdated CSI at the transmitter. The beamforming matrix is optimized based on the codeword pair criterion. A semi-closed-form optimization solution is derived for the simplified scenario. While in the design of unstructured STBC dependent on the CSI at the transmitter, STBC is not predetermined and unstructured with the maximum degrees of design freedom. The CSI at the transmitter is plagued by the quantization errors as well as the feedback delay. The code-construction process is based on the BLER union bound. The optimization problem can be solved by using an exhaustive search method with significant computational complexity.

Chapter 4

Combining Beamforming and Alamouti's STBC

4.1 Introduction

In Chapter 3, we have described the attractive combined system of beamforming and OSTBC proposed by Jongren *et al.* in [45], that takes into account the degree of the feedback CSI. The predetermined OSTBC is adapted to the available CSI at the transmitter by means of a linear transformation. The CSI is noisy and outdated due to the feedback delay, which is modelled by using a purely statistical approach, namely the channel mean feedback [93, 97].

Jongren *et al.* focus on examining the performance of the combined system based on the square beamforming matrix, (i.e., the dimension of the corresponding OSTBC is the same as the number of transmitting antennas), although it is mentioned that the combined system can be extended to handle the case of a non-square beamforming matrix in [45]. By using the square beamforming matrix, a new OSTBC of different dimension is required every time the number of transmitting antennas is changed. Also for complex constellation, OSTBC with full

code rate does not exist for arbitrary dimensions as discussed in Chapter 2. In addition, the computational and decoding complexities of the combined system increase significantly with the increase of the code dimension. It has been mentioned in Chapter 1 that these issues have motivated us to develop a simple system that may achieve a tradeoff between complexity and performance.

It is well-known that Alamouti's STBC is the unique and simplest OSTBC to provide full transmitting diversity and full code rate simultaneously for complex constellation, but only designed for two transmitting antennas. In general, increasing the number of transmitting antennas provides better system array gain or diversity gain. It is attractive, therefore, to extend the application of Alamouti's STBC for two transmitting antennas to more than two, using the idea of Jongren's combined system of beamforming and OSTBC. The new system will be significantly simpler than that discussed in [45] as the new combined system uses only the readily available Alamouti's STBC, while the performance will be better than the Alamouti scheme as the number of transmitting antennas increases. In addition, the beamforming matrix designed for the predetermined Alamouti's STBC becomes non-square in the case of more than two transmitting antennas. Therefore, the new combined system can retain full code rate as long as the number of time instants during the transmission of the codewords is equal to the number of symbols in the transmitted codewords.

Before continuing the discussion on the proposed combined beamforming and Alamouti's STBC, it is necessary to mention that in this chapter, as well as in the forthcoming one, we will concentrate our attention mainly on the MISO systems

in the simplified fading scenario.

The works on the BER performance of Jongren's combined system in [45] are carried out employing simulations, leaving the analytical performance evaluation of this type of closed-loop combined system as an open problem. The development of effective tools for the calculation of error probabilities is important for the application and design of this type of closed-loop combined systems, as the performance results can be obtained faster from these calculations than from the tedious simulations. Hence, in this chapter, we also theoretically analyze the new combined system in two scenarios involving perfect feedback CSI and imperfect feedback CSI, respectively, utilizing various methods. In the case of perfect CSI at the transmitter, we present two methods to calculate the error probabilities. The first one is the moment-generating function (MGF) approach and Gauss-Chebyshev quadrature rule [86], through which we derive the exact PEP and illustrate the system diversity property. Furthermore, we provide a tight union bound on the BER based on the derived exact PEP. The second one is the conditional probability method, which is more efficient to derive the closed-form expressions for the upper bound of PEP and the BER. In the case of imperfect CSI at the transmitter, the closed-form upper bound of PEP and the exact BER expressions involving only two double integrals are also derived by using the conditional probability method. With the exact BER expressions, the new combined system BER performance can be obtained much faster than the simulation, especially at high SNR. The upper bound on the PEP helps further analysis on the system diversity gain, coding gain and array gain.

4.2 System Model

Fig. 4.1 shows a combined system of beamforming and Alamouti's STBC, comprising M_t transmitting antennas and a single receiving antenna (MISO system). The

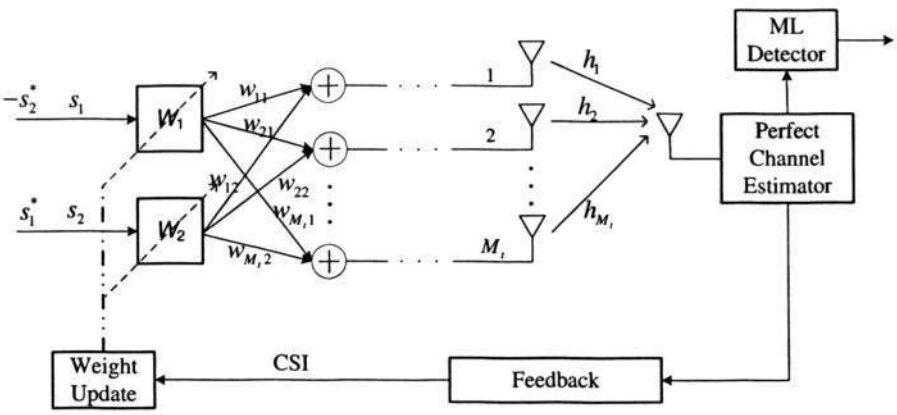

Figure 4.1: Block diagram of the system model

CSI is fed back from the receiver to the transmitter through a dedicated feedback link or estimated by using reciprocity in duplexing schemes. The beamforming weights are updated instantaneously and optimized to deliver the maximum power to the receiver according to the perfect or imperfect CSI at the transmitter. The associated channel model is assumed to be the simplified fading scenario as described in Chapter 3. The channel coefficients from the M_t transmitting antennas to the receiving antenna are denoted by the $1 \times M_t$ complex row vector $\mathbf{h}$ as follows:

$$\mathbf{h} = \begin{bmatrix} h_1 & h_2 & \cdots & h_{M_t} \end{bmatrix} \tag{4.1}$$

where h_i $(i = 1, 2, ..., M_t)$ is the ith circularly complex Gaussian distributed channel's parameter with zero-mean and variance $\sigma_h^2 = E\left[|h_i|^2\right]$. It is assumed that the channels are statistically identical, space-independent, time-correlated and satisfy

the quasi-static Rayleigh flat fading. The well-known Alamouti's STBC, proposed in [4], can be denoted by:

$$\mathbf{S} = \sqrt{E_s} \begin{bmatrix} s_1 & -s_2^* \\ s_2 & s_1^* \end{bmatrix} \tag{4.2}$$

where s_j $(j = 1, 2)$ denotes the modulated information data and E_s is the energy allocated to each symbol. Note that in Alamouti scheme described in Section 2.4.1, the energy for each symbol is halved, i.e., $E_s/2$, in order to ensure the same total radiated power as with one transmitting antenna. However, in the combined system of beamforming and Alamouti's STBC discussed in this chapter, the total transmitted power can be kept the same even though each symbol has the energy of E_s due to the normalization carried out in the beamforming procedure. The system data model can be expressed by:

$$\mathbf{Y} = \mathbf{hWS} + \mathbf{E} \tag{4.3}$$

where $\mathbf{Y}$ is a 1×2 row vector representing the received data at two time instants, i.e.,

$$\mathbf{Y} = [\ y_1 \quad y_2\ ] \tag{4.4}$$

and $\mathbf{W}$ is the $M_t \times L$ dimensional optimal beamforming matrix, which is adapted according to the CSI at the transmitter. Here, L is the length of orthogonal space-time block codewords and $L = 2$ for Alamouti's STBC. It is clear that $\mathbf{W}$ is a non-square matrix if $M_t > 2$. The noise vector $\mathbf{E}$ is the independent AWGN samples with zero-mean and variance $\sigma^2 = N_0/2$ per dimension, denoted by:

$$\mathbf{E} = [\ e_1 \quad e_2\ ] \tag{4.5}$$

4.2.1 The CSI at the transmitter

Although it is assumed that perfect CSI is available at the receiver for simplicity, the feedback CSI $\hat{\mathbf{h}}$ at the transmitter is not only noisy but may also be outdated due to the feedback delay, denoted by a $1 \times M_t$ dimensional complex row vector as follows,

$$\hat{\mathbf{h}} = \begin{bmatrix} \hat{h}_1 & \hat{h}_2 & \cdots & \hat{h}_{M_t} \end{bmatrix} \tag{4.6}$$

Each coefficient $\hat{h}_i$ $(i = 1, 2, \ldots, M_t)$ can be expressed by

$$\hat{h}_i = h_d + \epsilon \tag{4.7}$$

where $h_d \sim \mathcal{CN}(0, \sigma_h^2)$ is the outdated version of the true channel and $\epsilon \sim \mathcal{CN}(0, \sigma_\epsilon^2)$ is the AWGN of the feedback link. In view of the well-known Jakes model [41], the channel coefficients are samples of a stationary Gaussian process with an autocorrelation function proportional to $J_0(2\pi f_m \tau)$, where $J_0(\cdot)$ is the Bessel function of the first kind for zero-order, τ is the time delay and f_m is the maximum Doppler frequency. Since the channel coefficients are time-correlated, the outdated channel h_d is correlated with the current true channel h_i and the amount of such correlation is determined by the time it takes to feed back the CSI. In this case, we have

$$E[h_i \hat{h}_i^*] = E[h_i h_d^*] + E[h_i \epsilon^*] \tag{4.8}$$

The correlation between the AWGN ϵ and the true channel, h_i, is zero since h_i and ϵ are independent. Therefore, the noisy and outdated CSI $\hat{h}_i$ at the transmitter is correlated with the corresponding true channel h_i and uncorrelated with all others.

The correlation between $\hat{h}_i$ and h_i is the same as that between h_d and h_i, and the amount of such correlation is also determined by the feedback delay and not by the AWGN of the feedback channel. The normalized correlation coefficient ρ is introduced to describe the degree of correlation, where $\rho = E\left[h_i \hat{h}_i^*\right] / \sigma_h^2$, which is a measure of the feedback CSI quality ($0 \leq |\rho| \leq 1$). Here, $|\rho| \rightarrow 1$ means that we have perfect CSI at the transmitter, i.e., $h_i = \hat{h}_i$. On the other hand, $|\rho| \rightarrow 0$ corresponds to no CSI at the transmitter, i.e., h_i and $\hat{h}_i$ are uncorrelated. As the true channel coefficient, h_i, and its outdated version, h_d, are samples of the same Gaussian random process, they are jointly complex Gaussian distributed and this relation still remains between the true channel, h_i, and the CSI, $\hat{h}_i$, at the transmitter, as well as $\hat{h}_i \sim \mathcal{CN}(0, \sigma_h^2)$.

4.2.2 Non-square Beamforming Matrix

In Chapter 3, we described the design of the square optimal beamforming matrix for the predetermined OSTBC with the same size. A semi-closed-form optimization solution for the simplified fading scenario is obtained by using EVD method based on the covariance matrix of the CSI at the transmitter as described in Section 3.2.3. We have also shown the detailed procedure for determining the optimum eigenvalues in (3.33) and (3.34) for MISO systems. In order to couple the predetermined Alamouti's STBC with more than two transmitting antennas, however, a non-square beamforming matrix exploiting the CSI at the transmitter is required. In this section, the associated modification for the existing optimization solution described in Section 3.2.3 is presented for the design of the non-square optimal

beamforming matrix $\mathbf{W}$.

Since the desired beamforming matrix $\mathbf{W}$ for the predetermined Alamouti's STBC is non-square with dimension $M_t \times 2$, only the last two columns of the square $\mathbf{W}$ that correspond to the last two largest eigenvalues are retained. With a slight abuse of notation, the desired optimal beamforming matrix $\mathbf{W}$, obtained after the modification of (3.36), can be expressed by

$$\mathbf{W} = \hat{\mathbf{V}}\mathbf{\Lambda}^{1/2} = \begin{bmatrix} \mathbf{v}_1 & \mathbf{v}_2 \end{bmatrix} \begin{bmatrix} \sqrt{\lambda_1} & 0 \\ 0 & \sqrt{\lambda_2} \end{bmatrix} \tag{4.9}$$

where the eigenvector matrix $\hat{\mathbf{V}}$ only has the last two columns $\mathbf{v}_1$ and $\mathbf{v}_2$ left and the eigenvalue matrix $\mathbf{\Lambda}$ is modified to be a 2×2 dimensional matrix with only two eigenvalues $\{\lambda_1, \lambda_2\}$ on its diagonal. It follows that the power constraint given in (3.28) is also modified to

$$0 \leq \lambda_1 \leq \lambda_2 \leq 1, \tag{4.10}$$

$$\lambda_1 + \lambda_2 = 1. \tag{4.11}$$

Hence, the expressions for the eigenvalues $\{\lambda_1, \lambda_2\}$ are still the same as (3.33) and (3.34), given by

$$\lambda_1 = \max\left\{0, \frac{1}{\mu} - \frac{1}{\alpha\eta}\right\}, \qquad \lambda_2 = 1 - \lambda_1 \tag{4.12}$$

but the Lagrange multiplier μ is modified to become

$$\mu = \frac{\eta\left(3\kappa + |\rho|^2\|\hat{\mathbf{h}}\|^2 + \sqrt{6\kappa|\rho|^2\|\hat{\mathbf{h}}\|^2 + |\rho|^4\|\hat{\mathbf{h}}\|^4 + \kappa^2}\right)}{2(2+\alpha\eta)^2} \tag{4.13}$$

for the predetermined codeword matrix with two rows, where $\kappa = \alpha(2+\alpha\eta)$, $\eta = \delta_{min}E_s/4N_0$ and δ_{min} denotes the minimum squared Euclidean distance between

all pairs of Alamouti's space-time codewords. It is clear that the average SNR, $\gamma_0 = E_s/N_0$, is contained in η.

It is known that $\mathbf{v}_1$ and $\mathbf{v}_2$ are the normalized eigenvectors of $\mathbf{W}\mathbf{W}^{\mathcal{H}}$, associated with the eigenvalues λ_1 and λ_2, respectively. Following the development in [45], the optimum principle eigenvector $\mathbf{v}_2$ corresponding to the largest eigenvalue λ_2 can be chosen as

$$\mathbf{v}_2 = \frac{\hat{\mathbf{h}}^{\mathcal{H}}}{\|\hat{\mathbf{h}}\|} \tag{4.14}$$

The remaining eigenvector $\mathbf{v}_1$ corresponding to the eigenvalue λ_1 is chosen as

$$\mathbf{v}_1 = \frac{\tilde{\mathbf{h}}^{T}}{\|\hat{\mathbf{h}}\|} \tag{4.15}$$

by forming a vector $\tilde{\mathbf{h}}$ orthogonal to $\hat{\mathbf{h}}$ and $\|\tilde{\mathbf{h}}\| = \|\hat{\mathbf{h}}\|$.

Thus, the optimal beamforming matrix for the new combined system turns out to be given by

$$\begin{aligned} \mathbf{W} &= \frac{1}{\|\hat{\mathbf{h}}\|} \begin{bmatrix} \tilde{\mathbf{h}}^{T} & \hat{\mathbf{h}}^{\mathcal{H}} \end{bmatrix} \begin{bmatrix} \sqrt{\lambda_1} & 0 \\ 0 & \sqrt{\lambda_2} \end{bmatrix} \\ &= \frac{1}{\|\hat{\mathbf{h}}\|} \begin{bmatrix} \tilde{h}_1 & \hat{h}_1^* \\ \tilde{h}_2 & \hat{h}_2^* \\ \vdots & \vdots \\ \tilde{h}_{M_t} & \hat{h}_{M_t}^* \end{bmatrix} \begin{bmatrix} \sqrt{\lambda_1} & 0 \\ 0 & \sqrt{\lambda_2} \end{bmatrix} \end{aligned} \tag{4.16}$$

Notice that the beamforming in the respective directions of $\hat{\mathbf{h}}^{\mathcal{H}}$ and $\tilde{\mathbf{h}}^{T}$ is performed, and the eigenvalues λ_1 and λ_2 are used to instruct the allocation of the transmission power between the two beamforming directions. Therefore, as long as $\lambda_1 \neq \lambda_2$, the output power of the linear transformation is loaded unequally across the different antennas and the maximum power is delivered to the receiver due to the optimization of the transmitter weights according to the CSI.

The optimal beamforming matrix (4.16) is constructed under the assumption of simplified fading scenario. As described in [45] and [48], the simplified fading scenario is a specialized form of the general complex Gaussian fading assumption for illustrative purpose. However, it has remarkable effect on the construction procedure of beamforming matrix without the assumption. As described in [45], in the general case, a semi-closed-form solution, i.e., (4.16), of the optimization problem in (3.20) is not guaranteed. The existing fairly efficient numerical optimization technique is much more complex. Although the simplified fading scenario is assumed in this chapter, it is known from [45] that the development generalizes easily to all scenarios where the conditional covariance matrix of $\mathbf{R}_{\mathbf{hh}|\acute{\mathbf{h}}}$ is diagonal. One important example of such a scenario is an environment with Ricean fading. Moreover, there are a few special cases that permit a closed-form solution including the case of perfect CSI at the transmitter, the case of no CSI at the transmitter, the case of infinite SNR and the case of an SNR value tending to zero. Therefore, with the aforementioned scenarios, we conclude that there will be no significant effect if the simplified fading conditions are not satisfied.

4.3 Performance Analysis for Ideal Beamforming

In the case of ideal beamforming, the feedback CSI at the transmitter is assumed to be perfect, i.e., $\hat{h}_i = h_i$. It corresponds to the correlation coefficient $|\rho| = 1$ and the largest eigenvalue $\lambda_2 = 1$ hence $\lambda_1 = 0$. It means that all the transmitted power is allocated to the direction of the eigenvector $\mathbf{h}^{\mathcal{H}}$ corresponding to λ_2. From (4.16),

the optimal beamforming matrix for the combined system of ideal beamforming and Alamouti's STBC is given by

$$\mathbf{W} = \frac{1}{\|\mathbf{h}\|}\begin{bmatrix} \mathbf{0} & \mathbf{h}^{\mathcal{H}} \end{bmatrix} = \frac{1}{\|\mathbf{h}\|}\begin{bmatrix} 0 & h_1^* \\ 0 & h_2^* \\ \vdots & \vdots \\ 0 & h_{M_t}^* \end{bmatrix} \tag{4.17}$$

The transmission matrix $\mathbf{C} = \mathbf{WS}$ for the combined system of ideal beamforming and Alamouti's STBC is a $M_t \times 2$ dimensional matrix, expressed by

$$\mathbf{C} = \frac{\sqrt{E_s}}{\|\mathbf{h}\|}\begin{bmatrix} \mathbf{h}^{\mathcal{H}} s_2 & \mathbf{h}^{\mathcal{H}} s_1^* \end{bmatrix} \tag{4.18}$$

The beamforming in the direction of $\mathbf{h}^{\mathcal{H}}$ is performed. Since there are two symbols transmitted over two time instants across M_t transmitting antennas, the code has a full rate, $R = 1$. The diversity advantage of the ideal combined system can be shown from the system PEP performance in Section 4.3.2.1.

In the following, we provide two methods involving the MGF approach and the conditional probability method, to analyze the error probability performance of the ideal combined system. Firstly, by using a MGF approach [86] and the Gauss-Chebyshev quadrature rule [8], we calculate the exact PEP of the ideal combined system with any desired degree of accuracy, even though we cannot get the closed-form through MGF approach. Subsequently, an analytical union bound on the BER is derived based on the exact PEP. Secondly, we exploit and investigate the conditional probability method to derive the closed-form upper bound on PEP and the closed-form BER. The closed-form upper bound on PEP is important, as it is straightforward from the expression to get the system coding gain and diversity gain.

4.3.1 Moment-Generating Function Approach

4.3.1.1 The exact PEP

It is known from [86] that the system PEP for the conventional OSTBC is given by

$$P(\mathbf{S} \to \mathbf{S}') = E[Q(\sqrt{\xi})] = \frac{1}{2\pi j} \int_{c-j\infty}^{c+j\infty} \Phi_\xi(s) \left(2s\sqrt{1-2s}\right)^{-1} ds \tag{4.19}$$

where

$$\Phi_\xi(s) = E[\exp(-s\xi)] \tag{4.20}$$

is the MGF of the nonnegative random variable ξ, and c is a constant in the region of convergence of $\Phi_\xi(s)\left(\sqrt{1-2s}\right)^{-1}$ and a good choice is $c = 1/4$. The random variable ξ is introduced to denote

$$\xi = \frac{d^2(\mathbf{S}, \mathbf{S}')}{2N_0} = \frac{\|\mathbf{h}\boldsymbol{\Delta}\|_{\mathrm{F}}^2}{2N_0} = \frac{1}{2N_0}\mathbf{h}\boldsymbol{\Delta}\boldsymbol{\Delta}^{\mathcal{H}}\mathbf{h}^{\mathcal{H}} \tag{4.21}$$

where $\boldsymbol{\Delta}$ is the codeword difference matrix defined as $\boldsymbol{\Delta} = \mathbf{S} - \mathbf{S}'$. Due to the orthogonal nature of OSTBC, these codes have the appealing property that

$$\boldsymbol{\Delta}\boldsymbol{\Delta}^{\mathcal{H}} = \frac{\delta_{M_t} E_s}{M_t}\mathbf{I}_{M_t} \tag{4.22}$$

where δ_{M_t} is the squared Euclidean distance between the OSTBC codeword pair of $\mathbf{S}$ and $\mathbf{S}'$ designed for M_t transmitting antennas and $\mathbf{I}_{M_t}$ denotes the $M_t \times M_t$ dimensional identity matrix. The average energy for each symbol of OSTBC is normalized to be E_s/M_t to ensure the same total radiated power as with one transmitting antenna. Substituting (4.22) into (4.21) leads to

$$\xi = \frac{\delta_{M_t} E_s}{2N_0 M_t}\|\mathbf{h}\|^2. \tag{4.23}$$

For the new combined system of ideal beamforming and Alamouti's STBC, the system PEP is also given by (4.19), but the nonnegative random variable ξ must be modified to include the linear beamforming matrix, $\mathbf{W}$, to become

$$\xi_w = \frac{d^2(\mathbf{C}, \mathbf{C}')}{2N_0} = \frac{\|\mathbf{h}\mathbf{W}\mathbf{\Delta}_a\|_{\mathrm{F}}^2}{2N_0} = \frac{1}{2N_0}\mathbf{h}\mathbf{W}\mathbf{\Delta}_a\mathbf{\Delta}_a^{\mathcal{H}}\mathbf{W}^{\mathcal{H}}\mathbf{h}^{\mathcal{H}} \tag{4.24}$$

where $\mathbf{\Delta}_a$ is the codeword difference matrix for Alamouti's STBC defined in (4.2) and

$$\mathbf{\Delta}_a\mathbf{\Delta}_a^{\mathcal{H}} = \delta_2 E_s \mathbf{I}_2 \tag{4.25}$$

where δ_2 denotes the square Euclidean distance between the Alamouti's space-time block codeword pair and $\mathbf{I}_2$ represents the two dimensional identity matrix. It is worth noting that in the combined system, the average energy for each symbol of Alamouti's STBC is E_s. Nevertheless, the total transmitted power of the combined system is still the same as with one transmitting antenna. This is because the weights in the beamforming matrix are normalized by $\|\mathbf{h}\|$ to keep the total transmitted power the same as with one transmitting antenna. Thus, the modified random variable ξ_w is obtained by substituting (4.25) into (4.24),

$$\xi_w = \frac{\delta_2 E_s}{2N_0}\|\mathbf{h}\|^2. \tag{4.26}$$

By introducing $\widehat{\mathbf{\Delta}}$ such that

$$\widehat{\mathbf{\Delta}}\widehat{\mathbf{\Delta}}^{\mathcal{H}} = \delta_2 E_s \mathbf{I}_{M_t}, \tag{4.27}$$

the random variable ξ_w given in (4.24) can be re-written in another expression,

$$\xi_w = \frac{\|\mathbf{h}\widehat{\mathbf{\Delta}}\|_{\mathrm{F}}^2}{2N_0} = \frac{1}{2N_0}\mathbf{h}\widehat{\mathbf{\Delta}}\widehat{\mathbf{\Delta}}^{\mathcal{H}}\mathbf{h}^{\mathcal{H}} = \frac{d^2(\widehat{\mathbf{S}}, \widehat{\mathbf{S}}')}{2N_0}. \tag{4.28}$$

where $\widehat{\mathbf{\Delta}} = \widehat{\mathbf{S}} - \widehat{\mathbf{S}}'$. It means that from the random variable ξ_w point of view, the ideal combined system is equivalent to an OSTBC with the codeword difference matrix $\widehat{\mathbf{\Delta}}$.

By introducing $\mathbf{z} = \mathbf{h}^{\mathcal{H}}$ and $\mathcal{A} = \widehat{\mathbf{\Delta}}\widehat{\mathbf{\Delta}}^{\mathcal{H}}/(2N_0)$, we have mean $\mathbf{m} = E[\mathbf{z}] = \mathbf{0}$ and covariance matrix $\mathbf{\Sigma} = E[\mathbf{z}\mathbf{z}^{\mathcal{H}}] - \mathbf{m}\mathbf{m}^{\mathcal{H}} = \mathbf{I}_{M_t}$. As stated in [86], for a complex circularly distributed Gaussian random column vector $\mathbf{z} \sim \mathcal{CN}(\mathbf{m}, \mathbf{\Sigma})$ and a Hermitian matrix $\mathcal{A}$, we have

$$E[\exp\left(-\mathbf{z}^{\mathcal{H}}\mathcal{A}\mathbf{z}\right)] = \frac{\exp\left[-\mathbf{m}^{\mathcal{H}}\mathcal{A}(\mathbf{I} + \mathbf{\Sigma}\mathcal{A})^{-1}\mathbf{m}\right]}{\det(\mathbf{I} + \mathbf{\Sigma}\mathcal{A})}. \tag{4.29}$$

Hence, we obtain the MGF of ξ_w as

$$\begin{aligned}
\Phi_{\xi_w}(s) &= E[\exp(-s\xi_w)] = E[\exp\left(-s\mathbf{z}^{\mathcal{H}}\mathcal{A}\mathbf{z}\right)] \\
&= [\det(\mathbf{I}_{M_t} + s\mathbf{\Sigma}\mathcal{A})]^{-1} \\
&= \left[\det\left(\mathbf{I}_{M_t} + \frac{s\widehat{\mathbf{\Delta}}\widehat{\mathbf{\Delta}}^{\mathcal{H}}}{2N_0}\right)\right]^{-1} \\
&= \left(1 + \frac{s\delta_2 E_s}{2N_0}\right)^{-M_t}
\end{aligned} \tag{4.30}$$

and the PEP of the ideal combined system is expressed by

$$P(\mathbf{C} \to \mathbf{C}') = P(\widehat{\mathbf{S}} \to \widehat{\mathbf{S}}') = \frac{1}{2\pi j}\int_{c-j\infty}^{c+j\infty} \Phi_{\xi_w}(s)\left(2s\sqrt{1-2s}\right)^{-1} ds \tag{4.31}$$

Substituting (4.30) into (4.31), it can be observed that the integral operation over variable s does not change the power M_t of E_s/N_0 in the denominator of the expression for the PEP. Therefore, the power M_t of E_s/N_0 is the diversity advantage of the system [87], which is the maximum or full diversity for a MISO system with M_t transmitting antennas and one receiving antenna.

We now turn our attention to calculating the exact PEP through the MGF $\Phi_{\xi_w}(s)$ for the ideal combined system. By introducing

$$\Phi_{\Delta}(s) = \frac{\Phi_{\xi_w}(s)}{\sqrt{1-2s}} = \frac{1}{\sqrt{1-2s}} \left(1 + \frac{s\delta_2 E_s}{2N_0}\right)^{-M_t}, \tag{4.32}$$

we expand the real and imaginary parts in (4.31) according to the derivation in [86],

$$\begin{aligned} P(\mathbf{C} \to \mathbf{C}') &= \frac{1}{2\pi j} \int_{c-j\infty}^{c+j\infty} \frac{\Phi_{\Delta}(s)}{2s}\, ds \\ &= \frac{1}{4\pi} \int_{-\infty}^{+\infty} \frac{\Phi_{\Delta}(c+j\omega)}{c+j\omega}\, d\omega \\ &= \frac{1}{4\pi} \int_{-\infty}^{+\infty} \frac{c\mathsf{Re}[\Phi_{\Delta}(c+j\omega)] + \omega \mathsf{Im}[\Phi_{\Delta}(c+j\omega)]}{c^2+\omega^2}\, d\omega \\ &= \frac{1}{4\pi} \int_{-1}^{+1} \mathsf{Re}\left[\Phi_{\Delta}\left(c + jc\frac{\sqrt{1-x^2}}{x}\right)\right] \frac{dx}{\sqrt{1-x^2}} \\ &+ \frac{1}{4\pi} \int_{-1}^{+1} \frac{\sqrt{1-x^2}}{x} \mathsf{Im}\left[\Phi_{\Delta}\left(c + jc\frac{\sqrt{1-x^2}}{x}\right)\right] \frac{dx}{\sqrt{1-x^2}} \end{aligned} \tag{4.33}$$

where $\omega = c\sqrt{1-x^2}/x$, and $\mathsf{Re}(\cdot)$ and $\mathsf{Im}(\cdot)$ denote the real and imaginary parts, respectively, of their arguments. By using a Gauss-Chebyshev numerical quadrature rule with ν nodes, the integral in (4.33) can be written as

$$P(\mathbf{C} \to \mathbf{C}') = \frac{1}{4\nu} \sum_{k=1}^{\nu} \{\mathsf{Re}[\Phi_{\Delta}(c + jc\tau_k)] + \tau_k \mathsf{Im}[\Phi_{\Delta}(c + jc\tau_k)]\} + E_{\nu} \tag{4.34}$$

where $\tau_k = \tan[(k-0.5)\pi/\nu]$ and $E_{\nu} \to 0$ as $\nu \to \infty$. For numerical calculation, $\nu = 64$ is good enough. It is clear that the exact PEP for the ideal combined system can be worked out by replacing s with $c + jc\tau_k$ and substituting (4.32) into (4.34).

4.3.1.2 The union bound on the BER

The standard approach bounds the BER using a union bound as follows

$$\begin{aligned} P_{union} &= \frac{1}{K} \sum_{k,l=1,k\neq l}^{K} q_{kl} P(\mathbf{C}_k \rightarrow \mathbf{C}_l) \\ &= \frac{2}{K} \sum_{k=1,l=2,k<l}^{K} q_{kl} P(\mathbf{C}_k \rightarrow \mathbf{C}_l) \end{aligned} \tag{4.35}$$

where K is the number of codewords in the Alamouti's STBC and q_{kl} is the bit error probability of each error event due to transmitting $\mathbf{C}_k$ but deciding in favor of $\mathbf{C}_l$, i.e.,

$$q_{kl} = \frac{\text{number of error bits in event } (\mathbf{C}_k \rightarrow \mathbf{C}_l)}{\text{number of input bits per encoding interval}}. \tag{4.36}$$

For illustration purpose, we assume that BPSK modulation is adopted for the combined system of ideal beamforming and Alamouti's STBC. Thus the number of input bits per encoding interval is 2 and the number of codewords is $K = 4$. The input signals s_1 or s_2 is assumed to be $+\sqrt{E_s}$ or $-\sqrt{E_s}$, then the input data constellation is formed as,

$$\begin{bmatrix} \mathbf{s}^{(1)} \\ \mathbf{s}^{(2)} \\ \mathbf{s}^{(3)} \\ \mathbf{s}^{(4)} \end{bmatrix} = \sqrt{E_s} \begin{bmatrix} 1 & 1 \\ 1 & -1 \\ -1 & 1 \\ -1 & -1 \end{bmatrix} \tag{4.37}$$

where $\mathbf{s}^{(k)} = [s_1^{(k)}\ s_2^{(k)}]$ $(k = 1, \ldots, K)$ represents the input signal series per encoding interval, corresponding to the codeword $\mathbf{C}_k$. In this case, the union bound on the BER for the ideal combined system can be expressed by

$$\begin{aligned} P_{union} = &\frac{1}{2}\left[q_{12}P(\mathbf{C}_1 \rightarrow \mathbf{C}_2) + q_{13}P(\mathbf{C}_1 \rightarrow \mathbf{C}_3) + q_{14}P(\mathbf{C}_1 \rightarrow \mathbf{C}_4)\right] \\ &+ \frac{1}{2}\left[q_{23}P(\mathbf{C}_2 \rightarrow \mathbf{C}_3) + q_{24}P(\mathbf{C}_2 \rightarrow \mathbf{C}_4) + q_{34}P(\mathbf{C}_3 \rightarrow \mathbf{C}_4)\right] \end{aligned} \tag{4.38}$$

It can be seen that there is some overlapped area in the calculation of error bits. Hence, the weighted sum of the PEPs is the union bound rather than the exact

BER. It is known from (4.32) and (4.34) that the PEP $P(\mathbf{C}_k \rightarrow \mathbf{C}_l)$ fully depends on the squared Euclidean distance δ_{kl} between $\mathbf{C}_k$ and $\mathbf{C}_l$. It is obvious from (4.37) that

$$P(\mathbf{C}_1 \rightarrow \mathbf{C}_2) = P(\mathbf{C}_1 \rightarrow \mathbf{C}_3) = P(\mathbf{C}_2 \rightarrow \mathbf{C}_4) = P(\mathbf{C}_3 \rightarrow \mathbf{C}_4), \tag{4.39}$$

$$P(\mathbf{C}_1 \rightarrow \mathbf{C}_4) = P(\mathbf{C}_2 \rightarrow \mathbf{C}_3) \tag{4.40}$$

and

$$q_{12} = q_{13} = q_{24} = q_{34} = \frac{1}{2}, \quad q_{14} = q_{23} = 1. \tag{4.41}$$

Therefore, the union bound on the BER for the ideal combined system can be simplified as follows,

$$P_{union} = P(\mathbf{C}_1 \rightarrow \mathbf{C}_2) + P(\mathbf{C}_1 \rightarrow \mathbf{C}_4) \tag{4.42}$$

To get the union bound on the BER, only the PEPs $P(\mathbf{C}_1 \rightarrow \mathbf{C}_2)$ and $P(\mathbf{C}_1 \rightarrow \mathbf{C}_4)$ are required which can be obtained through (4.34). The numerical results are shown in Section 4.3.3 to demonstrate that the analytical union bound is very tight to the simulation results.

4.3.2 Conditional Probability Method

We have obtained the exact PEP with any desired degree of accuracy in the above subsection. However, the expression of the exact PEP obtained above does not explicitly show the characteristics of the ideal combined system, such as the diversity order and the coding gain, which are very important for the study of the ideal combined systems. In the following, we derive the closed-form upper bound of PEP

and the exact closed-form BER by using the conditional probability. The diversity, coding and array gains can be straightforwardly obtained from the closed-form upper bound of PEP.

4.3.2.1 The closed-form upper bound of PEP

Following the derivation procedure in [87], an equivalent channel $\mathbf{h}_{eq}$ is introduced to denote $\mathbf{hW}$. In the case of ideal beamforming, $\mathbf{h}_{eq}$ has the following expression,

$$\mathbf{h}_{eq} = \mathbf{hW} = \begin{bmatrix} 0 & \|\mathbf{h}\| \end{bmatrix} \tag{4.43}$$

Similar to [45] and [87], the upper bound of PEP of transmitting $\mathbf{C}$ and deciding in favor of $\mathbf{C}'$ at the decoder, conditioned on the equivalent channel, can be obtained and is given as follows,

$$P\left(\mathbf{C}, \mathbf{C}'|\mathbf{h}_{eq}\right) = Q\left(\sqrt{d^2(\mathbf{C}, \mathbf{C}')\frac{1}{2N_0}}\right) \leq \exp\left(-d^2(\mathbf{C}, \mathbf{C}')\frac{1}{4N_0}\right) \tag{4.44}$$

where $Q(\cdot)$ is the Gaussian Q function and $d^2(\mathbf{C}, \mathbf{C}')$ is given by

$$d^2(\mathbf{C}, \mathbf{C}') = \|\mathbf{h}(\mathbf{C} - \mathbf{C}')\|_{\mathrm{F}}^2 = \|\mathbf{h}_{eq}(\mathbf{S} - \mathbf{S}')\|_{\mathrm{F}}^2. \tag{4.45}$$

After following simple manipulations similar to [45] and [88], we have

$$d^2(\mathbf{C}, \mathbf{C}') = \mathbf{h}_{eq}\mathbf{A}\mathbf{h}_{eq}^{\mathcal{H}} \tag{4.46}$$

where $\mathbf{A}$ is the Hermitian code distance matrix, given by

$$\mathbf{A} = (\mathbf{S} - \mathbf{S}')(\mathbf{S} - \mathbf{S}')^{\mathcal{H}} = \delta_2 E_s \mathbf{I}_2 \tag{4.47}$$

due to the orthogonality of the Alamouti's STBC. In this case, the conditional upper bound of PEP on the true channel realization becomes

$$P\left(\mathbf{C}, \mathbf{C}'|\|\mathbf{h}\|^2\right) \leq \exp\left(-\frac{\delta_2 E_s}{4N_0}\|\mathbf{h}\|^2\right). \tag{4.48}$$

Since h_i is assumed to be statistically i.i.d complex Gaussian random variable with zero-mean and variance σ_h^2, then,

$$\|\mathbf{h}\|^2 = \sum_{i=1}^{M_t} |h_i|^2 \tag{4.49}$$

is central chi-square distributed with $n_f = 2M_t$ degrees of freedom. Let ξ_I represents the random variable $\|\mathbf{h}\|^2$, and according to [78], the PDF of $\|\mathbf{h}\|^2$ is given by

$$f_{\|\mathbf{h}\|^2}(\xi_I) = \frac{1}{\sigma_h^{2M_t}\Gamma(M_t)} \xi_I^{M_t-1} \exp\left(-\frac{\xi_I}{\sigma_h^2}\right). \tag{4.50}$$

where $\Gamma(\cdot)$ is the gamma function. By averaging both sides of (4.48) with respect to the distribution in (4.50), a non-conditional upper bound of PEP is obtained,

$$P(\mathbf{C}, \mathbf{C}') \leq \int_0^\infty \exp\left(-\frac{\delta_2 E_s}{4N_0}\xi_I\right) f_{\|\mathbf{h}\|^2}(\xi_I) d\xi_I = \left(1 + \frac{\delta_2 E_s}{4N_0}\sigma_h^2\right)^{-M_t} \tag{4.51}$$

At sufficiently high SNRs, the right-hand side of Inequality (4.51) can be approximated as

$$P(\mathbf{C}, \mathbf{C}') \leq 2^{-M_t} \left(\frac{1}{2}\delta_2 \sigma_h^2\right)^{-M_t} \left(\frac{E_s}{4N_0}\right)^{-M_t} \tag{4.52}$$

According to [87], the diversity advantage is the power of the SNR in the denominator of the expression for the PEP derived above, and the coding advantage is the approximate measure of the gain over an uncoded system operating with the same diversity advantage. Hence, the system achieves a diversity gain of M_t, which is the maximum or full diversity for a system with M_t transmitting antennas and a single receiving antenna. Therefore, the combined system of ideal beamforming and Alamouti's STBC can achieve the full diversity gain and full code rate simultaneously for complex constellation, which cannot be achieved at the same time by the conventional OSTBC in [89] except for the Alamouti scheme [4].

Comparing (4.52), for $M_t = 2$, with the upper bound of PEP for the Alamouti scheme given in [87] as

$$P(\mathbf{S}, \mathbf{S}') \leq \left(\frac{1}{2}\delta_2\sigma_h^2\right)^{-2} \left(\frac{E_s}{4N_0}\right)^{-2}, \tag{4.53}$$

it is observed that the ideal combined system has the same coding gain of $\frac{1}{2}\delta_2\sigma_h^2$ due to the same encoder as the Alamouti scheme. In addition, the base of the first term on the right-hand side of (4.52) indicates that the former has an array gain of 2 over the latter. The additional array gain of 2 is benefited from the perfect CSI at the transmitter and therefore a coherent combining effect at the receiver. This means that the ideal combined system with two transmitting antennas has 3dB performance gain over the Alamouti scheme though equal total transmission power is assumed. This can be explained as follows.

As described in (4.18), the ideal combined system transmits the same information data from M_t transmitting antennas simultaneously with different power allocation. At the receiver, the signals carrying the same information data with different weights are received within one time instant and hence are affected by one AWGN sample. To illustrate this, we consider two transmitting antennas and assume that $s_2\sqrt{E_s}$ denotes the information data and e_1 denotes the AWGN sample within one time instant. Then the transmitted signals from two transmitting antennas are $h_1^* s_2\sqrt{E_s}/\|\mathbf{h}\|$ and $h_2^* s_2\sqrt{E_s}/\|\mathbf{h}\|$, respectively. Therefore the received signal y_1 may be described as

$$y_1 = \frac{|h_1|^2}{\|\mathbf{h}\|} s_2\sqrt{E_s} + \frac{|h_2|^2}{\|\mathbf{h}\|} s_2\sqrt{E_s} + e_1 = \|\mathbf{h}\| s_2\sqrt{E_s} + e_1 \tag{4.54}$$

Consequently, the average SNR for each received signal before the ML detector at

the receiver is given by

$$\gamma_c = \|\mathbf{h}\|^2 \frac{E_s}{N_0}. \tag{4.55}$$

On the other hand, for the Alamouti scheme, the same information data are carried by two signals transmitted from two transmitting antennas with equal power allocation during two time instants. As a result, the two signals carrying the same information data are received at two time instants and hence are affected by two different AWGN samples. Following the above illustration, the two signals $s_1\sqrt{E_s/2}$ and $s_1^*\sqrt{E_s/2}$ from two transmitting antennas for the Alamouti scheme are transmitted at two different time instants. At the receiver, as stated in [4], the combined signal over two time instants after channel estimator and linear combiner is described as

$$\tilde{y}_1 = \|\mathbf{h}\|^2 s_1 \sqrt{\frac{E_s}{2}} + h_1^* e_1 + h_2 e_2^* \tag{4.56}$$

where e_1 and e_2 are the AWGN samples at two successive time instants. Therefore, the average SNR for each combined signal before the ML detector at the receiver is given by

$$\gamma_a = \|\mathbf{h}\|^2 \frac{E_s}{2N_0}. \tag{4.57}$$

Comparing (4.55) and (4.57), clearly, the ideal combined system has 3dB gain on the overall SNR over the Alamouti scheme, so also on the BER performance.

Furthermore, when we compare (4.52) with the upper bound of PEP for the conventional OSTBC, given by [87] as

$$P(\mathbf{S}, \mathbf{S}') \leq \left(\frac{1}{M_t}\delta_{M_t}\sigma_h^2\right)^{-M_t} \left(\frac{E_s}{4N_0}\right)^{-M_t} \tag{4.58}$$

the ideal combined system has the same full diversity gain of M_t as the conventional OSTBC. If we divide the right-hand side of (4.52) by the right-hand side of (4.58), under the same diversity condition M_t, we get the ideal combined system's overall performance gain of

$$2^{-M_t}\left(\frac{M_t\delta_2}{2\delta_{M_t}}\right)^{-M_t} \tag{4.59}$$

which includes a coding gain of

$$CG = 10\log\left(\frac{M_t\delta_2}{2\delta_{M_t}}\right) \quad \text{dB} \tag{4.60}$$

and an additional array gain of

$$AG = 10\log 2 \approx 3 \quad \text{dB}. \tag{4.61}$$

4.3.2.2 The closed-form BER

In the combined system of ideal beamforming and Alamouti's STBC, the received signals at two time instants are given respectively by

$$y_1 = \|\mathbf{h}\|\sqrt{E_s}s_2 + e_1 \tag{4.62}$$

and

$$y_2 = \|\mathbf{h}\|\sqrt{E_s}s_1^* + e_2 \tag{4.63}$$

Notice that the pre-coded information data s_1 and s_2 are decoupled completely, i.e., only one of the pre-coded information data is received at each time instant in the case of ideal beamforming. The received SNR for each signal is expressed as

$$\gamma_b = \|\mathbf{h}\|^2\gamma_0 = \xi_I\gamma_0 \tag{4.64}$$

where $\gamma_0 = E_s/N_0$ is the average SNR. For BPSK modulation, the exact BER expression is given as follows,

$$P_2 = \int_0^\infty Q\left(\sqrt{2\gamma_b}\right) f_{\gamma_b}(\gamma_b) d\gamma_b \tag{4.65}$$

where $f_{\gamma_b}(\gamma_b)$ is the PDF of γ_b which, by using (4.50), has the following expression,

$$f_{\gamma_b}(\gamma_b) = \frac{1}{\gamma_0} f_{\|\mathbf{h}\|^2}\left(\frac{\gamma_b}{\gamma_0}\right) = \frac{\gamma_b^{M_t-1}}{\Gamma(M_t)\left(\sigma_h^2\gamma_0\right)^{M_t}} \exp\left(-\frac{\gamma_b}{\sigma_h^2\gamma_0}\right). \tag{4.66}$$

Hence, the PDF of γ_b for the ideal combined system has the same form as that for the true MRC described by (14.4-13) in the Section 14.4.1 of [78], except that the parameter M_t in (4.66) denotes the number of transmitting antennas, while for the true MRC, the parameter L in (14.4-13) denotes the number of receiving antennas. It follows that (4.65) has the same closed-form solution as the true MRC system described by [78]

$$P_2 = \left[\frac{1}{2}(1-\mu_\gamma)\right]^{M_t} \sum_{k=0}^{M_t-1} \binom{M_t-1+k}{k} \left[\frac{1}{2}(1+\mu_\gamma)\right]^k \tag{4.67}$$

where, by definition

$$\mu_\gamma = \sqrt{\frac{\sigma_h^2\gamma_0}{1+\sigma_h^2\gamma_0}}. \tag{4.68}$$

Due to the special structure of the orthogonal Alamouti's code and the fact that only one column of $\mathbf{W}$ is nonzero, the ideal combined system becomes the pure ideal transmitter beamforming system with the optimized power allocation. In other words, the Alamouti's STBC has no effect on the combined system in the case of perfect CSI at the transmitter. The important conclusion of this section is that the ideal combined system not only can achieve full code rate and full diversity simultaneously, but also the optimum BER performance as the true MRC.

4.3.3 Numerical Results

In this thesis, unless otherwise stated, all numerical results are obtained in the simplified fading scenario under the assumption of $M_r = 1$, $E_s = 1$ and $\sigma_h^2 = 1$. For the combined system of beamforming and STBC, it is assumed that the variances σ^2 and σ_h^2 and the correlation coefficient ρ are perfectly known at the transmitter in order for the optimization to be carried out.

For fair comparison, all different systems are compared on the basis of the same effective bits per symbol (BPS) throughput given by

$$\text{BPS} = R \times m, \tag{4.69}$$

where m is the modulation throughput corresponding to $2^m = M$ for M-PSK modulation.

Fig. 4.2 shows the BER performance of the ideal combined system of beamforming and Alamouti's STBC as well as the conventional OSTBC for comparison. All the curves are obtained by Monte Carlo simulation. To keep the same BPS of 1bit/symbol, the system's parameters used for the various systems simulated are summarized in Table 4.1. In the ideal combined system of beamforming and Alamouti's STBC, BPSK modulation ($m = 1$) is used for any number of transmitting antennas. Thus the combined system has a BPS of 1bit/symbol since the transmission rate is unity as described in Section 4.3 and 4.4. For the conventional OSTBC, QPSK modulation ($m = 2$) is adopted for $M_t = 3$ or $M_t = 8$ transmitting antennas in order to achieve a BPS of 1bit/symbol because the adopted code has a rate of 1/2 [89]. It can be observed that the performance of the ideal

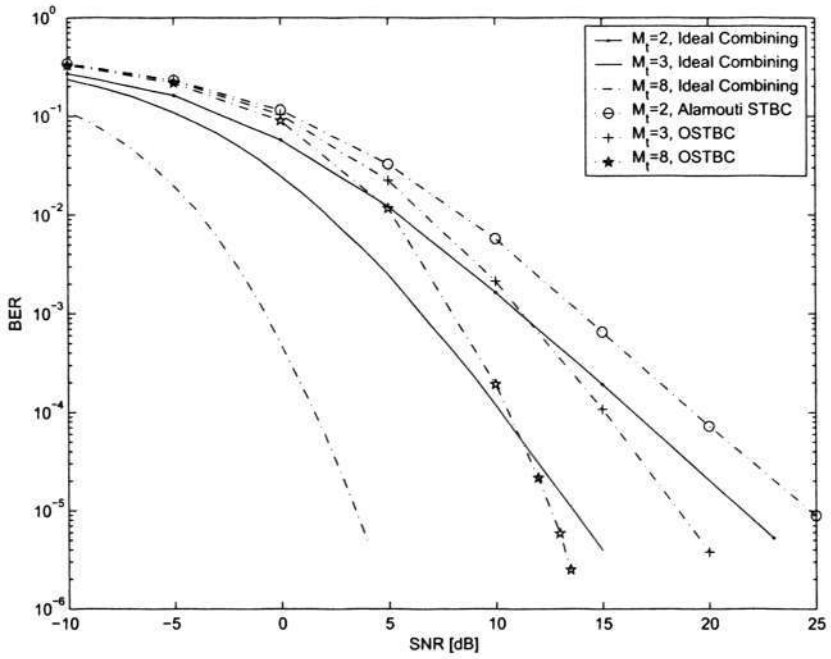

Figure 4.2: BER performance comparison between the ideal combined system and OSTBC

System	No. of Transmitting Antennas	Code Rate	Modulation	Modulation Throughput
Combined System	$M_t = 2$	$R = 1$	BPSK	$m = 1$
Combined System	$M_t = 3$	$R = 1$	BPSK	$m = 1$
Combined System	$M_t = 8$	$R = 1$	BPSK	$m = 1$
Alamouti's STBC	$M_t = 2$	$R = 1$	BPSK	$m = 1$
OSTBC	$M_t = 3$	$R = 1/2$	QPSK	$m = 2$
OSTBC	$M_t = 8$	$R = 1/2$	QPSK	$m = 2$

Table 4.1: System parameters used for simulation results shown in Fig. 4.2

combined system improves as the number of transmitting antenna increases. The ideal combined system has a great performance gain over the conventional OSTBC, including the classical Alamouti scheme. It is worth mentioning that the curve of the ideal combined system has the same slope as that of the conventional

OSTBC with the same number of antennas because both have the same full diversity. According to the discussion in Chapter 3 and [87], the minimum of the squared Euclidean distances between the OSTBC codeword pairs corresponds to the PEP of worst-case codeword pair, which is the dominant term in the union bound. Therefore, the minimum of δ_2 is $(\delta_2)_{min} = 4$ for BPSK modulation, the minimum of δ_3 is $(\delta_3)_{min} = 4$ for QPSK modulation and the minimum of δ_8 is $(\delta_8)_{min} = 4$ for QPSK modulation. From (4.60) and (4.61), the ideal combined system should have a total performance gain of $G = 10\log(M_t\delta_2/\delta_{M_t})$ dB involving coding gain CG and array gain AG over the corresponding conventional OSTBC with the same number of antennas. We can see from Fig. 4.2 that the ideal combined system for $M_t = 2$ is 3dB better than the Alamouti's STBC; for $M_t = 3$, the former is about 5dB better than the corresponding OSTBC; while the difference is 9dB for $M_t = 8$. Obviously, these simulation results confirm the conclusions of the discussion in Section 4.3.2.1.

Fig. 4.3 shows the union bound on the BER and the exact theoretical BER from the closed-form expressions for the combined system of ideal beamforming and Alamouti's STBC in the cases of $M_t = 2$, $M_t = 3$ and $M_t = 8$, respectively. The simulation results are also plotted for comparison. It is clearly seen that the numerical analysis in Section 4.3.1.2 provides a tight union bound on the BER for the ideal combined system. As the number of transmitting antennas increases, the analytical union bound agrees better with the simulation results. The figure also shows that the closed-form theoretical BER in (4.67) matches very well with the simulation results.

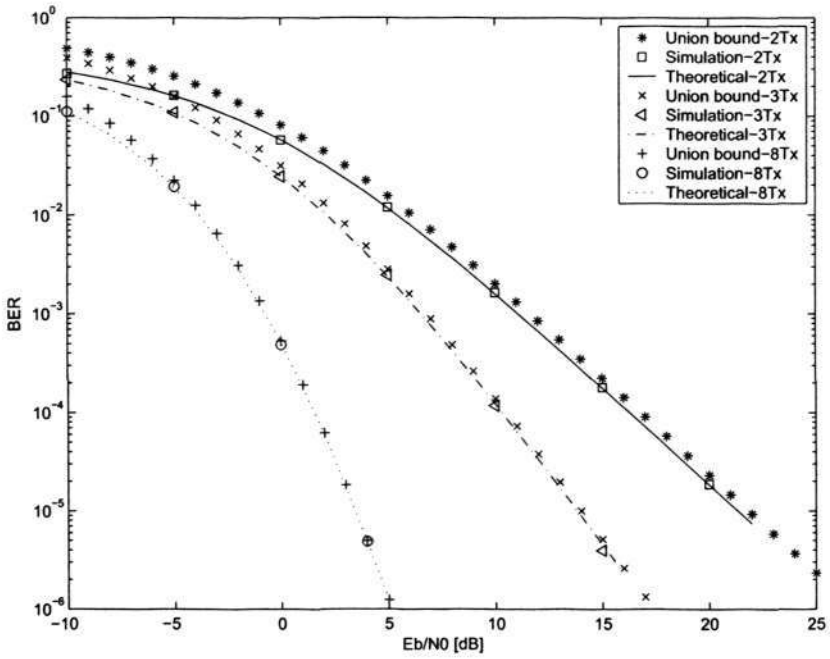

Figure 4.3: Comparison of union bound and simulation results for the ideal combined system

4.4 Performance Analysis for Non-ideal Beamforming

In the case of non-ideal beamforming, the feedback CSI at the transmitter is assumed to be imperfect. It corresponds to the feedback correlation coefficient $0 \leq |\rho| < 1$. Substituting (4.13) into (4.12) shows that the optimal eigenvalues λ_1 and λ_2 of the linear beamforming matrix in (4.16) are the functions of $\|\hat{\mathbf{h}}\|$ and the average SNR γ_0, i.e.,

$$\lambda_1 = fn\left(\|\hat{\mathbf{h}}\|, \gamma_0\right), \quad \lambda_2 = fn\left(\|\hat{\mathbf{h}}\|, \gamma_0\right). \tag{4.70}$$

Fig. 4.4 illustrates that the eigenvalue λ_1 is clearly decreasing as a function of $\|\hat{\mathbf{h}}\|$ and increasing as a function of E_s/N_0. Hence, for a given E_s/N_0, it remains that

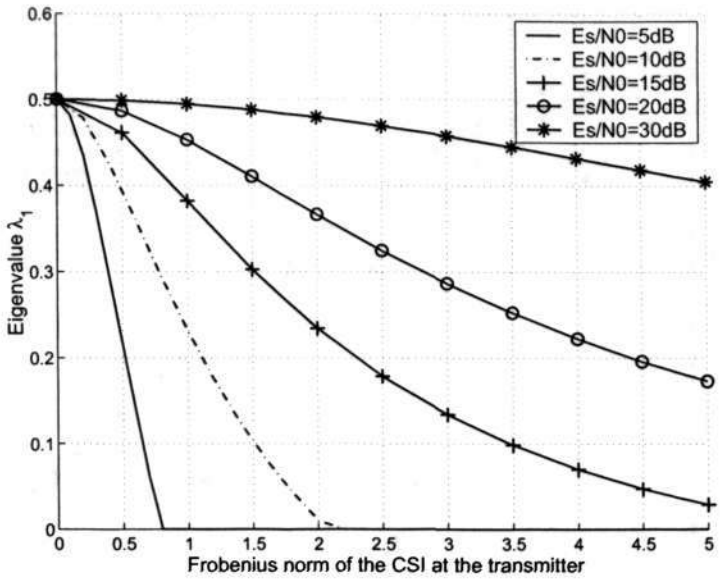

Figure 4.4: The relationship between λ_1 and $\|\hat{\mathbf{h}}\|$ or E_s/N_0

$0 \leq \lambda_1 \leq \frac{1}{2} \leq \lambda_2 \leq 1$. In the case of $\lambda_1 = 0$ and $\lambda_2 = 1$, beamforming in the direction of $\hat{\mathbf{h}}^{\mathcal{H}}$ is performed, i.e., all the transmitted power is allocated to this direction corresponding to the largest eigenvalue λ_2. On the other hand, in the case of $\lambda_1 \neq 0$ and $\lambda_2 \neq 1$, a part of the total transmitted power is allocated to $\hat{\mathbf{h}}^{\mathcal{H}}$ and the remaining power is allocated to the direction of $\tilde{\mathbf{h}}^{T}$, which is orthogonal to $\hat{\mathbf{h}}^{T}$.

Since the transmission matrix $\mathbf{C} = \mathbf{WS}$ for the non-ideal combined system is still a $M_t \times 2$ matrix, the code achieves full rate $R = 1$. The diversity gain can be derived by using the same method as in Section 4.3 from the closed-form upper bound of PEP expression. However, it is essential to obtain the distribution of the equivalent channel $\mathbf{h}_{eq}$ (introduced in Section 4.3) before discussing the system PEP and BER.

In the case of the non-ideal beamforming, the equivalent channel $\mathbf{h}_{eq}$ has the following expression,

$$\mathbf{h}_{eq} = \mathbf{h}\mathbf{W} = \frac{1}{\|\hat{\mathbf{h}}\|}\left[\begin{array}{cc} \sqrt{\lambda_1}\sum_{i=1}^{M_t} h_i\tilde{h}_i & \sqrt{\lambda_2}\sum_{i=1}^{M_t} h_i\hat{h}_i^* \end{array}\right] \tag{4.71}$$

By introducing

$$a = \frac{1}{\|\hat{\mathbf{h}}\|}\sum_{i=1}^{M_t} h_i\tilde{h}_i \quad \text{and} \quad b = \frac{1}{\|\hat{\mathbf{h}}\|}\sum_{i=1}^{M_t} h_i\hat{h}_i^*, \tag{4.72}$$

the equivalent channel $\mathbf{h}_{eq}$ can be rewritten as

$$\mathbf{h}_{eq} = \left[\begin{array}{cc} a\sqrt{\lambda_1} & b\sqrt{\lambda_2} \end{array}\right] \tag{4.73}$$

According to (4.46), $d^2(\mathbf{C}, \mathbf{C}')$ can be expressed by

$$d^2(\mathbf{C}, \mathbf{C}') = \delta_2 E_s \left(|a|^2\lambda_1 + |b|^2\lambda_2\right) = \delta_2 E_s z \tag{4.74}$$

where z is introduced to denote $(|a|^2\lambda_1 + |b|^2\lambda_2)$. It is obvious that the key of the solution is to find the PDF of z, $f_z(z)$.

4.4.1 Conditional PDF of a and b

It is reasonable to assume that the CSI $\hat{\mathbf{h}}$ at the transmitter and the true channel $\mathbf{h}$ are jointly complex Gaussian distributed as in Section 3.2.1 and Section 4.2.1. According to the discussion in Section 3.2, the mean and the variance matrices of $\mathbf{h}$ conditioned on $\hat{\mathbf{h}}$ for the MISO system in the simplified fading scenario are described respectively by

$$\mathbf{m}_{\mathbf{h}|\hat{\mathbf{h}}} = \rho\hat{\mathbf{h}} \tag{4.75}$$

$$\mathbf{R}_{\mathbf{h}\mathbf{h}|\hat{\mathbf{h}}} = \sigma_h^2(1 - |\rho|^2)\mathbf{I}_{M_t} = \alpha\mathbf{I}_{M_t} \tag{4.76}$$

where $0 < |\rho| < 1$ and $\alpha = \sigma_h^2(1 - |\rho|^2)$. The PDF of the true channel element h_i, conditioned on the CSI element $\hat{h}_i$ at the transmitter, is also a complex Gaussian PDF given by

$$h_i \sim \mathcal{CN}\left(\rho\hat{h}_i, \alpha\right), \tag{4.77}$$

and hence $h_i\tilde{h}_i$ and $h_i\hat{h}_i^*$ are also conditional complex Gaussian distributed as follows,

$$h_i\tilde{h}_i \sim \mathcal{CN}\left(\rho\hat{h}_i\tilde{h}_i, \alpha|\tilde{h}_i|^2\right) \tag{4.78}$$

$$h_i\hat{h}_i^* \sim \mathcal{CN}\left(\rho|\hat{h}_i|^2, \alpha|\hat{h}_i|^2\right). \tag{4.79}$$

It is assumed that the elements of both the true channel $\mathbf{h}$ and the CSI $\hat{\mathbf{h}}$ at the transmitter are statistically i.i.d, so do the elements of the two vectors' multiplication. Consequently, $a\|\hat{\mathbf{h}}\|$ and $b\|\hat{\mathbf{h}}\|$ are both the sum of M_t statistically independent complex Gaussian random variables with the following distribution,

$$a\|\hat{\mathbf{h}}\| \sim \mathcal{CN}\left(\rho\sum_{i=1}^{M_t}\hat{h}_i\tilde{h}_i, \alpha\|\tilde{\mathbf{h}}\|^2\right) \tag{4.80}$$

$$b\|\hat{\mathbf{h}}\| \sim \mathcal{CN}\left(\rho\|\hat{\mathbf{h}}\|^2, \alpha\|\hat{\mathbf{h}}\|^2\right). \tag{4.81}$$

From Section 4.2, we know that $\tilde{\mathbf{h}}$ and $\hat{\mathbf{h}}$ are orthogonal, i.e.,

$$\sum_{i=1}^{M_t}\hat{h}_i\tilde{h}_i = 0. \tag{4.82}$$

By utilizing (4.82) and $\|\tilde{\mathbf{h}}\| = \|\hat{\mathbf{h}}\|$, it is straightforward to arrive at

$$a \sim \mathcal{CN}(0, \alpha) \quad \text{and} \quad b \sim \mathcal{CN}\left(\rho\|\hat{\mathbf{h}}\|, \alpha\right). \tag{4.83}$$

Expanding the real and imaginary parts of a and b, we have the following results for $\lambda_1 \neq 0$ when $\|\hat{\mathbf{h}}\|$ is given:

$$\sqrt{\lambda_1}\mathsf{Re}(a) \sim \mathcal{N}(0, \frac{1}{2}\alpha\lambda_1), \tag{4.84}$$

$$\sqrt{\lambda_1}\mathsf{Im}(a) \sim \mathcal{N}(0, \frac{1}{2}\alpha\lambda_1) \tag{4.85}$$

$$\sqrt{\lambda_2}\mathsf{Re}(b) \sim \mathcal{N}(\rho\|\hat{\mathbf{h}}\|\sqrt{\lambda_2}, \frac{1}{2}\alpha\lambda_2), \tag{4.86}$$

$$\sqrt{\lambda_2}\mathsf{Im}(b) \sim \mathcal{N}(0, \frac{1}{2}\alpha\lambda_2) \tag{4.87}$$

Therefore, $\lambda_1|a|^2 = [\sqrt{\lambda_1}\mathsf{Re}(a)]^2 + [\sqrt{\lambda_1}\mathsf{Im}(a)]^2$ conditioned on $\|\hat{\mathbf{h}}\|$ has a central chi-square distribution with $n_f = 2$ degrees of freedom, and $\lambda_2|b|^2 = [\sqrt{\lambda_2}\mathsf{Re}(b)]^2 + [\sqrt{\lambda_2}\mathsf{Im}(b)]^2$ conditioned on $\|\hat{\mathbf{h}}\|$ has a noncentral chi-square distribution with $n_f = 2$ degrees of freedom.

4.4.2 Conditional PDF of z

The conditional PDF of z is analyzed in three scenarios as follows:

(i) $\lambda_1 = 0$, $\lambda_2 = 1$. It is seen from (4.74) that in this case, $z = |b|^2$, which is noncentral chi-square distributed random variable conditioned on $\|\hat{\mathbf{h}}\|$ with $n_f = 2$ degrees of freedom. From [78], the PDF of z conditioned on $\|\hat{\mathbf{h}}\|$ for $\lambda_1 = 0$ can be described by

$$f_{z|\|\hat{\mathbf{h}}\|}(z) = \frac{1}{\alpha}\exp\left(-\frac{z + |\rho|^2\|\hat{\mathbf{h}}\|^2}{\alpha}\right) I_0\left(\frac{2\rho\sqrt{z}}{\alpha}\|\hat{\mathbf{h}}\|\right) \tag{4.88}$$

where $I_\nu(\cdot)$ is the modified Bessel function of the first kind for the νth order.

(ii) $\lambda_1 = \frac{1}{2}$, $\lambda_2 = \frac{1}{2}$. Again from (4.74), the random variable $z = \frac{1}{2}|a|^2 + \frac{1}{2}|b|^2$ conditioned on $\|\hat{\mathbf{h}}\|$ becomes a noncentral chi-square distributed with $n_f = 4$ degrees of freedom. According to [78], the conditional PDF of z for $\lambda_1 = \frac{1}{2}$ is described by

$$f_{z|\|\hat{\mathbf{h}}\|}(z) = \frac{2\sqrt{2z}}{\alpha\rho\|\hat{\mathbf{h}}\|}\exp\left(-\frac{2z + |\rho|^2\|\hat{\mathbf{h}}\|^2}{\alpha}\right) I_1\left(\frac{2\rho\sqrt{2z}}{\alpha}\|\hat{\mathbf{h}}\|\right) \tag{4.89}$$

(iii) $0 < \lambda_1 < \frac{1}{2}, \frac{1}{2} < \lambda_2 < 1$. The random variable z conditioned on $\|\hat{\mathbf{h}}\|$ is the sum of an independent noncentral chi-square distributed random variable $\lambda_2|b|^2$ and a central chi-square distributed random variable $\lambda_1|a|^2$. According to Equation (5.45) of [85], we can get the conditional PDF of z for $0 < \lambda_1 < \frac{1}{2}$ as follows,

$$f_{z|\|\hat{\mathbf{h}}\|}(z) = \frac{1}{\lambda_1 \alpha \rho \|\hat{\mathbf{h}}\|} \sqrt{\frac{z}{\lambda_2}} \exp\left[-\frac{z + \lambda_2|\rho|^2\|\hat{\mathbf{h}}\|^2}{\lambda_2 \alpha}\right] \times \sum_{i=0}^{\infty} \left[\frac{\sqrt{z}(\lambda_1 - \lambda_2)}{\lambda_1\sqrt{\lambda_2}\rho\|\hat{\mathbf{h}}\|}\right]^i I_{1+i}\left(\frac{2\rho\|\hat{\mathbf{h}}\|}{\alpha}\sqrt{\frac{z}{\lambda_2}}\right) \tag{4.90}$$

4.4.3 Non-conditional PDF of z

The conditional PDFs of z given above, are all conditioned on the vector norm of the CSI at the transmitter $\|\hat{\mathbf{h}}\|$. The real and imaginary parts of each element $\hat{h}_i$ are statistically i.i.d Gaussian random variables with zero-mean and variance $\frac{1}{2}\sigma_h^2$. Clearly, from (3.32), $\|\hat{\mathbf{h}}\|^2$ is central chi-square distributed with $n_f = 2M_t$ degrees of freedom. Hence, $\|\hat{\mathbf{h}}\|$ has a generalized Rayleigh distribution. Let $\hat{\xi}$ denote the random variable $\|\hat{\mathbf{h}}\|$, then the PDF of $\|\hat{\mathbf{h}}\|$ has the form [78]:

$$f_{\|\hat{\mathbf{h}}\|}(\hat{\xi}) = \frac{2\hat{\xi}^{2M_t-1}}{\sigma_h^{2M_t}\Gamma(M_t)} \exp\left(-\frac{\hat{\xi}^2}{\sigma_h^2}\right), \quad \hat{\xi} \geq 0 \tag{4.91}$$

The PDF of z can be obtained by substituting (4.91) and (4.88) or (4.89) or (4.90) into the following equation,

$$f_z(z) = \int_0^{\infty} f_{z|\|\hat{\mathbf{h}}\|}(z) f_{\|\hat{\mathbf{h}}\|}(\hat{\xi}) d\hat{\xi}. \tag{4.92}$$

Fig. 4.5 depicts the PDFs of the coefficient z with $M_t = 2$, $\rho = 0.9$, $\sigma_h^2 = 1$ and $E_b/N_0 = 5, 15$ dB, respectively. The simulation results are the amplitudes of the

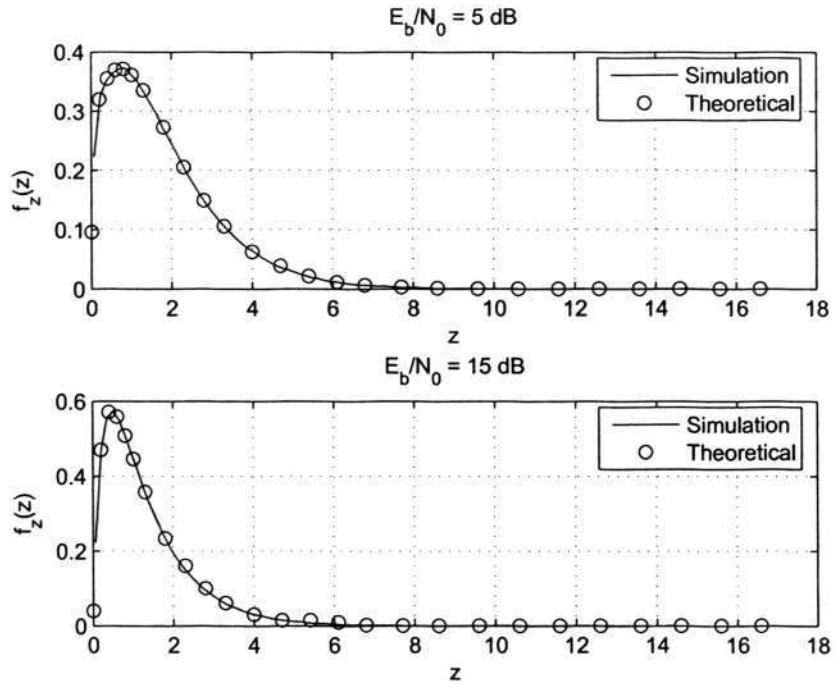

Figure 4.5: The relationship between λ_1 and $\|\hat{\mathbf{h}}\|$ or E_s/N_0

histograms averaged over 1000 000 Monte Carlo feedback realizations. The theoretical results are calculated from (4.92). It can be seen that the simulation results coincide with the theoretical analysis very well. It verifies that the theoretical analysis about the coefficient z's distribution is indeed viable and efficient.

To consider the system performance gain, we should turn our attention into the range of high SNR. Fig. 4.4 shows that the eigenvalue λ_1 approaches $\frac{1}{2}$ at sufficiently high SNR for all values of $\|\hat{\mathbf{h}}\|$, and, therefore, $f_z(z)$ in (4.92) can be simplified for the case of high SNR. It is known that the modified Bessel function of the first kind, $I_\nu(\cdot)$, has a close relationship with the Bessel function of the first kind, $J_\nu(\cdot)$, as follows,

$$I_\nu(x) = j^{-\nu} J_\nu(jx). \tag{4.93}$$

Hence, (4.89) can be rewritten as

$$f_{z|\|\hat{\mathbf{h}}\|}(z) = -j\frac{2\sqrt{2z}}{\alpha\rho\|\hat{\mathbf{h}}\|}\exp\left(-\frac{2z+|\rho|^2\|\hat{\mathbf{h}}\|^2}{\alpha}\right)J_1\left(j\frac{2\rho\sqrt{2z}}{\alpha}\|\hat{\mathbf{h}}\|\right) \tag{4.94}$$

Using the integration formula given in [24],

$$\int_0^\infty x^\mu e^{-tx^2}J_\nu(\beta x)\,dx = \frac{\beta^\nu\Gamma\left(\frac{1}{2}\nu+\frac{1}{2}\mu+\frac{1}{2}\right)}{2^{\nu+1}t^{\frac{1}{2}(\mu+\nu+1)}\Gamma(\nu+1)}\,{}_1F_1\left(\frac{\mu+\nu+1}{2};\nu+1;-\frac{\beta^2}{4t}\right) \tag{4.95}$$

with the constraints $\mathsf{Re}(t) > 0$ and $\mathsf{Re}(\mu+\nu) > -1$, where ${}_1F_1(\cdot;\cdot;\cdot)$ denotes the confluent Hypergeometric function, the non-conditional PDF of z in (4.92) reduces, for high SNR, to

$$f_z(z) = 4z\frac{\alpha^{M_t-2}}{\sigma_h^{2M_t}}\exp\left(-\frac{2z}{\alpha}\right)\,{}_1F_1\left(M_t;2;\frac{2\rho^2 z}{\alpha}\right). \tag{4.96}$$

4.4.4 The Exact BER

In the combined system of non-ideal beamforming and Alamouti's STBC, the received signal before decoding are given by

$$y_1 = a\sqrt{\lambda_1}s_1 - b\sqrt{\lambda_2}s_2^* + e_1 \tag{4.97}$$

and

$$y_2 = a\sqrt{\lambda_1}s_2 + b\sqrt{\lambda_2}s_1^* + e_2 \tag{4.98}$$

After intelligent processing at the receiver, the overall SNR γ_b for each signal is given by

$$\gamma_b = (|a|^2\lambda_1 + |b|^2\lambda_2)\gamma_0 = z\gamma_0. \tag{4.99}$$

Since z is a random variable with the PDF of $f_z(z)$, γ_b is a random variable with the PDF

$$f_{\gamma_b}(\gamma_b) = \frac{1}{\gamma_0}f_z\left(\frac{\gamma_b}{\gamma_0}\right). \tag{4.100}$$

For BPSK modulation, it is well known that the exact BER expression is

$$P_2 = \int_0^\infty Q\left(\sqrt{2\gamma_b}\right) f_{\gamma_b}(\gamma_b) d\gamma_b = \frac{1}{\gamma_0}\int_0^\infty Q\left(\sqrt{2\gamma_b}\right) f_z(\frac{\gamma_b}{\gamma_0}) d\gamma_b \tag{4.101}$$

By applying $f_z(z)$ in (4.92) into the integrand of the above equation and calculating the integral, we get the exact BER for the combined system of the non-ideal beamforming ($|\rho| < 1$) and Alamouti's STBC. Using the exact BER expression which is a double integrals, the combined system BER performance can be obtained much faster than the simulation, especially at high SNR.

4.4.5 The Closed-form Upper Bound of PEP

The BER expression obtained above consists of integral function. In order to analyze and investigate the diversity, coding and array gains of the non-ideal combined system, a closed-form upper bound of PEP is derived. The conditional upper bound of PEP on the equivalent channel is described by

$$P\left(\mathbf{C}, \mathbf{C}'|\mathbf{h}_{eq}\right) \leq \exp\left(-d^2(\mathbf{C}, \mathbf{C}')\frac{1}{4N_0}\right) = \exp\left(-\frac{\delta_2 E_s}{4N_0} z\right) \tag{4.102}$$

Since it is known from Fig. 4.4 that λ_1 approaches to $\frac{1}{2}$ at sufficiently high SNR, the upper bound of PEP is derived by averaging both sides of (4.102) with respect to the distribution in (4.96), i.e.,

$$P\left(\mathbf{C}, \mathbf{C}'\right) \leq \frac{4\alpha^{M_t-2}}{\sigma_h^{2M_t}} \int_0^\infty z \exp\left[-\left(\frac{2}{\alpha} + \frac{\delta_2 E_s}{4N_0}\right) z\right] \; {}_1F_1\left(M_t; 2; \frac{2\rho^2 z}{\alpha}\right) dz \tag{4.103}$$

Again using the formulas given in [24],

$$\int_0^\infty x^{\mu-1} \exp(-sx) \; {}_1F_1(\nu; c; kx) dx = \Gamma(\mu) s^{-\mu} F\left(\nu, \mu; c; ks^{-1}\right) \tag{4.104}$$

and

$$F(-k,\beta;\beta;-x)=(1+x)^k, \tag{4.105}$$

equation (4.103) can be simplified and rewritten as

$$\begin{aligned} P(\mathbf{C},\mathbf{C}') &\leq \frac{4\alpha^{M_t-2}}{\sigma_h^{2M_t}}\left(\frac{2}{\alpha}+\frac{\delta_2 E_s}{4N_0}\right)^{-2} F\left(M_t,2;2;\rho^2\left(1+\frac{\alpha\delta_2 E_s}{8N_0}\right)^{-1}\right) \\ &\leq \frac{4\alpha^{M_t-2}}{\sigma_h^{2M_t}}\left(\frac{2}{\alpha}+\frac{\delta_2 E_s}{4N_0}\right)^{-2}\left[1-\rho^2\left(1+\frac{\alpha\delta_2 E_s}{8N_0}\right)^{-1}\right]^{-M_t} \end{aligned} \tag{4.106}$$

At sufficiently high SNR, the last factor approaches to one, hence the inequality (4.106) is further reduced to

$$P(\mathbf{C},\mathbf{C}') \leq \left(\alpha^{-\frac{M_t-2}{2}}\sigma_h^{M_t-2}\right)^{-2}\left(\frac{1}{2}\delta_2\sigma_h^2\right)^{-2}\left(\frac{E_s}{4N_0}\right)^{-2} \tag{4.107}$$

Thus a diversity advantage of 2 and a coding advantage of $\frac{1}{2}\delta\sigma_h^2$ are achieved, with an additional array gain of $\alpha^{-\frac{M_t-2}{2}}\sigma_h^{M_t-2}$ over the normal single transmitter and receiver systems. Notice that the diversity gain of the non-ideal combined system remains at 2 regardless of the number of transmitting antennas. Therefore, increasing the number of transmitting antennas has no effect on improving the diversity order of the non-ideal combined system. In [76], the authors show that array gain arises from the coherent combining effect of multiple antennas at the receiver or transmitter or both. The effect of array gain is similar to that of coding gain (i.e., it causes a left parallel shift in the BER vs SNR curves). Equation (4.107) shows that increasing the number of transmitting antennas M_t can improve the array gain of the non-ideal combined system.

From the discussion in Section 4.3, we know that the ideal combined system has full diversity advantage of M_t, a coding advantage of $\frac{1}{2}\delta\sigma_h^2$ and an additional

array gain of 2 over the normal single transmitter and receiver systems. The performance difference between the non-ideal and ideal combined systems is that the non-ideal combined system has an improvement in the array advantage, but a loss in diversity advantage.

Compared with the Alamouti scheme, the non-ideal combined system has the same coding gain due to the same encoder and the same diversity order of 2 regardless of the number of transmitting antennas. When $M_t = 2$, the non-ideal combined system has no additional array gain over the Alamouti scheme at high SNR, as can be seen from (4.107). However, a small performance gain can be expected at low SNR. The statement is reasonable in view of that the non-ideal combined system combines the benefits of the conventional beamforming and Alamouti scheme and therefore the non-ideal combined system should have more performance gain over Alamouti scheme. It is shown above that the non-ideal combined system has similar performance to Alamouti scheme at high SNR. Therefore, its performance gain over Alamouti scheme should appear at low SNR. The mathematical analysis can also verify the statement. In the case of imperfect CSI at the transmitter, if the SNR value tends to 0, the first term of $\mathbf{\Psi}_{\bar{k}\bar{l}}$ in (3.12) also approaches to 0. $\mathbf{\Psi}_{\bar{k}\bar{l}} \approx \frac{1}{\alpha}\mathbf{I}_{M_t M_r}$. It turns out that the performance result is similar to the one derived in the case of perfect CSI at the transmitter. It is known from Section 4.3 and Fig. 4.2 that the ideal combined system with perfect CSI at the transmitter has a small performance gain over Alamouti scheme due to its additional array gain. Therefore, as the SNR decreases, the curve of the non-ideal combined system approaches to that of the ideal combined system. Thus, a small performance

gain of the non-ideal combined system can be expected over Alamouti scheme at low SNR. It is worth noting, that these conclusions are true only because of the assumption that the channel estimation is perfect at the receiver, regardless of the SNR. In practice, at low SNR the channel estimation becomes very poor at the receiver and the feedback CSI becomes useless. Therefore, we cannot expect any gain at all for the non-ideal combined system over the Alamouti scheme even at low SNR. Hence, with the assumption of perfect channel estimation at the receiver, the performance of the former is slightly better than the latter at low SNR while it approaches the latter at high SNR, as illustrated in Fig. 4.7. When $M_t > 2$, it can be obtained that the former has an additional array gain of $AG = \alpha^{-\frac{M_t-2}{2}}\sigma_h^{M_t-2}$ over the latter from dividing the right-hand side of (4.107) by that of (4.53).

Although the non-ideal combined system has a worse diversity gain compared with the corresponding OSTBC for $M_t > 2$, but has an additional array gain. Consequently, at specific BER value, the non-ideal combined Alamouti's code and beamforming may have better performance gain than the conventional OSTBC system because the array gain of the former is much larger than the diversity gain of the latter.

To compare with the conventional combined system of beamforming and OSTBC, its upper bound of PEP can be derived by following similar derivation procedure for the non-ideal combined system of beamforming and Alamouti's STBC. It is straightforward to obtain the upper bound of PEP for the conventional combined

system to be,

$$P(\mathbf{C}, \mathbf{C}') \leq \left(\frac{1}{M_t}\delta_{M_t}\sigma_h^2\right)^{-M_t}\left(\frac{E_s}{4N_0}\right)^{-M_t} \tag{4.108}$$

It can be observed that the upper bound of PEP for the conventional combined system has the same expression as the conventional OSTBC in (4.58). It means that the conventional combined system has the same coding gain and diversity gain as OSTBC. However, it has no additional array gain at high SNR, unlike the proposed combined system of beamforming and Alamouti's STBC. This justifies the simulation results in [45] that at high SNR, the performance of the conventional combined system approaches to that of the conventional OSTBC. Similar to the conventional OSTBC, the performance improvement due to the diversity gain of the conventional combined system overwhelms that of the proposed combined system due to the array gain at high SNR.

4.4.6 Numerical Results

Numerical results are provided to demonstrate the performance analyses developed in this section and to compare the new combined beamforming and Alamouti's STBC system with the conventional methods — conventional OSTBC and conventional combined system of beamforming and OSTBC. For fair comparison, all different systems are kept at a BPS of 1bit/symbol as described in Section 4.3.3.

Fig. 4.6 shows the BER performances of the combined system of beamforming and Alamouti's STBC with different number of transmitting antennas, obtained by theoretical analysis and Monte Carlo simulations. The variance of the channel coefficients was arbitrarily set at $\sigma_h^2 = 1$ and the feedback quality was set to $\rho = 0.9$.

It can be seen that the theoretical BER and the simulation results matched very

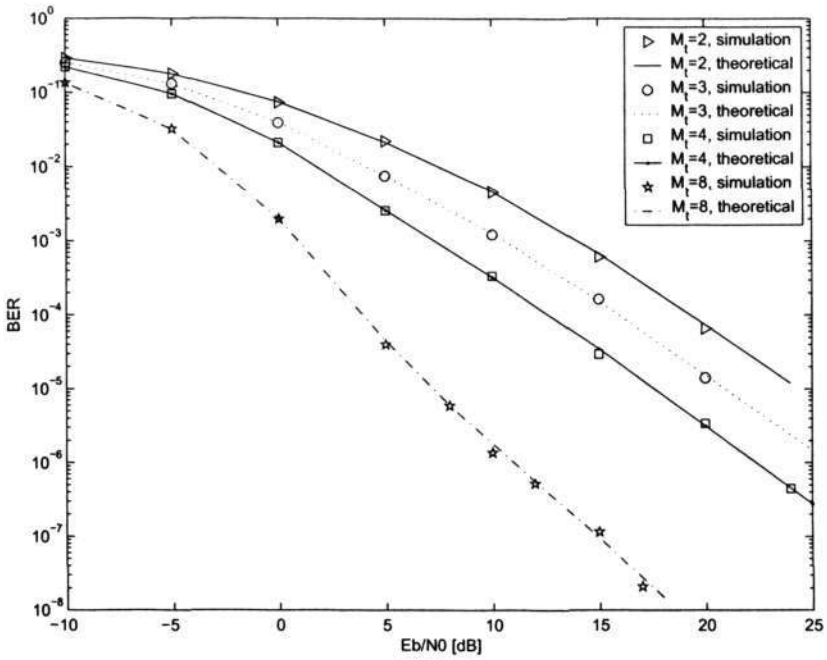

Figure 4.6: Comparison of simulation and theoretical results for the combined system BER of beamforming and Alamouti's STBC with different number of antennas

well regardless of the number of transmitting antennas. Therefore, the exact BER expression in (4.101) is effective to compute the BER for the combined system of beamforming and Alamouti's STBC with multiple transmitting antennas. It is known from Section 4.4 that the non-ideal combined system has the same diversity gain of 2 regardless of the number of transmitting antennas and an array gain of $\alpha^{-\frac{M_t-2}{2}}\sigma_h^{M_t-2}$. As described in [87], the diversity gain and coding gain are derived at sufficiently high SNR. Equation (4.106) in Section 4.4.5 is also approximated to Equation (4.107) for high SNR. The power of the SNR in the denominator of Equation (4.107) denotes the diversity gain of the system, which embodies the slope of the performance curve at high SNR. Hence, it only makes sense for high SNR.

The slope of the performance curve varies at low to medium SNR. For example, at some low SNR range, the slope of the curve for eight transmitting antennas is less than 2, while at some medium SNR range, the slope is higher than 2. Both the slopes can not indicate the system diversity gain. At high SNR, the slope of the curve is stable, which indicates the diversity gain. The curves in Fig. 4.6 have the same slope at sufficiently high SNR, which confirms that the non-ideal combined systems have the same diversity gain regardless of the number of transmitting antennas. Furthermore, this figure also confirms that due to the array gain, an approximately 3.6dB performance improvement can be achieved for each increment of the number of transmitting antennas, for example, from $M_t = 2$ to $M_t = 3$, as well as from $M_t = 3$ to $M_t = 4$.

Theoretically, from the above observation we can conclude that the BER will improve indefinitely as we increase the number of transmitting antennas. However, this is impossible in practice. One of the explicit explanations is as follows. Before we can coherently combine y_1 and y_2 in (4.97) and (4.98) at the receiver, we need synchronization process using pilot signals for each antenna. Our simulations are conducted under the assumption that synchronization can be achieved regardless of the signal power at each antenna. However, as the number of transmitting antennas increases, the power of pilot signals becomes lower and lower under the condition of the same total transmission power. If this pilot power is too low, then there is no way to synchronize and also to estimate the CSI at the receiver. Hence, the system performance cannot continually improve with the increase of the number of transmitting antennas in practice.

The BER performance comparison between the combined system and the conventional OSTBC for different antennas is depicted in Fig. 4.7. In the legend of

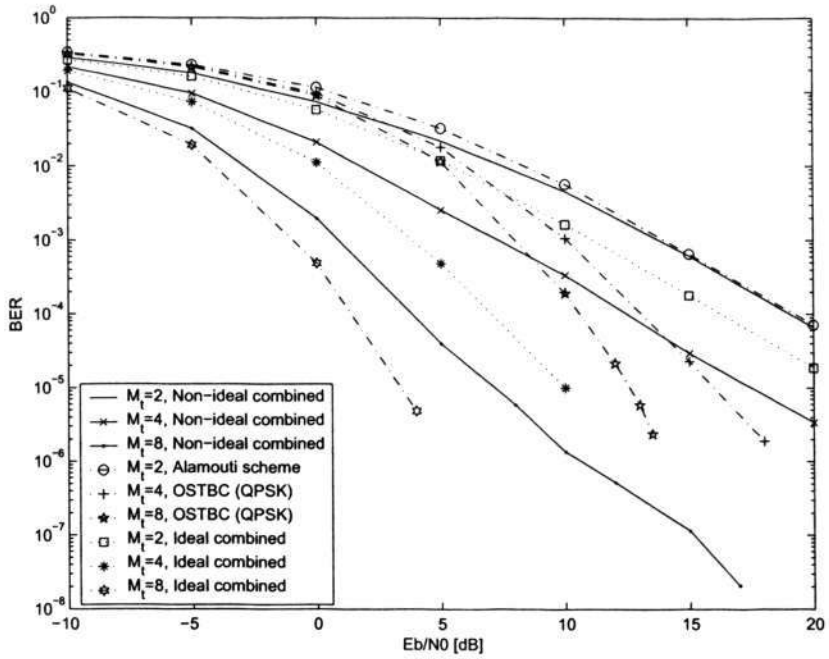

Figure 4.7: Comparison of the combined system and the conventional OSTBC for the system BER

this figure, "Non-ideal" represents the simulation result of the combined system of non-ideal beamforming and Alamouti's STBC with the CSI imperfection set to $\rho = 0.9$; "Ideal" denotes the simulation result of the combined system of ideal beamforming and Alamouti's STBC with $\rho = 1$; and "OSTBC" is used to denote the simulation of the conventional OSTBC without beamforming as proposed in [89]. As seen, the curves of the ideal combined systems have the same slope as the corresponding conventional OSTBC due to the same diversity gain, while they all have a parallel shift to the left over the corresponding conventional OSTBC due to the array gain AG and the coding gain CG, discussed in Section 4.3.

The curves of the non-ideal combined systems are all parallel to that of Alamouti scheme at high SNR because all of them have the same diversity gain of 2. For two transmitting antennas, the curve of the non-ideal combined system approaches the one of Alamouti scheme as the SNR increases. For more than two transmitting antennas, the curves of the non-ideal combined system have a parallel shift to the left over Alamouti scheme due to the additional array gain of $\alpha^{-\frac{M_t-2}{2}}\sigma_h^{M_t-2}$. The non-ideal combined system combines the advantages of both beamforming and Alamouti scheme. Clearly, the performance of the non-ideal combined system improves significantly over the Alamouti scheme as the number of antennas increases to more than two.

In the case of four transmitting antennas, although the performance of the non-ideal combined system is worse than that of the conventional OSTBC at high SNR, as expected, it is much better than the conventional OSTBC at the low SNR of the practically useful region of the BER values due to the array gain. As the number of transmitting antennas increases to 8, it is obvious that the advantage of array gain overwhelms the diversity gain at the desired BER.

Fig. 4.8 shows the performance comparison between the combined system of beamforming and Alamouti's STBC and the combined conventional OSTBC with beamforming as proposed in [45]. To keep the same BPS of 1bit/symbol, the system parameters used for different combined systems are summarized in Table 4.2. The combined system of beamforming and Alamouti's STBC can achieve the same BER performance as the conventional combined system of beamforming and OSTBC at low SNR. But, at high SNR, the performance of the latter is much better

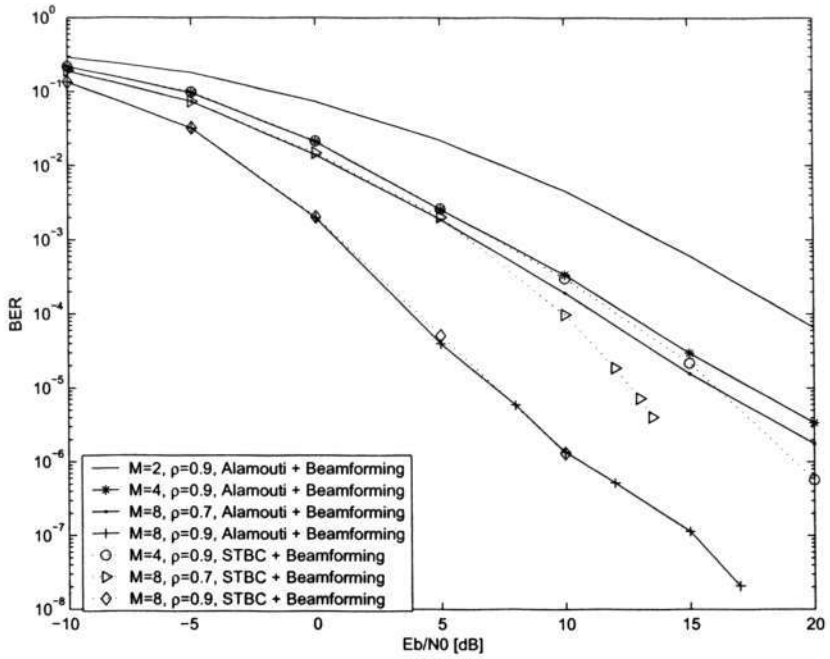

Figure 4.8: Performance comparison of the combined system of beamforming and Alamouti's STBC with the conventional combined system of beamforming and OSTBC

Combined System	No. of Transmitting Antennas	Code Rate	Modulation	Modulation Throughput
Alamouti and Beamforming	$M_t = 2$	$R = 1$	BPSK	$m = 1$
Alamouti and Beamforming	$M_t = 4$	$R = 1$	BPSK	$m = 1$
Alamouti and Beamforming	$M_t = 8$	$R = 1$	BPSK	$m = 1$
OSTBC and Beamforming	$M_t = 4$	$R = 1/2$	QPSK	$m = 2$
OSTBC and Beamforming	$M_t = 8$	$R = 1/2$	QPSK	$m = 2$

Table 4.2: System parameters implemented in this comparison of Fig. 4.8

than that of the former. This is due to the conventional combined system has more diversity gain when the number of transmitting antennas is greater than 2. However, the combined beamforming and Alamouti's STBC system has much lower computational complexity, and it remains at full code rate for more than

2 transmitting antennas, which cannot be achieved by the conventional combined system. Furthermore, no new STBC of different dimension is required every time the number of antennas is changed, as the same Alamouti's STBC is used in the combined system regardless of the number of antennas. In this way, the design phase can be made simpler.

Meanwhile, it is observed from Fig. 4.8 that the performance improvement of the conventional combined system over the combined beamforming and Alamouti's STBC decreases as the number of transmitting antennas increases. For example, for four transmitting antennas and $\rho = 0.9$, the investigated combined system starts to show worse performance than the conventional combined system when the BER is below the level of 3×10^{-4}, while for eight transmitting antennas, the point of departure is at BER$= 6 \times 10^{-6}$. Moreover, the performance improvement of the conventional combined system decreases more seriously as the CSI imperfection ρ increases. For example, for eight transmitting antennas, the point of departure for the two systems' performances for $\rho = 0.7$ is at 2×10^{-3}. Therefore, the combined system of beamforming and Alamouti's STBC has a great advantage for a large number of transmitting antennas and good feedback quality.

4.5 Summary

In this chapter, a beamforming technique based on the CSI at the transmitter is employed to combine the Alamouti's STBC with more than two transmitting antennas in order to get more diversity gain or array gain while keeping the full code rate. Two scenarios are considered to investigate the performance of the

proposed system: one is the perfect CSI at the transmitter and the other one is the imperfect CSI at the transmitter. For the perfect CSI, a closed-form BER expression is derived, while for the imperfect CSI case, the exact BER expression involving only double integrals is given. With the BER expressions, the system BER performance can be obtained much faster than the simulation, especially at high SNR. The upper bound of PEP for the proposed system over the two scenarios are also derived to further analyze the diversity gain, coding gain and array gain. With the upper bound of PEP, it is convenient to compare the proposed system with the conventional OSTBC as well as the existing combined system of beamforming and OSTBC. Numerical results demonstrate that though the non-ideal Alamouti combined system does not improve the diversity gain of two, the array gain advantage of the combined system may overwhelm the diversity gain of the conventional OSTBC at the desired SNR, especially for a large number of transmitting antennas. With imperfect CSI at the transmitter, the comparison between the proposed system and the existing combined system of beamforming and OSTBC shows that, although the performance of the former is much worse than that of the latter at high SNR, the former performs as well as the latter at low to medium SNR. However, the Alamouti combined system is much simpler to design and retains full code rate regardless of the number of transmitting antennas. For any number of transmitting antennas, the Alamouti combined system requires no new STBC of different dimension to be designed. Therefore, the combined system of beamforming and Alamouti's STBC can achieve a tradeoff between performance and complexity especially for a large number of transmitting antennas and good

feedback quality.

Chapter 5

Joint Design of Beamforming and Linear STBC

5.1 Introduction

A few research works [10, 29, 45, 48, 56–58, 69, 96, 97] have been published which discuss how to incorporate the perfect or imperfect CSI at the transmitter into the design of optimal transmitter. In [29, 69, 96], the design of transmitter beamformer considering the imperfect CSI was addressed. In [45, 56–58, 97], the transmitter beamforming and a predetermined OSTBC are combined into one single low-complexity transmission mode based on the perfect or imperfect CSI at transmitter. The design of unstructured STBC that uses the quantized and outdated CSI at the transmitter is investigated in [48] and reviewed in Chapter 3 in this thesis. The efficient codes in [48] are found by optimizing the design criterion based on the union bound on the BLER technique, using a simple gradient search algorithm. The goal of the union bound criterion is herein to minimize the BLER. The numerical gradient search is a locally optimal algorithm. To remedy this, it should be repeated several times, each with different initialization and selecting

the best of the resulting solutions. All of these design schemes are based on various design criteria for different purposes.

It is known that there are many design criteria exist for pursuing the optimal transmitting diversity design, including capacity criterion [38, 39], mutual information criterion [22, 27, 69, 70, 93] (which specifies the theoretical achievable maximum rate of reliable communication in the absence of delay and processing constraints), expected SNR criterion [69] and error probability criterion including the worst-case PEP [45], the symbol error rate (SER) [9], the Chernoff bound on the SER [98] and the union bound on the BLER [48], etc. The well-known rank criterion and determinant criterion [87] for the design of space-time codes are derived from the worst-case PEP. Subsequently, a trace criterion is proposed in [94] for the design of space-time codes in the case of high diversity order.

In [48], the union bound on the BLER criterion is adopted, based on the feedback CSI which is available at the transmitter. Since each current transmitted codeword is also known at the transmitter, it should be exploited to further improve the system performance. Hence, in this chapter, we propose a new performance criterion taking both the feedback CSI at the transmitter and the current transmitted codewords into account. Meanwhile, the BER performance criterion has always come to our attention, which is striving to minimize the system BER rather than the BLER.

It is known from [48] that the unstructured STBC adopted in Chapter 3 has an important issue of decoding complexity. These codes require an exhaustive search over all codewords. For codes with a moderate number of codewords, the resulting

computational complexity may be tolerable, but for high-rate applications, the high decoding complexity essentially excludes the use of unstructured codes. On the other hand, linear structure may be a more appealing choice for high-rate applications, since it often permits the use of decoding algorithms [42, 92] with significantly lower complexity than an exhaustive search, at the price of lower performance.

In this chapter, we propose to jointly design the linear STBC and beamforming based on the new performance criterion. A simple genetic algorithm (SGA) is utilized to search the best solution, which is a global optimization method rather than the local optimization gradient search algorithm adopted in [48]. The imperfect feedback CSI is considered under two different and fairly general models in the form of noisy or quantized measurement as in [69]. The new design criterion and the resulting optimization problem for two CSI models are developed, respectively. In addition, we analyze some special cases and give some examples of the jointly-designed code in order to understand the system behavior deeply and also to help explain the simulation results. Benefiting from the new performance criterion, the jointly-designed code has advantage in both BLER and BER performances, although the linear structure of the code limits the freedom of design, over the unstructured code used in Chapter 3. This is illustrated by numerical results.

5.2 System Model

We consider a MISO narrowband wireless communication system making use of linear STBC based on the available CSI at the transmitter. Fig. 5.1 illustrates

such a system model comprising M_t transmitting antennas and a single receiving antenna. The CSI is fed back from the receiver to the transmitter through a

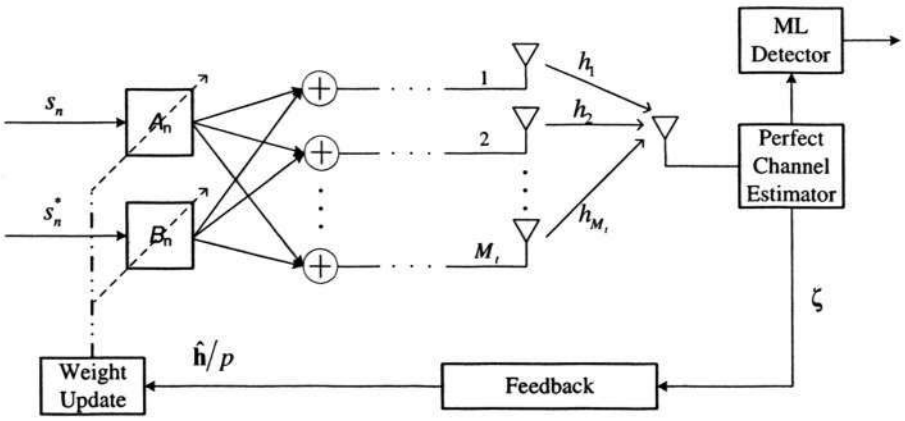

Figure 5.1: Block diagram of the system model

dedicated feedback link or estimated by using reciprocity in duplexing schemes. We assume that the channel estimate at the receiver is perfect and the linear STBC are used. The codeword matrices in such linear STBC [17, 47, 48, 52] are formed as linear combinations of some information carrying symbols, each weighted by a corresponding matrix that spreads the information both in time and space. Let N denote the number of such symbols corresponding to a codeword and let the set $\mathcal{A} = \{s^i\}_{i=1}^{|\mathcal{A}|}$ of signal points s^i represent the constellation alphabet from which the symbols are chosen. Here, $|\mathcal{A}|$ denotes the cardinality of the set $\mathcal{A}$. For each codeword, the corresponding part of the message to be transmitted is mapped into symbol s_n and its conjugate s_n^* with $s_n, s_n^* \in \mathcal{A}$, forming two parallel sequences $s_1, s_2, \ldots, s_N$ and $s_1^*, s_2^*, \ldots, s_N^*$. These two sequences are then used to compute

the transmitted codeword according to

$$\mathbf{C} = \sum_{n=1}^{N} (s_n \mathbf{A}_n + s_n^* \mathbf{B}_n) \tag{5.1}$$

where $\mathbf{A}_n, \mathbf{B}_n$ are $M_t \times L$ weighting matrices used for spreading the information both in time and space. Enumerating over all symbol sequences gives $K = |\mathcal{A}|^N$ potentially different codewords. Depending on the message to be communicated, the linear STBC encoder chooses which, out of the K codewords, to transmit. Since the codewords are of length L, the code rate is $R = N/L$ and the spectral efficiency of the linear STBC is $\eta_{se} = N \log_2(|\mathcal{A}|)/L$ bits/s/Hz. The choices of $\mathcal{A}$, N, and L thus allow an appropriate tradeoff between data rate and time redundancy.

Traditionally, $\{\mathbf{A}_n, \mathbf{B}_n\}_{n=1}^N$ is a set of fixed transmitter weighting matrices, such as OSTBC as discussed in Chapter 2. The combined system of beamforming and Alamouti's STBC for BPSK modulation proposed in Chapter 4 can be also viewed as a subclass of $M_t \times 2$ dimensional linear STBC with $N = 2$ and code rate of $R = 1$, where the weighting matrix of the Alamouti's STBC is predetermined while the weighting matrix of beamforming is adapted separately to the perfect or imperfect channel characteristics according to the CSI at the transmitter. Because of orthogonality of Alamouti's STBC, the performance of the combined system is suboptimal.

In this chapter, we jointly design the beamforming and linear STBC dependent on the CSI at the transmitter. For simplicity and for the purpose of comparing with the related work in [45, 48, 56–58], BPSK modulation is adopted. Thus, the input symbols of (5.1) become no imaginary parts and the weighting matrix $\mathbf{B}_n$

is incorporated into the weighting matrix $\mathbf{A}_n$. The number of symbols, N, and the length L of the block codeword are set to be equal, $N = L$, to ensure the jointly-designed system remains a full code rate $R = N/L = 1$. However, it is straightforward to generalize the proposed method to the linear STBC with any length, any symbols and other M-PSK modulations. Note that the specified jointly-designed codes, which has a full code rate, can be expressed by,

$$\mathbf{C} = \sum_{n=1}^{N} s_n \mathbf{A}_n \tag{5.2}$$

where $\{\mathbf{A}_n\}_{n=1}^{N}$ are adjusted according to the CSI at the transmitter. Let E_s represent the average energy per information symbol and let $\mathcal{C}$ denote the codeword constellation, i.e., $\mathcal{C} = \{\mathbf{C}_k\}_{k=1}^{K}$. Due to BPSK modulation, we have $|\mathcal{A}| = 2$, thus $K = 2^N$. In order to ensure the average output power per symbol epoch to be E_s, the constraint

$$\sum_{k=1}^{K} \|\mathbf{C}_k\|_{\mathrm{F}}^2 = E_s K \log_2 K \tag{5.3}$$

is imposed under the assumption that all the codewords are transmitted with equal probability.

The complex baseband received data model may be written as follows,

$$\mathbf{Y} = \mathbf{h}\mathbf{C} + \mathbf{E} \tag{5.4}$$

where $\mathbf{Y}$ is a $1 \times L$ row vector $\mathbf{Y} = [\ y_1 \quad y_2 \quad \cdots \quad y_L\ ]$ representing the received data over L time intervals, $\mathbf{E} = [\ e_1 \quad e_2 \quad \cdots \quad e_L\ ]$ is the independent AWGN samples with zero-mean and variance $\sigma^2 = N_0/2$ per dimension and $\mathbf{h}$ is a $1 \times M_t$ complex row vector denoting the channel coefficients from the M_t transmitting antennas to the single receiving antenna, which is further discussed in Section 5.2.1.

5.2.1 The channel model

The associated fading model is again assumed to be the so-called *simplified fading scenario* as in [45, 48] for illustrative purpose. The complex channel vector $\mathbf{h} = \begin{bmatrix} h_1 & h_2 & \cdots & h_{M_t} \end{bmatrix}$ consists of M_t statistically normalized identical and independent coefficients. The coefficient h_i $(i = 1, 2, \ldots, M_t)$ is the ith circularly complex Gaussian distributed channel's parameter with zero-mean and variance $\sigma_h^2 = E\left[|h_i|^2\right]$. The channels are assumed to be time-correlated and satisfy the quasi-static Rayleigh flat fading.

At the receiver, the $1 \times M_t$ row vector $\boldsymbol{\zeta}$, with elements $\{\zeta_i\}$, is used to represent the *initial channel information* which is fed back to the transmitter. In view of the well-known Jakes fading model [41], the following assumptions are reasonable. The initial channel information $\boldsymbol{\zeta}$ is a delayed copy of the current true channel $\mathbf{h}$ due to the feedback delay and the time-varying nature of the wireless channel. Since the channel coefficients are time-correlated, the outdated version $\boldsymbol{\zeta}$ is correlated, to an arbitrary degree, with the current true channel $\mathbf{h}$. In the simplified fading scenario, each element ζ_i is correlated with the corresponding coefficient h_i, and uncorrelated with all others. The amount of such correlation is determined by the time it takes to feed back the CSI. The normalized correlation coefficient ρ is introduced to describe the degree of correlation, where $\rho = E[h_i \zeta_i^*] / \sigma_h^2$, which is a measure of the initial channel information quality as used in [45, 48]. More precisely, we further assume that $\mathbf{h}$ and $\boldsymbol{\zeta}$ are jointly complex Gaussian since they are samples of the same time-correlated stationary Gaussian random process. Their

distribution is completely characterized by the mean vector $\mathbf{m_h} = \mathbf{m_\zeta} = \mathbf{0}$, the covariance matrices $\mathbf{R_{hh}} = \mathbf{R_{\zeta\zeta}} = \sigma_h^2 \mathbf{I}_{M_t}$ and the cross-covariance $\mathbf{R_{h\zeta}} = \sigma_h^2 \rho \mathbf{I}_{M_t}$, where $\mathbf{I}_{M_t}$ is the $M_t \times M_t$ dimensional identity matrix. It is shown in [45, 48] that the mean and the covariance matrix of $\mathbf{h}$ conditioned on $\boldsymbol{\zeta}$ is described respectively by

$$\mathbf{m_{h|\zeta}} = \rho\boldsymbol{\zeta}, \quad \mathbf{R_{hh|\zeta}} = \sigma_h^2(1 - |\rho|^2)\mathbf{I}_{M_t} = \alpha \mathbf{I}_{M_t} \tag{5.5}$$

5.2.2 The CSI at the transmitter

Besides the feedback delay, the CSI at the transmitter may also suffer from the noise in the feedback link or the quantization errors. In the following, we consider two different and fairly general models that capture the salient features of practical systems about the feedback CSI at the transmitter in the form of noisy or quantized measurement as in [69].

5.2.2.1 Noisy CSI

In this model, it is assumed that the CSI obtained at the transmitter is corrupted by the AWGN of the feedback link, which can be expressed by

$$\hat{\mathbf{h}} = \boldsymbol{\zeta} + \boldsymbol{\epsilon} \tag{5.6}$$

where the AWGN $\boldsymbol{\epsilon} \sim \mathcal{CN}(0, \sigma_\epsilon^2)$. From (5.6), it follows that

$$E[h_i \hat{h}_i^*] = E[h_i \zeta_i^*] + E[h_i \epsilon_i^*]. \tag{5.7}$$

The correlation between the AWGN $\boldsymbol{\epsilon}$ and the true channel, $\mathbf{h}$, is zero since h_i and its corresponding ϵ_i are independent. Therefore, the noisy and outdated CSI $\hat{h}_i$ at the transmitter is correlated with the current true channel h_i. The correlation

between $\hat{h}_i$ and h_i is the same as that between ζ_i and h_i, and the amount of such correlation is also determined by the feedback delay and not by the AWGN of the feedback channel, i.e., $E\left[h_i\hat{h}_i^*\right]/\sigma_h^2 = \rho$. The detailed explanation is discussed in Chapter 4. Hence, we opt for ρ as the quality describing the CSI at the transmitter. Perfect CSI at the transmitter corresponds to $\rho \to 1$, as discussed in [56]. No CSI at the transmitter corresponds to $\rho \to 0$ and in the other cases of imperfect CSI at the transmitter, $0 < |\rho| < 1$.

5.2.2.2 Quantized CSI

As an alternative model for the CSI at the transmitter that matched to most classes of practical systems, we consider a scenario as in [48] in which the initial channel information is quantized into a b-bit integer $p = f_n(\boldsymbol{\zeta}) \in \{0, 1, \ldots, 2^b - 1\}$, which is transported to the transmitter via a dedicated feedback link. The feedback link is assumed to have an ideal feedback channel, i.e., it does not introduce any bit errors. Consequently, the integer p represents the quantized CSI available at the transmitter. It is used to choose the jointly-designed linear STBC $\mathcal{C}$ from a set of 2^b different codes $\mathcal{C}(p)$.

As in [48], we will implement b-bit *uniform scalar quantization of the phases* of $\zeta_i/\zeta_1, i = 2, \ldots, M_t$, for the closed-loop MISO system model. The quantizer $f_n(\boldsymbol{\zeta})$ divides the space of the initial channel information vector $\boldsymbol{\zeta}$ into 2^b regions $\{O_p\}_{p=0}^{2^b-1}$, based on the mapping $\boldsymbol{\zeta} \in O_p \Rightarrow f_n(\boldsymbol{\zeta}) = p$. The codebook vectors $\{\hat{\boldsymbol{\zeta}}(p)\}_{p=0}^{2^b-1}$ are given by

$$\hat{\boldsymbol{\zeta}}(p) = \left[\begin{array}{cccc} 1 & e^{j\phi_{\tau_0(p)}} & \cdots & e^{j\phi_{\tau_{M_t-2}(p)}} \end{array}\right] \tag{5.8}$$

where $\phi_{\tau_\nu(p)} = 2\pi\tau_\nu(p)/2^{\bar{b}}, \nu = 0, \ldots, M_t - 2$, $\bar{b} = b/(M_t - 1)$ represents the number of bits per complex-valued dimension and $\tau_\nu(p) \in \{0, 1, \ldots, 2^{\bar{b}} - 1\}$ has the relation of $p = \sum_{\nu=0}^{M_t-2} \tau_\nu(p) 2^{\bar{b}\nu}$. Thus, the specific quantization function is defined by

$$p = f_n(\boldsymbol{\zeta}) = \arg \min_{p \in \{0,1,\ldots,2^b-1\}} \left\| \frac{\boldsymbol{\zeta}}{\zeta_1} - \hat{\boldsymbol{\zeta}}(p) \right\|^2 \tag{5.9}$$

The detailed explanation for uniform phase quantization scheme is given in Chapter 3. This quantization scheme is very practical since it is closely related to the feedback scheme adopted by the closed-loop mode of 3G WCDMA system [1].

5.3 Performance Criterion For Joint Design

In practice, the channel information is estimated at the receiver via transmitting pilot symbols or training sequence. The knowledge of transmitter weighting matrix can also be obtained through the same method. For example, a known training sequence is used to detect the transmitter weighting matrix in [49]. More specifically, we can even detect the transmitter weighting matrix and the channel information jointly via the same pilot symbols or training sequence. In this scenario, the detecting of transmitter weighting matrix does not increase the complexity of the receiver seriously. However, both issues of the transmitter weighting matrix detection and the channel estimation go beyond the discussion range of our thesis. Therefore, it is assumed that the ML decoding algorithm is employed based on the perfect channel estimate and the perfect knowledge of transmitter weighting matrix at the receiver, as adopted in [45]. This assumption allows us to isolate the impact on system performance of different degrees of knowledge about the channel

at the transmitter, which is the focus of this thesis. Under this assumption, we propose a new performance criterion for the joint design of beamforming and linear STBC.

From [45], we know that the worst-case PEP, conditioned on the CSI at the transmitter, is the dominating term in the union bound for the combined system of beamforming and the predetermined OSTBC. Hence, the closed-form expression for the performance criterion in [45] is derived from the upper bound of the worst-case PEP conditioned on the CSI at the transmitter, as described in Chapter 3. However, in this chapter, the performance criterion is derived from the weighted sum of the only associated PEPs with respect to the current transmitted codeword, conditioned on the CSI at the transmitter. This criterion is reasonable in view of the fact that the worst-case PEP is not exactly the dominating term of the union bound for the linear STBC without the requirement of orthogonality. Meanwhile, our performance criterion is also different from the performance criterion used in [47, 48] and discussed in Chapter 3, which is based on purely the union bound principle without considering the current transmitted codewords. Following Section 5.2, we develop the performance criteria for the jointly-designed codes in two cases of the noisy and quantized CSI at the transmitter as follows.

5.3.1 Code design for noisy CSI

It is known from Section 5.2 that the jointly-designed linear STBC $\mathcal{C}$ contains K codewords $\{\mathbf{C}_1, \ldots, \mathbf{C}_K\}$ for the given $\{\mathbf{A}_n\}_{n=1}^{N}$. The PEP $P(\mathbf{C}_k \rightarrow \mathbf{C}_l)$ represents the probability that the ML decoding metric for codeword $\mathbf{C}_l$ is smaller than the

metric for $\mathbf{C}_k$, conditioned on the event that $\mathbf{C}_k$ was transmitted, where $k, l \in 1, \ldots, K$ and $k \neq l$. Similar to [45, 58, 87] and Chapter 3, the upper bound of PEP of transmitting $\mathbf{C}_k$ and deciding in favor of $\mathbf{C}_l$ at the decoder, conditioned on the true channel $\mathbf{h}$ and the CSI $\hat{\mathbf{h}}$, can be obtained and is given as follows,

$$\begin{aligned} P\left(\mathbf{C}_k \to \mathbf{C}_l | \mathbf{h}, \hat{\mathbf{h}}\right) &= Q\left(\sqrt{d^2(\mathbf{C}_k, \mathbf{C}_l)\frac{1}{2N_0}}\right) \\ &\leq \frac{1}{2}\exp\left(-d^2(\mathbf{C}_k, \mathbf{C}_l)\frac{1}{4N_0}\right) \end{aligned} \tag{5.10}$$

where $d^2(\mathbf{C}_k, \mathbf{C}_l)$ is given by

$$\begin{aligned} d^2(\mathbf{C}_k, \mathbf{C}_l) &= \|\mathbf{h}(\mathbf{C}_k - \mathbf{C}_l)\|_{\mathrm{F}}^2 \\ &= \mathbf{h}(\mathbf{C}_k - \mathbf{C}_l)(\mathbf{C}_k - \mathbf{C}_l)^{\mathcal{H}}\mathbf{h}^{\mathcal{H}} \end{aligned} \tag{5.11}$$

It is assumed in Section 5.2.1 that the CSI $\hat{\mathbf{h}}$ at the transmitter and the true channel $\mathbf{h}$ are jointly complex Gaussian distributed. As shown in [45], the mean vector and the variance matrix of $\mathbf{h}$ conditioned on $\hat{\mathbf{h}}$ is described respectively by

$$\mathbf{m}_{\mathbf{h}|\hat{\mathbf{h}}} = \rho\hat{\mathbf{h}}, \quad \text{and} \quad \mathbf{R}_{\mathbf{hh}|\hat{\mathbf{h}}} = \sigma_h^2(1 - |\rho|^2)\mathbf{I}_{M_t} = \alpha\mathbf{I}_{M_t}. \tag{5.12}$$

The PDF of $\mathbf{h}$ conditioned on $\hat{\mathbf{h}}$ is also complex Gaussian, given in [45] as follows,

$$p_{\mathbf{h}|\hat{\mathbf{h}}}\left(\mathbf{h}|\hat{\mathbf{h}}\right) = \frac{\exp\left[-(\mathbf{h} - \mathbf{m}_{\mathbf{h}|\hat{\mathbf{h}}})\mathbf{R}_{\mathbf{hh}|\hat{\mathbf{h}}}^{-1}(\mathbf{h} - \mathbf{m}_{\mathbf{h}|\hat{\mathbf{h}}})^{\mathcal{H}}\right]}{\pi^{M_t}\det\left(\mathbf{R}_{\mathbf{hh}|\hat{\mathbf{h}}}\right)} \tag{5.13}$$

The upper bound of PEP, conditioned on the CSI $\hat{\mathbf{h}}$, is formed by averaging both sides of (5.10) over the distribution in (5.13),

$$P\left(\mathbf{C}_k \to \mathbf{C}_l | \hat{\mathbf{h}}\right) \leq \frac{1}{2}\int \exp\left(-\frac{d^2(\mathbf{C}_k, \mathbf{C}_l)}{4N_0}\right) p_{\mathbf{h}|\hat{\mathbf{h}}}\left(\mathbf{h}|\hat{\mathbf{h}}\right) d\mathbf{h} \tag{5.14}$$

After following simple manipulations similar to [45], we have

$$P\left(\mathbf{C}_k \to \mathbf{C}_l | \hat{\mathbf{h}}\right) \leq \frac{\exp\left[\mathbf{m}_{\mathbf{h}|\hat{\mathbf{h}}}\mathbf{R}_{\mathbf{hh}|\hat{\mathbf{h}}}^{-1}(\boldsymbol{\Psi}_{kl}^{-1} - \mathbf{R}_{\mathbf{hh}|\hat{\mathbf{h}}})\mathbf{R}_{\mathbf{hh}|\hat{\mathbf{h}}}^{-1}\mathbf{m}_{\mathbf{h}|\hat{\mathbf{h}}}^{\mathcal{H}}\right]}{2\det\left(\mathbf{R}_{\mathbf{hh}|\hat{\mathbf{h}}}\right)\det(\boldsymbol{\Psi}_{kl})} \tag{5.15}$$

where

$$\mathbf{\Psi}_{kl} = (\mathbf{C}_k - \mathbf{C}_l)(\mathbf{C}_k - \mathbf{C}_l)^{\mathcal{H}}/4N_0 + \mathbf{R}^{-1}_{\mathbf{hh}|\hat{\mathbf{h}}}. \tag{5.16}$$

Taking the logarithm, neglecting parameter-independent terms and reformulating the exponent in (5.15) lead to the so-called *codeword pair criterion* used in [45] as

$$V(\mathbf{C}_k \to \mathbf{C}_l|\hat{\mathbf{h}}) = \frac{\exp\left(\mathbf{m}_{\mathbf{h}|\hat{\mathbf{h}}}\mathbf{R}^{-1}_{\mathbf{hh}|\hat{\mathbf{h}}}\mathbf{\Psi}^{-1}_{kl}\mathbf{R}^{-1}_{\mathbf{hh}|\hat{\mathbf{h}}}\mathbf{m}^{\mathcal{H}}_{\mathbf{h}|\hat{\mathbf{h}}}\right)}{\det(\mathbf{\Psi}_{kl})}. \tag{5.17}$$

Now our attention is turned onto deriving the weighted sum of the only associated PEPs conditioned on the CSI at the transmitter. For the purpose of illustration we describe the associated design process in the case of $N = L = 2$ and $K = 2^N = 4$. The modulated information data s_1/s_2 are assumed to be $+\sqrt{E_s}$ or $-\sqrt{E_s}$ for BPSK modulation. The information data constellation is formed as,

$$\begin{bmatrix} \mathbf{s}^{(1)} \\ \mathbf{s}^{(2)} \\ \mathbf{s}^{(3)} \\ \mathbf{s}^{(4)} \end{bmatrix} = \sqrt{E_s} \begin{bmatrix} 1 & 1 \\ 1 & -1 \\ -1 & 1 \\ -1 & -1 \end{bmatrix} \tag{5.18}$$

where $\mathbf{s}^{(k)} = [s_1^{(k)}\ s_2^{(k)}](k = 1, \ldots, K)$ represents the input information series to the jointly-designed linear STBC, corresponding to the codeword $\mathbf{C}_k$. Since the input information series $\mathbf{s}^{(k)}$ is known at the transmitter, it is just required to calculate the weighted sum of the PEPs associated with $\mathbf{C}_k$ rather than the union bound of the BER. Consequently, the performance criterion with the noisy CSI at the transmitter is defined as,

$$W(\mathbf{A}_1, \mathbf{A}_2|\hat{\mathbf{h}}, \mathbf{s}^{(k)}) = \sum_{l=1, l\neq k}^{K} q_{kl} V(\mathbf{C}_k \to \mathbf{C}_l|\hat{\mathbf{h}}) \tag{5.19}$$

where q_{kl} is the number of error bits between the codeword pair $\mathbf{C}_k, \mathbf{C}_l$. In the following, we give a detailed description of the parameters in the performance criterion (5.19).

In the first case when the input information series is $\mathbf{s}^{(1)}$, i.e., $k = 1$, the transmitted codeword is $\mathbf{C}_1$. The associated parameters with respect to $\mathbf{C}_1$ are given as follows,

$$\mathbf{\Psi}_{12} = \gamma \mathbf{A}_2 \mathbf{A}_2^{\mathcal{H}} + \mathbf{R}^{-1}_{\mathbf{hh}|\hat{\mathbf{h}}}, \tag{5.20}$$

$$\mathbf{\Psi}_{13} = \gamma \mathbf{A}_1 \mathbf{A}_1^{\mathcal{H}} + \mathbf{R}^{-1}_{\mathbf{hh}|\hat{\mathbf{h}}}, \tag{5.21}$$

$$\mathbf{\Psi}_{14} = \gamma \left(\mathbf{A}_1 \mathbf{A}_1^{\mathcal{H}} + \mathbf{A}_2 \mathbf{A}_1^{\mathcal{H}} + \mathbf{A}_1 \mathbf{A}_2^{\mathcal{H}} + \mathbf{A}_2 \mathbf{A}_2^{\mathcal{H}} \right) + \mathbf{R}^{-1}_{\mathbf{hh}|\hat{\mathbf{h}}} \tag{5.22}$$

where $\gamma = E_s/N_0$. It is obvious that $q_{12} = q_{13} = 1$ while $q_{14} = 2$ in (5.19). Then by substituting (5.20), (5.21), (5.22) and (5.17) into the performance criterion in (5.19), it takes on the equivalent form as

$$\begin{aligned} W(\mathbf{A}_1, \mathbf{A}_2|\hat{\mathbf{h}}, \mathbf{s}^{(1)}) = & \frac{\exp\left(\mathbf{m}_{\mathbf{h}|\hat{\mathbf{h}}} \mathbf{R}^{-1}_{\mathbf{hh}|\hat{\mathbf{h}}} \mathbf{\Psi}_{12}^{-1} \mathbf{R}^{-1}_{\mathbf{hh}|\hat{\mathbf{h}}} \mathbf{m}^{\mathcal{H}}_{\mathbf{h}|\hat{\mathbf{h}}}\right)}{\det(\mathbf{\Psi}_{12})} \\ & + \frac{\exp\left(\mathbf{m}_{\mathbf{h}|\hat{\mathbf{h}}} \mathbf{R}^{-1}_{\mathbf{hh}|\hat{\mathbf{h}}} \mathbf{\Psi}_{13}^{-1} \mathbf{R}^{-1}_{\mathbf{hh}|\hat{\mathbf{h}}} \mathbf{m}^{\mathcal{H}}_{\mathbf{h}|\hat{\mathbf{h}}}\right)}{\det(\mathbf{\Psi}_{13})} \\ & + \frac{2\exp\left(\mathbf{m}_{\mathbf{h}|\hat{\mathbf{h}}} \mathbf{R}^{-1}_{\mathbf{hh}|\hat{\mathbf{h}}} \mathbf{\Psi}_{14}^{-1} \mathbf{R}^{-1}_{\mathbf{hh}|\hat{\mathbf{h}}} \mathbf{m}^{\mathcal{H}}_{\mathbf{h}|\hat{\mathbf{h}}}\right)}{\det(\mathbf{\Psi}_{14})} \end{aligned} \tag{5.23}$$

In the second case of $\mathbf{s}^{(2)}$, i.e., $k = 2$, the transmitted codeword is $\mathbf{C}_2$. The associated parameters with respect to $\mathbf{C}_2$ are given as follows,

$$\mathbf{\Psi}_{21} = \gamma \mathbf{A}_2 \mathbf{A}_2^{\mathcal{H}} + \mathbf{R}^{-1}_{\mathbf{hh}|\hat{\mathbf{h}}} = \mathbf{\Psi}_{12}, \tag{5.24}$$

$$\mathbf{\Psi}_{24} = \gamma \mathbf{A}_1 \mathbf{A}_1^{\mathcal{H}} + \mathbf{R}^{-1}_{\mathbf{hh}|\hat{\mathbf{h}}} = \mathbf{\Psi}_{13}, \tag{5.25}$$

$$\mathbf{\Psi}_{23} = \gamma \left(\mathbf{A}_1 \mathbf{A}_1^{\mathcal{H}} - \mathbf{A}_2 \mathbf{A}_1^{\mathcal{H}} - \mathbf{A}_1 \mathbf{A}_2^{\mathcal{H}} + \mathbf{A}_2 \mathbf{A}_2^{\mathcal{H}} \right) + \mathbf{R}^{-1}_{\mathbf{hh}|\hat{\mathbf{h}}} \tag{5.26}$$

Here, $q_{21} = q_{24} = 1$ while $q_{23} = 2$. We rewrite the performance criterion in (5.19)

by using (5.24), (5.25), (5.26) and (5.17) as

$$W(\mathbf{A}_1, \mathbf{A}_2|\hat{\mathbf{h}}, \mathbf{s}^{(2)}) = \frac{\exp\left(\mathbf{m}_{\mathbf{h}|\hat{\mathbf{h}}}\mathbf{R}^{-1}_{\mathbf{hh}|\hat{\mathbf{h}}}\boldsymbol{\Psi}^{-1}_{12}\mathbf{R}^{-1}_{\mathbf{hh}|\hat{\mathbf{h}}}\mathbf{m}^{\mathcal{H}}_{\mathbf{h}|\hat{\mathbf{h}}}\right)}{\det(\boldsymbol{\Psi}_{12})} + \frac{\exp\left(\mathbf{m}_{\mathbf{h}|\hat{\mathbf{h}}}\mathbf{R}^{-1}_{\mathbf{hh}|\hat{\mathbf{h}}}\boldsymbol{\Psi}^{-1}_{13}\mathbf{R}^{-1}_{\mathbf{hh}|\hat{\mathbf{h}}}\mathbf{m}^{\mathcal{H}}_{\mathbf{h}|\hat{\mathbf{h}}}\right)}{\det(\boldsymbol{\Psi}_{13})} + \frac{2\exp\left(\mathbf{m}_{\mathbf{h}|\hat{\mathbf{h}}}\mathbf{R}^{-1}_{\mathbf{hh}|\hat{\mathbf{h}}}\boldsymbol{\Psi}^{-1}_{23}\mathbf{R}^{-1}_{\mathbf{hh}|\hat{\mathbf{h}}}\mathbf{m}^{\mathcal{H}}_{\mathbf{h}|\hat{\mathbf{h}}}\right)}{\det(\boldsymbol{\Psi}_{23})} \tag{5.27}$$

Similar to the derivation in the first and second cases, it is straightforward to obtain the conditional performance criterion for $\mathbf{s}^{(3)}$ and $\mathbf{s}^{(4)}$ respectively as

$$W(\mathbf{A}_1, \mathbf{A}_2|\hat{\mathbf{h}}, \mathbf{s}^{(3)}) = W(\mathbf{A}_1, \mathbf{A}_2|\hat{\mathbf{h}}, \mathbf{s}^{(2)}), \tag{5.28}$$

due to $\boldsymbol{\Psi}_{31} = \boldsymbol{\Psi}_{13}$, $\boldsymbol{\Psi}_{32} = \boldsymbol{\Psi}_{23}$ and $\boldsymbol{\Psi}_{34} = \boldsymbol{\Psi}_{12}$, and

$$W(\mathbf{A}_1, \mathbf{A}_2|\hat{\mathbf{h}}, \mathbf{s}^{(4)}) = W(\mathbf{A}_1, \mathbf{A}_2|\hat{\mathbf{h}}, \mathbf{s}^{(1)}) \tag{5.29}$$

due to $\boldsymbol{\Psi}_{41} = \boldsymbol{\Psi}_{14}$, $\boldsymbol{\Psi}_{42} = \boldsymbol{\Psi}_{13}$ and $\boldsymbol{\Psi}_{43} = \boldsymbol{\Psi}_{12}$.

Since $\{\mathbf{A}_1, \mathbf{A}_2\}$ are adjusted according to each transmitted codeword besides the CSI at the transmitter, the power constraint should be considered for each codeword. In this chapter, we restrict the output power during every symbol epoch to be E_s, then the average output power per symbol epoch is sure to be E_s. Thus, the power constraint for the new performance criterion is modified to

$$\|\mathbf{C}_k\|_{\mathrm{F}}^2 = E_s \log_2 K = NE_s \tag{5.30}$$

which satisfies the constraint in (5.3). In this example, the power constraint of (5.30) can be further simplified and expressed by

$$\frac{1}{E_s}\|\mathbf{C}_k\|_{\mathrm{F}}^2 = tr\left[\mathbf{A}_1\mathbf{A}_1^{\mathcal{H}} + \mathbf{A}_2\mathbf{A}_2^{\mathcal{H}} + \tau_k\left(\mathbf{A}_2\mathbf{A}_1^{\mathcal{H}} + \mathbf{A}_1\mathbf{A}_2^{\mathcal{H}}\right)\right] = 2 \tag{5.31}$$

where $\tau_k = s_1^{(k)} s_2^{(k)} / E_s$. It is clear that $\tau_1 = \tau_4 = 1$ and $\tau_2 = \tau_3 = -1$.

We jointly design the codes by minimizing the performance criterion with respect to every input information series $\mathbf{s}^{(k)}$ subject to the constraint of (5.31) as follows,

$$\{\mathbf{A}_1, \mathbf{A}_2\} = \arg \min_{tr\left[\mathbf{A}_1\mathbf{A}_1^{\mathcal{H}} + \mathbf{A}_2\mathbf{A}_2^{\mathcal{H}} + \tau_k\left(\mathbf{A}_2\mathbf{A}_1^{\mathcal{H}} + \mathbf{A}_1\mathbf{A}_2^{\mathcal{H}}\right)\right]=2} W(\mathbf{A}_1, \mathbf{A}_2|\hat{\mathbf{h}}, \mathbf{s}^{(k)}) \tag{5.32}$$

where $k = 1, \ldots, K$. A strategy for numerically solving (5.32) is presented in Section 5.4.

Although it is a difficult task to explicitly characterize the optimal set of codewords from the optimization problem in (5.32), we will, in the following paragraphs, present the analyses of the optimal codewords for a few special cases in order to understand the behavior of the transmitter, and also to help explain the simulation results in Section 5.6.

For the special case of high SNR, i.e., $\gamma \to \infty$, the codeword pair criterion in (5.17) converges to the limit function, as derived in [45, 48],

$$V_\infty(\mathbf{C}_k \to \mathbf{C}_l|\hat{\mathbf{h}}) = \frac{1}{\det(\mathbf{\Psi}_{kl})}. \tag{5.33}$$

The performance criterion in (5.19) for high SNR becomes

$$\begin{aligned} W(\mathbf{A}_1, \mathbf{A}_2|\hat{\mathbf{h}}, \mathbf{s}^{(k)}) &= \sum_{l=1, l\neq k}^{K} q_{kl} V_\infty(\mathbf{C}_k \to \mathbf{C}_l|\hat{\mathbf{h}}) \\ &= \sum_{l=1, l\neq k}^{K} \frac{q_{kl}}{\det(\mathbf{\Psi}_{kl})}. \end{aligned} \tag{5.34}$$

By using $\widehat{\mathbf{C}}_k = \mathbf{C}_k / \sqrt{2E_s}$ to re-parameterize the optimization problem and substituting (5.12) into (5.16), we have

$$\mathbf{\Psi}_{kl} = \gamma \mathbf{\Phi}_{kl} + \frac{1}{\alpha}\mathbf{I}_{M_t} \tag{5.35}$$

where $\mathbf{\Phi}_{kl} = (\widehat{\mathbf{C}}_k - \widehat{\mathbf{C}}_l)(\widehat{\mathbf{C}}_k - \widehat{\mathbf{C}}_l)^{\mathcal{H}}$ is a Hermitian square matrix. Obviously, $\mathbf{\Phi}_{kl}$ can be $\mathbf{A}_1\mathbf{A}_1^{\mathcal{H}}$, $\mathbf{A}_2\mathbf{A}_2^{\mathcal{H}}$ or $\mathbf{A}_1\mathbf{A}_1^{\mathcal{H}} + \mathbf{A}_2\mathbf{A}_2^{\mathcal{H}} \pm (\mathbf{A}_2\mathbf{A}_1^{\mathcal{H}} + \mathbf{A}_1\mathbf{A}_2^{\mathcal{H}})$ according to the mapping (5.2). Due to the EVD theorem [33], the $M_t \times M_t$ matrix $\mathbf{\Phi}_{kl}$ can be written as

$$\mathbf{\Phi}_{kl} = \mathbf{\Gamma}\mathbf{\Sigma}_{kl}\mathbf{\Gamma}^{\mathcal{H}} \tag{5.36}$$

where $\mathbf{\Gamma}$ is a $M_t \times M_t$ unitary matrix, and $\mathbf{\Sigma}_{kl}$ is a $M_t \times M_t$ diagonal matrix whose elements are given as

$$\beta_{11} \geq \beta_{22} \geq \cdots \geq \beta_{rr} > \beta_{r+1,r+1} = \cdots = \beta_{M_tM_t} = 0 \tag{5.37}$$

where β_{rr} represents the rth eigenvalue of $\mathbf{\Phi}_{kl}$ and r is the rank of $\mathbf{\Phi}_{kl}$ and $r \leq \min\{M_t, L\}$. Therefore, $\mathbf{\Psi}_{kl}$ is also a Hermitian square matrix and can be formulated using the EVD method as

$$\mathbf{\Psi}_{kl} = \gamma\mathbf{\Gamma}\mathbf{\Sigma}_{kl}\mathbf{\Gamma}^{\mathcal{H}} + \frac{1}{\alpha}\mathbf{\Gamma}\mathbf{I}_{M_t}\mathbf{\Gamma}^{\mathcal{H}} = \mathbf{\Gamma}\left(\gamma\mathbf{\Sigma}_{kl} + \frac{1}{\alpha}\mathbf{I}_{M_t}\right)\mathbf{\Gamma}^{\mathcal{H}} \tag{5.38}$$

Thus,

$$\det(\mathbf{\Psi}_{kl}) = \det\left(\gamma\mathbf{\Sigma}_{kl} + \frac{1}{\alpha}\mathbf{I}_{M_t}\right) = \prod_{i=1}^{M_t}\left(\gamma\beta_{ii} + \frac{1}{\alpha}\right) = \frac{1}{\alpha^{M_t-r}}\prod_{i=1}^{r}\left(\gamma\beta_{ii} + \frac{1}{\alpha}\right) \tag{5.39}$$

Substituting (5.39) into the performance criterion (5.34) for high SNR, it can be seen that r should be as large as possible to guarantee the criterion in (5.34) is minimized. Hence, $r = \min\{M_t, L\}$ in the asymptotically optimal code. From [25, 87], it means that the diversity gain of the jointly-designed code in the noisy CSI measurement model is $\min\{M_t, L\}$.

For the special case of combining beamforming and Alamouti's STBC, the

weighting matrices of Alamouti's STBC are predetermined, which are given by

$$\bar{\mathbf{A}}_1 = \begin{bmatrix} 1 & 0 \\ 0 & 1 \end{bmatrix}, \qquad \bar{\mathbf{A}}_2 = \begin{bmatrix} 0 & 1 \\ -1 & 0 \end{bmatrix} \tag{5.40}$$

for BPSK modulation, and the weighting matrix of beamforming $\mathbf{W}$ is adapted according to the available CSI at the transmitter. Accordingly, the weighting matrices of the combined system are given by

$$\mathbf{A}_1 = \mathbf{W}\bar{\mathbf{A}}_1, \qquad \mathbf{A}_2 = \mathbf{W}\bar{\mathbf{A}}_2. \tag{5.41}$$

Thus, we have

$$\mathbf{A}_1\mathbf{A}_1^{\mathcal{H}} = \mathbf{W}\mathbf{W}^{\mathcal{H}} = \mathbf{A}_2\mathbf{A}_2^{\mathcal{H}} \tag{5.42}$$

$$\mathbf{A}_2\mathbf{A}_1^{\mathcal{H}} + \mathbf{A}_1\mathbf{A}_2^{\mathcal{H}} = \mathbf{W}\left(\bar{\mathbf{A}}_2\bar{\mathbf{A}}_1^{\mathcal{H}} + \bar{\mathbf{A}}_1\bar{\mathbf{A}}_2^{\mathcal{H}}\right)\mathbf{W}^{\mathcal{H}} = \mathbf{0} \tag{5.43}$$

due to the orthogonal nature of Alamouti's STBC. To illustrate that the new performance criterion produces the same effect as the codeword pair criterion for this special case, we give an example of inputting the information series, $\mathbf{s}^{(1)}$, to the encoder. In this case, (5.20), (5.21) and (5.22) become

$$\mathbf{\Psi}_{12} = \mathbf{\Psi}_{13} = \gamma\mathbf{A}_1\mathbf{A}_1^{\mathcal{H}} + \mathbf{R}^{-1}_{\mathbf{hh}|\hat{\mathbf{h}}} \tag{5.44}$$

$$\mathbf{\Psi}_{14} = 2\gamma\mathbf{A}_1\mathbf{A}_1^{\mathcal{H}} + \mathbf{R}^{-1}_{\mathbf{hh}|\hat{\mathbf{h}}} \tag{5.45}$$

The codeword pair criteria corresponding to the terms $\mathbf{\Psi}_{12}$, $\mathbf{\Psi}_{13}$ and $\mathbf{\Psi}_{14}$ are implicitly proportional to $\mathbf{A}_1\mathbf{A}_1^{\mathcal{H}}$. Hence, the new performance criterion (5.19) is implicitly proportional to $\mathbf{A}_1\mathbf{A}_1^{\mathcal{H}}$, since the new performance criterion is just the weighted summation of these codeword pair criteria. This results in that optimizing the worst-case codeword pair criterion has the same effect as the proposed

optimization problem in (5.32). Simultaneously, it verifies the assumption of [45] that the codeword pair criterion, corresponding to the worst-case PEP containing the term $\mathbf{A}_1\mathbf{A}_1^{\mathcal{H}}$ or $\mathbf{A}_2\mathbf{A}_2^{\mathcal{H}}$, is the dominant term in the union bound criterion on the BLER as well as the proposed performance criterion for this special case.

Even though the codeword pair criterion has the same effect on the code design as the new performance criterion in the case of combining beamforming and predetermined OSTBC, it can not be used for the proposed jointly-designed code. Without the requirement of orthogonality, the term $\mathbf{A}_1\mathbf{A}_1^{\mathcal{H}}$ in (5.42) may not be equal to the term $\mathbf{A}_2\mathbf{A}_2^{\mathcal{H}}$ and the sum of the cross terms, $\mathbf{A}_1\mathbf{A}_2^{\mathcal{H}} + \mathbf{A}_2\mathbf{A}_1^{\mathcal{H}}$, in (5.43) may not equal to zero. This means that the individual codeword pair criterion does not possess the aforementioned proportionality. Hence, optimizing the worst-case codeword pair criterion does not mean that the weighted summation of the codeword pair criteria achieves the optimum as what the new performance criterion aims to achieve.

5.3.2 Code design for quantized CSI

Given the quantized CSI, the integer p, the transmitter determines the current channel code $\mathcal{C} = \{\mathbf{C}_k\}_{k=1}^{K}$ from a set $\{\mathcal{C}(p)\}$ of codes. Following Section 5.3.1, we start by exploiting the upper bound of the conditional PEP of transmitting $\mathbf{C}_k^{(p)}$ and deciding in favor of $\mathbf{C}_l^{(p)}$ at the decoder, so as to obtain

$$\begin{aligned} P\left(\mathbf{C}_k^{(p)} \to \mathbf{C}_l^{(p)} | \mathbf{h}, \boldsymbol{\zeta}\right) &= Q\left(\sqrt{d^2(\mathbf{C}_k^{(p)}, \mathbf{C}_l^{(p)}) \frac{1}{2N_0}}\right) \\ &\leq \frac{1}{2} \exp\left(-d^2(\mathbf{C}_k^{(p)}, \mathbf{C}_l^{(p)}) \frac{1}{4N_0}\right) \\ &= \frac{1}{2} \exp\left(-\|\mathbf{h}(\mathbf{C}_k^{(p)} - \mathbf{C}_l^{(p)})\|_{\mathrm{F}}^2 \frac{1}{4N_0}\right) \end{aligned} \tag{5.46}$$

Due to the jointly complex Gaussian relationship of $\mathbf{h}$ and $\boldsymbol{\zeta}$, the PDF of $\mathbf{h}$ conditioned on $\boldsymbol{\zeta}$ is given as follows

$$p_{\mathbf{h}|\boldsymbol{\zeta}}(\mathbf{h}|\boldsymbol{\zeta}) = \frac{\exp\left[-(\mathbf{h}-\mathbf{m}_{\mathbf{h}|\boldsymbol{\zeta}})\mathbf{R}_{\mathbf{hh}|\boldsymbol{\zeta}}^{-1}(\mathbf{h}-\mathbf{m}_{\mathbf{h}|\boldsymbol{\zeta}})^{\mathcal{H}}\right]}{\pi^{M_t}\det\left(\mathbf{R}_{\mathbf{hh}|\boldsymbol{\zeta}}\right)} \tag{5.47}$$

By averaging both sides of (5.46) over the distribution in (5.47) and executing the same manipulations as in [45] and [48], we have

$$P\left(\mathbf{C}_k^{(p)} \to \mathbf{C}_l^{(p)}|\boldsymbol{\zeta}\right) \leq \frac{\exp\left[\mathbf{m}_{\mathbf{h}|\boldsymbol{\zeta}}\mathbf{R}_{\mathbf{hh}|\boldsymbol{\zeta}}^{-1}\left((\boldsymbol{\Psi}_{kl}^{(p)})^{-1}-\mathbf{R}_{\mathbf{hh}|\boldsymbol{\zeta}}\right)\mathbf{R}_{\mathbf{hh}|\boldsymbol{\zeta}}^{-1}\mathbf{m}_{\mathbf{h}|\boldsymbol{\zeta}}^{\mathcal{H}}\right]}{2\det\left(\mathbf{R}_{\mathbf{hh}|\boldsymbol{\zeta}}\right)\det(\boldsymbol{\Psi}_{kl}^{(p)})} \tag{5.48}$$

where

$$\boldsymbol{\Psi}_{kl}^{(p)} = (\mathbf{C}_k^{(p)}-\mathbf{C}_l^{(p)})(\mathbf{C}_k^{(p)}-\mathbf{C}_l^{(p)})^{\mathcal{H}}/4N_0 + \mathbf{R}_{\mathbf{hh}|\boldsymbol{\zeta}}^{-1}. \tag{5.49}$$

Similarly, we take the logarithm, neglect parameter independent terms and reformulate the exponent in (5.48) according to the process in [48]. Thus, referring to the derivation in Section 3.3, the modified *codeword pair criterion* with the quantized CSI at the transmitter can be written as

$$V(\mathbf{C}_k^{(p)} \to \mathbf{C}_l^{(p)}|p) = \frac{\exp\left\{tr\left((\boldsymbol{\Psi}_{kl}^{(p)})^{-1}\mathbf{R}_{\mathbf{hh}|\boldsymbol{\zeta}}^{-1}E[\mathbf{m}_{\mathbf{h}|\boldsymbol{\zeta}}^{\mathcal{H}}\mathbf{m}_{\mathbf{h}|\boldsymbol{\zeta}}|p]\mathbf{R}_{\mathbf{hh}|\boldsymbol{\zeta}}^{-1}\right)\right\}}{\det(\boldsymbol{\Psi}_{kl}^{(p)})} \tag{5.50}$$

where

$$E[\mathbf{m}_{\mathbf{h}|\boldsymbol{\zeta}}^{\mathcal{H}}\mathbf{m}_{\mathbf{h}|\boldsymbol{\zeta}}|p] = |\rho|^2 E[\boldsymbol{\zeta}^{\mathcal{H}}\boldsymbol{\zeta}|p] \tag{5.51}$$

according to (5.5). The expectation in the expression of (5.51) can be obtained from the corresponding sample estimates taken from a Monte Carlo simulation of the quantization process in the feedback link. Similar to the derivation in Section 5.3.1, the performance criterion for the jointly-designed linear STBC with respect to the current transmitted codeword $\mathbf{C}_k^{(p)}$ in the case of quantized CSI at

the transmitter is the weighted sum of the PEPs associated with $\mathbf{C}_k^{(p)}$, given as follows,

$$W(\mathbf{A}_1^{(p)}, \mathbf{A}_2^{(p)}, \ldots, \mathbf{A}_N^{(p)}|p, \mathbf{s}^{(k)}) = \sum_{l=1, l\neq k}^{K} q_{kl} V(\mathbf{C}_k^{(p)} \rightarrow \mathbf{C}_l^{(p)}|p) \tag{5.52}$$

For the special case of high SNR, i.e., $\gamma \rightarrow \infty$, the codeword pair criterion with the quantized CSI at the transmitter in (5.50) converges to the limit function, as derived in [48],

$$V_\infty(\mathbf{C}_k^{(p)} \rightarrow \mathbf{C}_l^{(p)}|p) = \frac{1}{\det(\mathbf{\Psi}_{kl}^{(p)})}. \tag{5.53}$$

The quantized CSI measurement model's performance criterion in (5.52) for high SNR becomes

$$\begin{aligned} W(\mathbf{A}_1^{(p)}, \mathbf{A}_2^{(p)}, \ldots, \mathbf{A}_N^{(p)}|p, \mathbf{s}^{(k)}) &= \sum_{l=1, l\neq k}^{K} q_{kl} V_\infty(\mathbf{C}_k^{(p)} \rightarrow \mathbf{C}_l^{(p)}|p) \\ &= \sum_{l=1, l\neq k}^{K} \frac{q_{kl}}{\det(\mathbf{\Psi}_{kl}^{(p)})}. \end{aligned} \tag{5.54}$$

Similar to the derivation in Section 5.3.1, we can also obtain that performing the design procedure of the quantized CSI measurement model for high SNR ensures that the jointly-designed codes have a diversity gain of $r = \min\{M_t, L\}$. Note also that the criterion in (5.54) does not depend on neither the quantized feedback CSI p nor the channel statistics. Thus, as the SNR increases, the feedback CSI becomes redundant.

For the special case of no feedback CSI, i.e., $\rho = 0$ and $b = 0$, the codeword pair criterion in (5.50) becomes

$$V(\mathbf{C}_k^{(0)} \rightarrow \mathbf{C}_l^{(0)}|0) = \frac{1}{\det(\mathbf{\Psi}_{kl}^{(0)})}. \tag{5.55}$$

due to the mean vector of $\mathbf{h}$ conditioned on $\boldsymbol{\zeta}$, $\mathbf{m}_{\mathbf{h}|\boldsymbol{\zeta}} = \mathbf{0}$. Note that (5.55) has the same expression as the limit function in (5.53). This similarity means that the jointly-designed code with the quantized feedback CSI at a sufficiently high SNR approaches to that without the feedback CSI. The jointly-designed code in the case of no feedback CSI is like an upper bound of the optimal codes.

It is known from Chapter 3 that the uniform phase-quantization method adopted in this work exhibits certain symmetries, i.e., the quantized regions are rotated copies of each other, which means that the codebook vectors in (5.8) can be expressed in terms of the first codebook vector as

$$\hat{\boldsymbol{\zeta}}(p) = \hat{\boldsymbol{\zeta}}(0)\boldsymbol{\Theta}_p \tag{5.56}$$

where $p = 0, \ldots, 2^b - 1$ and the $M_t \times M_t$ dimensional unitary rotation matrix $\boldsymbol{\Theta}_p$ in Chapter 3 becomes a diagonal matrix depending on p in MISO system,

$$\boldsymbol{\Theta}_p = \begin{bmatrix} 1 & 0 & \cdots & 0 \\ 0 & e^{j\phi_{\tau_0(p)}} & \cdots & \vdots \\ \vdots & \vdots & \ddots & 0 \\ 0 & \cdots & 0 & e^{j\phi_{\tau_{M_t-2}(p)}} \end{bmatrix} \tag{5.57}$$

which rotates $\hat{\boldsymbol{\zeta}}(0)$ to the desired position. This quantization symmetry together with the symmetrical statistics of the simplified fading scenario leads to the symmetric feedback of MISO system satisfying the following conditions, as described in Section 3.3,

$$E[\mathbf{m}_{\mathbf{h}|\boldsymbol{\zeta}}^{\mathcal{H}}\mathbf{m}_{\mathbf{h}|\boldsymbol{\zeta}}|p] = \tilde{d}\ \boldsymbol{\Theta}_p \mathbf{U} \boldsymbol{\Theta}_p^{\mathcal{H}} \tag{5.58}$$

$$\mathbf{R}_{\mathbf{hh}|\boldsymbol{\zeta}} = d\ \mathbf{I}_{M_t} \tag{5.59}$$

where $\mathbf{U}$ is a constant $M_t \times M_t$ matrix corresponding to $E[\boldsymbol{\zeta}^{\mathcal{H}}\boldsymbol{\zeta}|p = 0]$, which can be obtained from the corresponding sample estimates by using Monte Carlo simulation

of the quantization function in the feedback link. Here, $\mathbf{U}$ can be evaluated prior to the code search, due to its independence from the codewords. From (5.51) and (5.5), it is clear that $\tilde{d} = |\rho|^2$ and $d = \alpha$.

This symmetrical nature can be exploited to reduce the computational complexity of the code design process significantly. In order to carry the symmetry of the feedback over to a corresponding symmetry of the codes, we let $\mathbf{C}_k^{(p)} = \mathbf{\Theta}_p \tilde{\mathbf{C}}_k$ following the method in [48], where $\tilde{\mathbf{C}}_k = \sum_{n=1}^{N} s_n^{(k)} \tilde{\mathbf{A}}_n$. Substituting this mapping, together with (5.58) and (5.59) into (5.50) results in the new form of the codeword pair criterion,

$$V(\mathbf{\Theta_p}\tilde{\mathbf{C}}_k \rightarrow \mathbf{\Theta}_p\tilde{\mathbf{C}}_l|p) = \frac{\exp\left[(|\rho|^2/\alpha^2) tr\left(\widetilde{\mathbf{\Psi}}_{kl}^{-1}\mathbf{U}\right)\right]}{\det(\widetilde{\mathbf{\Psi}}_{kl})} = V(\tilde{\mathbf{C}}_k \rightarrow \tilde{\mathbf{C}}_l) \qquad (5.60)$$

where

$$\widetilde{\mathbf{\Psi}}_{kl} = (\tilde{\mathbf{C}}_k - \tilde{\mathbf{C}}_l)(\tilde{\mathbf{C}}_k - \tilde{\mathbf{C}}_l)^{\mathcal{H}} \frac{1}{4N_0} + \frac{1}{\alpha}\mathbf{I}_{M_t}. \qquad (5.61)$$

It is obvious that (5.60) is independent of the integer p, then the proposed performance criterion of (5.52) also becomes independent of p as,

$$W(\tilde{\mathbf{A}}_1, \tilde{\mathbf{A}}_2, \ldots, \tilde{\mathbf{A}}_N |\, \mathbf{s}^{(k)}) = \sum_{l=1, l\neq k}^{K} q_{kl} V(\tilde{\mathbf{C}}_k \rightarrow \tilde{\mathbf{C}}_l). \qquad (5.62)$$

Thus we only need to jointly design the specified code $\tilde{\mathcal{C}} = \{\tilde{\mathbf{C}}_k\}_{k=1}^{K}$ by minimizing the above performance criterion (5.62) while subjecting it to the power constraint in (5.30) to arrive at

$$\{\tilde{\mathbf{A}}_n\}_{n=1}^{N} = \arg \min_{\|\tilde{\mathbf{C}}_k\|_{\mathrm{F}}^2 = NE_s} W(\tilde{\mathbf{A}}_1, \tilde{\mathbf{A}}_2, \ldots, \tilde{\mathbf{A}}_N |\, \mathbf{s}^{(k)}). \qquad (5.63)$$

where $k = 1, 2, \ldots, K$. The jointly-designed code $\mathcal{C}(p)$ corresponding to the quantized CSI of p can be constructed through the linear mapping $\mathbf{A}_n^{(p)} = \mathbf{\Theta}_p \tilde{\mathbf{A}}_n$.

It is known from (5.57) that $\mathbf{\Theta}_0 = \mathbf{I}_{M_t}$. Then $\mathbf{A}_n^{(0)} = \mathbf{\Theta}_0 \tilde{\mathbf{A}}_n = \tilde{\mathbf{A}}_n$. Thus, only $\{\mathbf{A}_n^{(0)}\}_{n=1}^N$ are needed to be searched and the remaining weighting matrices $\mathbf{A}_n^{(p)}, p = 1, \ldots, 2^b - 1$ are obtained through the rotation $\mathbf{A}_n^{(p)} = \mathbf{\Theta}_p \mathbf{A}_n^{(0)}$. The look-up table $\{\mathcal{C}(p)\}_{p=0}^{2^b-1}$ is formed by collecting the 2^b jointly-designed linear STBC. The required transmission matrix $\mathbf{C}_k^{(p)}$ is selected from the look-up table dependent on the feedback CSI p, and the input information series $\mathbf{s}^{(k)}$. Hence, the design process for the quantized CSI measurement model is substantially expedited and the memory required to store the code is drastically reduced. Since the quantized feedback CSI, the b-bit integer p, is limited, the search of weighting matrices can be performed off-line and the look-up tables can also be constructed off-line.

Our real interest for the system design is to minimize the BER performance. Therefore, we propose the design criterion as given in (5.52) to minimize the BER performance as much as possible, while [48] uses different design criterion, summing over all codeword pairs based on the union bound criterion on the BLER as follows

$$W(\mathcal{C}|p) = \sum_{k,l=1,k<l}^{K} V(\mathbf{C}_k \rightarrow \mathbf{C}_l|p) \tag{5.64}$$

which assumes that all the information series are transmitted with equal likelihood. The design goal in [48] is to minimize the BLER. However, although the proposed design criterion does give a better BER performance as compared with the union bound criterion used in [48], the gain is not as expected. This will be explained later in Section 5.5 and 5.6.

5.4 Numerical Optimization

The optimization problems of (5.32) and (5.63) are non-convex and difficult to solve analytically in general. Numerical optimization techniques are therefore required to implement the design procedure. In [48], a simple gradient search algorithm is used, but the resulting solutions can only be expected to be locally optimal. This algorithm must be remedied by repeating the gradient search several times using different initial guesses. Here, we use a SGA described in [23] to numerically find the global optimum. SGA is a stochastic global search method by applying the principle of survival of the fittest to produce better and better approximations to a solution. Hence, repetition using different initial guesses is not required. The SGA as a random search process provides no limits regarding the required time and search effort to reach a global solution. We give an upper limit in the search effort. Generally, the upper limit in the search effort will affect the performance of the proposed system more or less. However, to fairly compare with the proposed system, the performances of the jointly-designed unstructured code are also obtained by using SGA with the same upper limit in the search effort as the proposed jointly-designed linear code. The methods we adopt for solving each of the major components of SGA in this work are outlined in Table 5.1.

Note that the time it takes to complete such jointly-designed procedure depends on the size of the problem. The number of the elements in each weighting matrix is $M_t \times L$. There are $N = \log_2 K$ weighting matrices for each codeword. Here, the real part and imaginary part of each weighting element are encoded as a binary

Components of SGA	Methods adopted
Solution Representation	Gray binary-coded and logarithmic scaling
Fitness Function	linear ranking
Selection Function	stochastic universal sampling
Crossover	single-point crossover
Mutation	binary mutation
Reinsertion	fitness-based reinsertion
Termination	specified maximum number of generations

Table 5.1: Major components implemented in this work

string by employing Gray coding, respectively. Hence, the number of parameters in the design criterion is $N_{par} = 2M_t L \log_2 K$.

In the noisy CSI measurement model, the SGA exhaustive search of the optimal weighting matrices must be executed for every transmission since the transmitting codeword and the current noisy CSI at the transmitter vary for every update. It is a very tedious work and needs remarkable computing power. On the other hand, in the quantized CSI measurement model, the design procedure may be performed off-line and the transmission scheme can be efficiently implemented by using the look-up tables and the symmetrical nature of the quantization method discussed in Section 5.3.2. Resulted from the symmetry of BPSK modulation, we only need to execute the SGA search for $K/2$ codewords. Therefore, the total number of parameters required to search in the design procedure is $N_{ttlpar} = N_{par}K/2 = M_t LK \log_2 K$. The complexity order of designing the proposed jointly-designed linear code is $K/2\mathcal{O}(2M_t L \log_2 K)$. It is obvious that the

time it takes to perform the design procedure becomes prohibitive as K grows large, resulting in an essentially unsolvable code design problem.

As shown in [48], the total number of parameters required to search in the existing jointly-designed unstructured code is $\hat{N}_{ttlpar} = 2\hat{N}_{par} = 2M_tLK$. The order of complexity on designing the existing jointly-designed unstructured code is $\mathcal{O}(2M_tLK)$. To compare fairly with the unstructured code with $M_t = 2, L = 2, K = 4$ used in [48], we design the jointly-designed linear code with the same system parameters. We can see that the total number of parameters required to search in the jointly-designed linear code is $2 \times 2 \times 4 \times 2 = 32$, which is equivalent to that of the unstructured code as shown in [48]. However, N_{ttlpar} is larger than $\hat{N}_{ttlpar}$ as long as $\log_2 K > 2$. Nevertheless, since the SGA search for each codeword of the jointly-designed linear code is independent, the $K/2$ times of search can be executed simultaneously over different platforms. Thus, for the jointly-designed linear code, the number of parameters required to search in each platform is $N_{par} = 2M_tL\log_2 K$, which is much less than $\hat{N}_{ttlpar}$ as K increases. It is obvious that the $K/2$ times of independent search of the jointly-designed linear code relieves the complexity burden required by the code design problem for large K remarkably compared with the unstructured code.

Moreover, the new performance criterion also reduces the computing power. In the new performance criterion, only $K-1$ PEPs between the current transmitted codeword $\mathbf{C}_k$ and other codewords $\{\mathbf{C}_l\}_{l=1}^{K}\,(l \neq k)$ are required to be calculated. On the other hand, the existing performance criterion adopted in [48] is based on the union bound of BLER, i.e., it must calculate $(K-1)K/2$ PEPs between all

codewords. Also the computational complexity of the new performance criterion is much less than the existing performance criterion adopted in [48] as K increases.

Note that the linear structure imposed into the code design makes it possible for the use of decoding algorithms with significantly lower complexity than an exhaustive search utilized by the unstructured joint design in [48]. Since our attention is focused on the transmitter design and the performance comparison, the decoding algorithms with lower complexity are not exploited and discussed in this thesis.

5.5 Examples of Jointly-Designed Code

In this section, a few illustrative examples of the quantized CSI measurement model should suffice to appreciate the extent of the improvement that can be achieved by the jointly-designed code using the proposed performance criterion and the described design procedures. All jointly-designed codes are obtained under the assumption of the simplified fading scenario in the MISO system with a power budget of $E_s = 1$, the fading variance of $\sigma_h^2 = 1$ and BPSK modulation. Other choices are certainly possible but usually do not affect the conclusions in any major way.

To compare and analyze, two types of codes with $M_t = 2$, $L = 2$, $K = 4$ are presented in Table 5.2 and Table 5.3.

Wherein, one type of codes in Table 5.2 comes from [48] reviewed in Chapter 3, the other type in Table 5.3 is the jointly-designed codes based on our proposed performance criterion and design procedures. It is known from (3.61) and (5.61)

Jongren's Unstructured Codes		
	$\rho = 0$	
$\mathbf{C}_1^{(0)}$	$-0.71126 + j\ 0.36087$	$+0.40735 - j\ 0.44435$
	$-0.58663 + j\ 0.14285$	$-0.65934 + j\ 0.44859$
$\mathbf{C}_2^{(0)}$	$+0.01832 + j\ 0.21581$	$+0.08399 + j\ 0.97295$
	$+0.81098 + j\ 0.54269$	$-0.18061 - j\ 0.12080$
$\mathbf{C}_3^{(0)}$	$+0.15579 + j\ 0.09515$	$-0.94038 - j\ 0.28723$
	$+0.20541 - j\ 0.96129$	$-0.00773 - j\ 0.18309$
$\mathbf{C}_4^{(0)}$	$+0.53715 - j\ 0.67183$	$+0.44904 - j\ 0.24136$
	$-0.42976 + j\ 0.27575$	$+0.84767 - j\ 0.14470$
	$\rho = 0.95$	
$\mathbf{C}_1^{(0)}$	$-0.92111 + j\ 0.37685$	$-0.04889 - j\ 0.10390$
	$-0.88850 + j\ 0.32513$	$-0.30045 + j\ 0.10687$
$\mathbf{C}_2^{(0)}$	$+0.48440 + j\ 0.49155$	$-0.03616 + j\ 0.72504$
	$+0.67026 + j\ 0.56673$	$-0.09747 + j\ 0.46532$
$\mathbf{C}_3^{(0)}$	$+0.24692 - j\ 0.47884$	$-0.77306 - j\ 0.34031$
	$+0.25685 - j\ 0.72680$	$-0.55128 - j\ 0.31430$
$\mathbf{C}_4^{(0)}$	$+0.18980 - j\ 0.38956$	$+0.85812 - j\ 0.28083$
	$-0.03860 - j\ 0.16506$	$+0.94920 - j\ 0.25788$

Table 5.2: Jongren's unstructured code $\mathcal{C}(0)$ for different ρ [48].

that both types of the codes are constructed depending on the required E_b/N_0. That is, with different E_b/N_0, the constructed codes are different. For fair comparison, all these codes presented in Table 5.2 and Table 5.3 are designed for a noise variance per dimension of $\sigma^2 = 0.05$, corresponding to an E_b/N_0 of 10dB, which are one set of the many sets of codes used to obtain the results for a range of E_b/N_0 values plotted in Fig. 5.3 and Fig. 5.4. The initial channel information quality, ρ, are set to 0 and 0.95, representing an open-loop system and a closed-loop system, respectively. In the latter case, $b = 2$ bits are used to quantize the initial channel information employing the uniform phase-quantization scheme de-

Proposed Jointly-Designed Codes $\mathbf{C}_k^{(0)} = s_1^{(k)}\mathbf{A}_1^{(0)} + s_2^{(k)}\mathbf{A}_2^{(0)}$			
		$\rho = 0$	
$\mathbf{s}^{(1)}$ or $\mathbf{s}^{(4)}$	$\mathbf{A}_1^{(0)}$	$-5.5092 + j\ 4.2137$	$-0.8301 + j\ 5.0567$
		$+2.3206 + j\ 0.6652$	$+0.6930 + j\ 3.1398$
	$\mathbf{A}_2^{(0)}$	$+4.7610 - j\ 4.1221$	$+0.3823 - j\ 5.5368$
		$-2.9647 - j\ 0.7931$	$-0.3754 - j\ 2.4552$
$\mathbf{s}^{(2)}$ or $\mathbf{s}^{(3)}$	$\mathbf{A}_1^{(0)}$	$-0.7655 + j\ 5.7103$	$+0.0537 + j\ 0.2645$
		$-5.8983 - j\ 3.4813$	$-0.2242 - j\ 5.9835$
	$\mathbf{A}_2^{(0)}$	$+0.0017 + j\ 5.5976$	$+0.5816 + j\ 0.6107$
		$-5.7341 - j\ 4.0903$	$-0.8729 - j\ 5.5575$
		$\rho = 0.95$	
$\mathbf{s}^{(1)}$ or $\mathbf{s}^{(4)}$	$\mathbf{A}_1^{(0)}$	$-1.5146 + j\ 1.4258$	$-1.0407 - j\ 0.7126$
		$-0.2336 - j\ 0.6245$	$-2.2582 + j\ 1.4231$
	$\mathbf{A}_2^{(0)}$	$+1.4998 - j\ 0.9506$	$+0.7586 + j\ 1.5457$
		$+0.8098 + j\ 1.0044$	$+1.7486 - j\ 0.9089$
$\mathbf{s}^{(2)}$ or $\mathbf{s}^{(3)}$	$\mathbf{A}_1^{(0)}$	$-0.7936 + j\ 0.1713$	$+1.6652 + j\ 2.1990$
		$+0.7218 + j\ 1.2609$	$-0.1359 + j\ 1.4421$
	$\mathbf{A}_2^{(0)}$	$-1.7418 + j\ 0.0805$	$+1.9595 + j\ 2.1224$
		$-0.1860 + j\ 1.1728$	$-0.5338 + j\ 1.5421$

Table 5.3: The proposed jointly-designed code $\mathcal{C}(0)$ for different ρ.

scribed in Section 5.2.2. The proposed jointly-designed linear codes with $M_t = 4$, $N = L = 4$, $K = 16$ and $b = 6$ for $E_b/N_0 = 10$dB, which is one set of the many sets of codes used to obtain the results for a range of values plotted in Fig. 5.5 and Fig. 5.6, are shown in Appendix A. In both tables, only the codewords of the first code $\mathcal{C}(0)$ are explicitly displayed. This constitutes all the required codes in the case of no feedback CSI ($\rho = 0$). In the case of $\rho = 0.95$, the feedback is symmetric, as explained in Section 5.3.2. The remaining codes $\mathcal{C}(p), p = 1, 2, 3$ are obtained through the relation $\mathbf{C}_k^{(p)} = \mathbf{\Theta}_p \mathbf{C}_k^{(0)}$, where $\mathbf{\Theta}_p$ is 2×2 dimensional

diagonal matrix as follows,

$$\mathbf{\Theta}_p = \begin{bmatrix} 1 & 0 \\ 0 & \exp\left(j\frac{p\pi}{2}\right) \end{bmatrix}. \tag{5.65}$$

Let $\mathbf{\Xi}$ denotes the Euclidean distance matrix of the code, where each element ε_{ij} represents the Euclidean distance between the ith codeword and the jth codeword, i.e., $\varepsilon_{ij} = \|\mathbf{C}_i - \mathbf{C}_j\|_{\mathrm{F}}$.

In the case of no feedback CSI, from Table 5.2, we can obtain the Euclidean distance matrix for Jongren's unstructured codes as follows,

$$\mathbf{\Xi}_0^U = \begin{bmatrix} 0 & 2.3094 & 2.3094 & 2.3094 \\ 2.3094 & 0 & 2.3094 & 2.3094 \\ 2.3094 & 2.3094 & 0 & 2.3094 \\ 2.3094 & 2.3094 & 2.3094 & 0 \end{bmatrix} \tag{5.66}$$

where the subscript "0" represents $\rho = 0$ and the superscript "U" denotes the unstructured code. Note that any pair of codewords has the same Euclidean distance of 2.3094. This means that no matter which codeword is transmitted, deciding in favor of any one of the other three codewords has equal likelihood. Thus all PEPs of the unstructured code has the same effect on the union bound of the BLER according to (5.55) and (5.64).

On the other hand, for the proposed jointly-designed code in Table 5.3 with $\rho = 0$, the transmitted weighting matrices are adaptive according to the input information data series. When $\mathbf{s}^{(1)}$ is input to the jointly-designed encoder, the Euclidean distance matrix for $\mathbf{s}^{(1)}$ is given by

$$\mathbf{\Xi}_0^J(\mathbf{s}^{(1)}) = \begin{bmatrix} 0 & 18.5525 & 19.0297 & 2.8284 \\ 18.5525 & 0 & 37.4786 & 19.0297 \\ 19.0297 & 37.4786 & 0 & 18.5525 \\ 2.8284 & 19.0297 & 18.5525 & 0 \end{bmatrix} \tag{5.67}$$

where the superscript "J" denotes the jointly-designed linear code. Obviously, the Euclidean distance between $\mathbf{C}_1$ and $\mathbf{C}_4$ is the minimum, i.e., the PEP between

$\mathbf{C}_1$ and $\mathbf{C}_4$ is the worst-case PEP, and also the dominating term in the case that $\mathbf{s}^{(1)}$ is input. Hence, the event of inputting $\mathbf{s}^{(1)}$ and deciding in favor of $\mathbf{s}^{(4)}$ at the decoder is the most likely. When $\mathbf{s}^{(2)}$ is input to the jointly-designed linear encoder, the Euclidean distance matrix for $\mathbf{s}^{(2)}$ is given by

$$\Xi_0^J(\mathbf{s}^{(2)}) = \begin{bmatrix} 0 & 21.2887 & 21.5433 & 42.7393 \\ 21.2887 & 0 & 2.8284 & 21.5433 \\ 21.5433 & 2.8284 & 0 & 21.2887 \\ 42.7393 & 21.5433 & 21.2887 & 0 \end{bmatrix} \tag{5.68}$$

where the Euclidean distance between $\mathbf{C}_2$ and $\mathbf{C}_3$ is the minimum. Hence, in the case that $\mathbf{s}^{(2)}$ is the input, the event of deciding in favor of $\mathbf{s}^{(3)}$ at the decoder is the most likely. According to the similar derivation, we can deduce that when $\mathbf{s}^{(3)}$ is the input, $\mathbf{s}^{(2)}$ is the most likely to be decided, while when $\mathbf{s}^{(4)}$ is the input, $\mathbf{s}^{(1)}$ is the most likely decision. It is known that $q_{14} = q_{23} = q_{32} = q_{41} = 2$. Therefore, when the event of one codeword error happens, the case of two error bits in this event is the most likely. It means that the BER performance of the jointly-designed system is very close to its BLER performance, as illustrated in Section 5.6.

5.6 Numerical Results

To illustrate the jointly code design based on the new performance criterion, we present a few examples and examine their performance, and compare them with the two typical hybrid open-loop and closed-loop MISO systems with partial CSI in this section. For all examined cases, the simplified fading scenario with perfect knowledge of σ^2, σ_h^2 and ρ is assumed and the variance of the channel coefficient is set to be $\sigma_h^2 = 1$.

For fair comparison, all investigated systems are compared on the basis of the

same effective BPS throughput given by BPS = code rate $\times$ m, where m is selected from $2^m = M$ corresponding to M-PSK modulation. Since BPSK modulation ($m = 1$) is assumed and a BPS of 1bit/symbol is adopted, all of these codes are required to have full code rate.

To demonstrate the performance advantage of the jointly-designed transmission method over the non-integrated design of combined system, we compare the proposed jointly-designed code with the combined system of beamforming and predetermined Alamouti's STBC described in Chapter 4. Since the latter is considered in the case of noisy and outdated CSI without quantization, the jointly-designed code is also investigated under this assumption. The latter has the orthogonal nature and the beamforming matrix is designed separately (from the Alamouti's STBC) according to the CSI at the transmitter in order to adapt the predetermined Alamouti's STBC to the channel. A simple semi-closed-form optimization solution can be derived from the codeword pair criterion. The proposed jointly-designed code, on the other hand, is based on the new performance criterion without the constraint of orthogonality. A numerical optimization algorithm requiring an exhaustive search is needed to obtain the suitable code. Therefore, the proposed jointly-designed system is more complex than the combined beamforming and Alamouti's STBC system. The available CSI at the transmitter is the same for both systems with the initial channel information quality set to $\rho = 0.9$. In Fig. 5.2, the BER as a function of the E_b/N_0 is depicted for the above two systems with various number of transmitting antennas and the same system parameters of $N = L = 2$ and $K = 4$. It can be seen that at the BER level of 1×10^{-4},

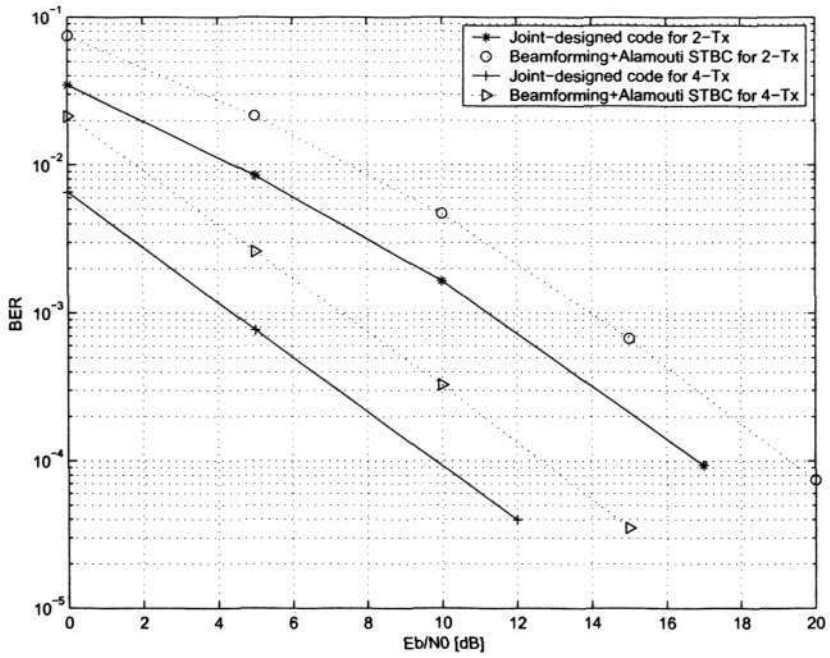

Figure 5.2: BER performance comparison of the proposed jointly-designed code with the combined system of beamforming and Alamouti's STBC in the case of noisy CSI, $N = L = 2$ and $K = 4$.

the jointly-designed code has about 2.5dB performance gain over the combined system of beamforming and Alamouti's STBC for both $M_t = 2$ and $M_t = 4$. Thus, the performance advantage comes at the price of higher computational complexity especially for the noisy CSI, which has been discussed in Section 5.4.

To prove the benefit of the new joint design with the new performance criterion suggested in this thesis, we compare the proposed jointly-designed code with the existing jointly-designed unstructured code proposed in [48]. The jointly-designed procedure in [48] is based on the quantized CSI as this can be performed off-line and the transmission scheme can be efficiently implemented by using lookup tables and making use of the symmetrical nature of the quantization method discussed in

Section 5.3.2. In this way, the computational complexity is significantly reduced. Due to this reason, the comparison between the two jointly-designed systems is carried out under the case of quantized CSI at the transmitter. The proposed joint-design uses linear structure STBC and is based on the new performance criterion, while the joint-design in [48] does not have the limit of code structure and is based on the well-known union bound technique. Fig. 5.3 shows the BLER performance of the two schemes for two transmitting antennas with the same system parameters of $N = L = 2$ and $K = 4$. For both jointly-designed schemes, ρ is set to 0 and 0.95, to study the impact of the initial channel information quality on the performance, and $\bar{b} = b = 2$ bits is exploited to coarsely quantize the initial channel information by using the uniform phase-quantization method. Note that the scenario of $\rho = 0$ also corresponds to an open-loop system which includes the conventional OSTBC [89]. Therefore, the OSTBC system is also presented in the comparison as a benchmark. It can be observed from the figure, the BLER performance of the OSTBC as well as the unstructured code agrees with the results in [48]. According to the analysis of [48], the unstructured code should have better performance than all the other corresponding block codes, since structure generally limits the degrees of freedom in the design. On the contrary, however, the proposed jointly-designed code with linear structure, regardless of the initial channel information quality ρ, has about 3.5 dB performance gain over the unstructured code at the high SNR, which shows the advantage of the new design criterion that takes the current transmitted codewords into account. In addition, the curve of the jointly-designed code for $\rho = 0$ looks like an upper bound, and the curve of the jointly-designed

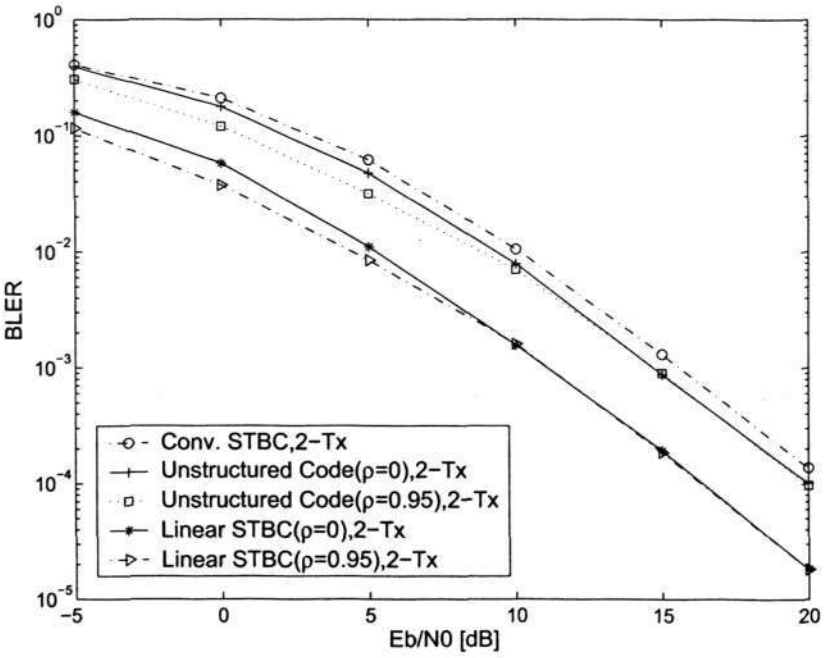

Figure 5.3: BLER performance comparison of the proposed jointly-designed linear code with the existing jointly-designed unstructured code in the case of quantized CSI, $M_t = 2$, $N = L = 2$, $K = 4$ and $b = 2$.

code for $\rho = 0.95$ approaches to it at high SNR, as the discussion for the special case of no feedback CSI in Section 5.3.2.

The BER as a function of the E_b/N_0 for the above two jointly-designed schemes as well as the benchmark, corresponding OSTBC (Alamouti), is depicted in Fig. 5.4. As it can be seen, the unstructured code in the case of $\rho = 0$ has nearly the same BER performance as the OSTBC. It turns out that the conventional OSTBC is one of the optimum solutions for the BER performance with respect to the standard union bound criterion used by the unstructured code in [48]. This is reasonable in view of that the unstructured code has a lot in common and even shares the pairwise orthogonality property (2.20) with the conventional OSTBC, although

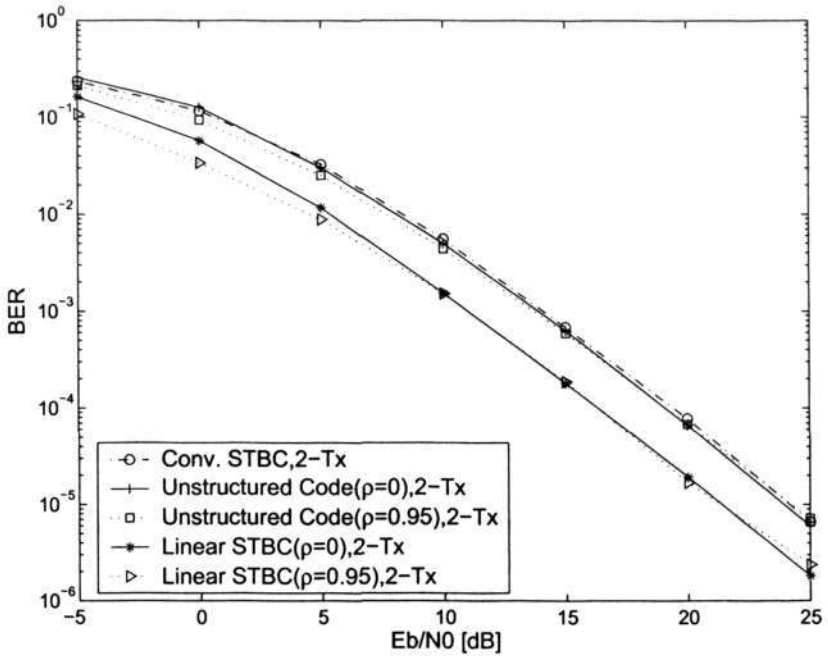

Figure 5.4: BER performance comparison of the proposed jointly-designed linear code with the existing jointly-designed unstructured code in the case of quantized CSI, $M_t = 2$, $N = L = 2$, $K = 4$ and $b = 2$.

typically with a nonconstant coefficient in (2.20), as described in [48].

Consistently, benefiting from the new performance criterion, the BER performance of the proposed jointly-designed code with linear structure is still better than that of the unstructured code, regardless of the quality of the initial channel information ρ. Whereas the BER performance gain of the proposed jointly-designed code over the unstructured code is less than 3 dB, which is smaller than the BLER performance gain. When we compare the BER curves in Fig. 5.3 with the BLER curves in Fig. 5.4 of the same proposed jointly-designed code, it is observed that the former is still on the left of the latter, although the two groups of curves are very close. This is due to the PEP of the error event with two error bits is dominant

in the new performance criterion, as discussed in Section 5.5.

Nevertheless, for the unstructured code, resulted from the freedom of design, every PEP nearly has the same value in the union bound criterion, as given in Section 5.5. It is known that the union bound on the BLER is obtained by summing over all the PEPs, while the union bound on the BER is the weighted summation of all the PEPs. Therefore, for the unstructured code proposed in [48], the difference (about 1dB) of the BER performance over the BLER performance is relatively more than that for the proposed jointly-designed code.

The BLER/BER versus E_b/N_0 for the aforementioned three schemes with four transmitting antennas and the code length of $L = 4$ are presented in Fig. 5.5 and Fig. 5.6, respectively. Since $\bar{b} = b/(M_t - 1) = 2$ bits are used, the quantization is roughly as coarse as in the above case of two transmitting antennas and the code length of $L = 2$. As expected, the BLER performances of the OSTBC and the unstructured code obtained by using the SGA agree well with the simulation results displayed in [48], which is obtained through the gradient search algorithm. It is clear that the gains due to the new performance criterion increase substantially with more transmitting antennas. For four transmitting antennas, the proposed jointly-designed code has more than 6 dB BLER performance gain and more than 5 dB BER performance gain over the existing jointly-designed unstructured code. At high SNR, the performance curves for $\rho = 0.95$ also approach to those for $\rho = 0$. It means that the feedback CSI has less effect on the performance improvement as SNR increases. However, as the number of quantization bits, b, increases, the two groups of performance curves for $\rho = 0.95$ and for $\rho = 0$ approach at lower BER

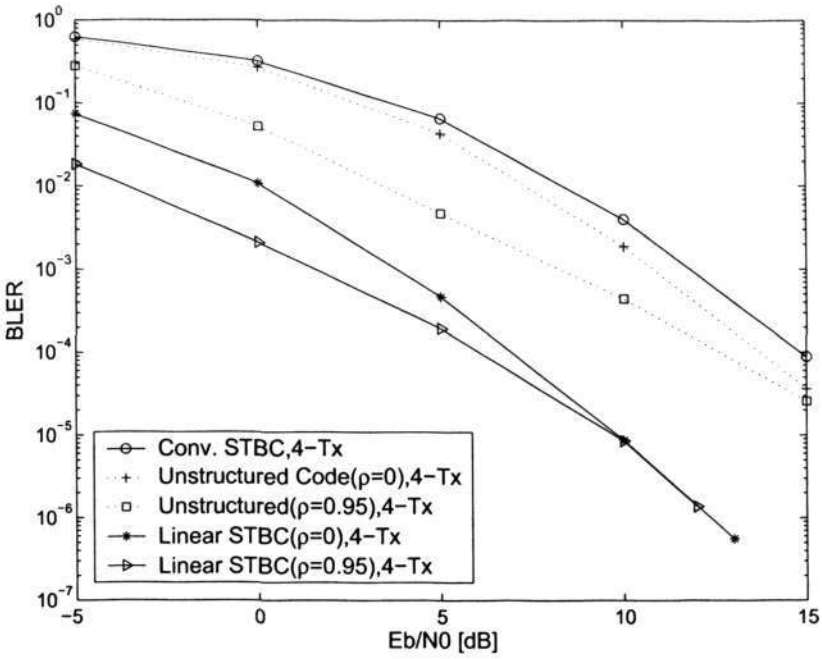

Figure 5.5: BLER performance comparison of the proposed jointly-designed linear code with the existing jointly-designed unstructured code in the case of quantized CSI, $M_t = 4$, $N = L = 4$, $K = 16$ and $b = 6$.

level.

The above performance results are obtained under the assumption of simplified fading scenario. It is discussed in Chapter 4 that the construction procedure of beamforming matrix is affected significantly without the assumption of simplified fading scenario. However, similar to [48], the code-construction process of the proposed jointly-designed linear code in this chapter is still suitable for the general complex Gaussian fading. The two jointly-designed schemes in [48] and this chapter have the same expression of the codeword pair criterion (5.50), although the value of (5.50) for the simplified fading scenario is different from that for the general complex Gaussian fading. Therefore, the new performance criterion is still

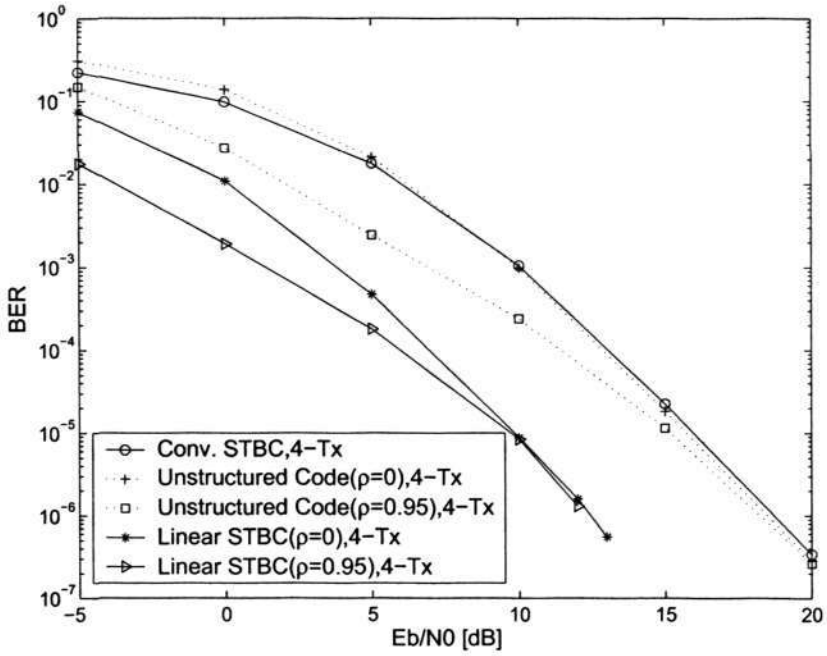

Figure 5.6: BER performance comparison of the proposed jointly-designed linear code with the existing jointly-designed unstructured code in the case of quantized CSI, $M_t = 4$, $N = L = 4$, $K = 16$ and $b = 6$.

more efficient than the one proposed in [48] since the difference of the two performance criteria is just the summation law of (5.50) corresponding to the individual codeword. It results in that for the general complex Gaussian fading, the proposed jointly-designed linear code still has better performance than the unstructured code proposed in [48].

5.7 Summary

In this chapter, under the assumption that the receiver has perfect channel estimation and weighting matrices detection, we propose a new performance criterion conditioned on the feedback CSI and the current transmitted codewords at the transmitter. Based on the new performance criterion, we incorporate the imper-

fect feedback CSI into the joint design of beamforming and linear STBC. Moreover, in order to simplify the optimal procedure, we adopt SGA (which is a globe numerical optimization algorithm) as an alternative choice replacing the simple gradient search (which is a local numerical optimization algorithm) employed in Chapter 3.

The simulation results show that the jointly-designed code has a diversity gain of $r = L$ for $M_t \geq L$, which agrees with the theoretical analysis of in Section 5.3.1 and 5.3.2. More importantly, these simulation results illustrate the jointly-designed code has more performance gain in both BLER and BER than the unstructured STBC, even though the latter has more degrees of design freedom than the former. They simultaneously justify the proposed performance criterion.

Chapter 6

Conclusion and Future Work

6.1 Conclusion

This thesis mainly concentrates on the study of the reduced-complexity design of two types of closed-loop MISO combined systems of beamforming and STBC over the slow Rayleigh flat fading channels. The first type is the combined beamforming and predetermined STBC, where only the beamforming matrix is the free parameter that can be adjusted. The second one considers beamforming and STBC as the whole transmission matrix to be jointly designed. The simplified fading scenario and perfect channel estimation at the receiver are assumed throughout the thesis. The feedback CSI from the receiver to the transmitter are modelled by mean feedback, in which the CSI resides in the mean of the distribution, with the covariance modelled as white proportional to an identity matrix. In the first type of the combined systems, the feedback CSI is assumed to be noisy and outdated due to the feedback delay without quantization while quantization is adopted in the second type.

The existing combined system of beamforming and predetermined OSTBC can

achieve full diversity gain, however, it becomes significantly complex with the price of reduced bandwidth efficiency as the number of transmitting antennas increases. To achieve a tradeoff between performance and complexity, we are motivated to investigate a simple combined system of beamforming and predetermined Alamouti's STBC in Chapter 4. The Alamouti's STBC can be incorporated with more than two transmitting antennas via the beamforming technique. A semi-closed-form optimization solution for the beamforming matrix is obtained from the worst-case codeword pair criterion. Simulation and theoretical analysis of the simple combined system are conducted to demonstrate its great advantage especially for a large number of transmitting antennas and good feedback quality.

From the performance point of view, the joint design of beamforming and STBC is preferable, although only numerical search approaches can be adopted to find the optimum solution. In this type of the combined systems, the feedback CSI is assumed to be quantized or unquantized, and outdated with an ideal feedback channel model. Although the existing CSI dependent unstructured code has an excellent performance, its typical drawback for high data rate scenario is the substantial decoding complexity incurred by the lack of structure in the code. Therefore, we propose to impose the linear structure into the code-construction process in Chapter 5, since linear code designs often permit the use of decoding algorithms with significantly lower complexity than an exhaustive search. However, the structure nature generally limits the degrees of freedom in the code design, which results in performance penalty. To remedy this, we propose a more efficient performance criterion for the jointly-designed linear code than the union bound

on the BLER criterion for the unstructured code. In addition, a global numerical optimization algorithm, SGA, is adopted to replace the gradient search technique which is a local numerical optimization algorithm. The simulation results show that the jointly-designed linear code has much performance improvement over the unstructured code based on the efficient performance criterion.

6.2 Future Work

In the simplified fading scenario, the transmitting antennas are assumed to be separated far apart enough that the channel realizations between two antennas are independent. But in practice, the channels between different transmitting antennas are impossible to be independent completely. Therefore, the channel correlation between two antennas should be considered in the future work. Although the channel correlation has been considered by Zhou *et al.* in [97], it is assumed that the feedback CSI is modelled as covariance feedback rather than mean feedback in his paper. The future work should investigate the impact of channel correlation on the performance of both types of the combined systems.

As discussed in Chapter 4, theoretically, the array gain expressed in decibels (dB) of the non-ideal combined system of beamforming and Alamouti's STBC will improve linearly as the number of transmitting antennas increases. This is due to the assumption of ideal synchronization process regardless of the signal power allocated at each antenna. In the future work, the possible number of transmitting antennas before the system breaks down can be studied.

In addition, both types of combined systems are designed under the assumption

that the transmitter weighting matrix can be detected perfectly at the receiver throughout the thesis. However, in practice, the detection is carried out using pilot signals or a known training sequence such as in [49]. Hence, the imperfect transmitting weights detection can be studied in the future work.

In the jointly-designed beamforming and linear STBC system, the CSI at the transmitter is assumed to suffer from feedback delay and quantization. Feedback channel bit errors are not considered in the feedback link. Therefore, for future work, vector quantization [15, 49] can be used as a replacement of the uniform phase-quantization method used in this thesis for non-ideal feedback channel in order to avoid the damaging effects caused by these errors.

Although the imperfect channel estimation at the transmitter is taken into account, the channel detection at the receiver is assumed to be perfect in this thesis. In the absence of accurate channel estimates at the receiver, the complexity of ML sequence detection grows exponentially with the length of the sequence. For future work, Expectation Maximization (EM) algorithm to jointly estimate the CSI and MAP symbol at the receiver can be employed. The EM algorithm [63, 64] is a general iterative procedure for ML estimation under certain conditions. It is often applied to a variety of estimation problem in the case of the absence of certain data such as in [6, 11, 13, 19, 73]. The EM-based receiver has a very low computational complexity, and it is often used for space time coded systems [53] and STBC-OFDM systems [62].

The closed-loop combined system of beamforming and STBC is employed in the single user scenario in this thesis. The system can also be generalized for

multiuser CDMA systems in the future works.

Author's Publications

Journal Paper

(i) Jin Liu and Erry Gunawan, "Combining ideal beamforming and Alamouti space-time block codes," *IEE Electron. Lett.*, Vol. 39, No. 17, pp. 1258-1259, Aug. 2003.

(ii) Jin Liu and Erry Gunawan, "Exact bit-error rate analysis for the combined system of beamforming and Alamouti's space-time block code," *IEEE Microwave and Wireless Components Letters (MWCL)*, Vol. 14, NO. 8, pp. 398-400, Aug. 2004.

(iii) Jin Liu and Erry Gunawan, "Combining beamforming and Alamouti's space-time block codes," submitted to *IEEE Trans. Commun.*, 2004.

(iv) Jin Liu and Erry Gunawan, "Joint design of beamforming and linear space-time block codes," submitted to *IEEE Trans. Wireless Commun.*, 2005.

Conference Paper

(i) Jin Liu and Erry Gunawan, "Combining beamforming and space-time block codes with outer turbo codes," in *Proc. Euro. Conf. on Wireless Technologies (ECWT2003)*, Munich, Germany, Oct. 2003.

(ii) Jin Liu and Erry Gunawan, "An exact union bound on the BER for the combined system of ideal beamforming and Alamouti's STBC," in *Proc. IEEE ICICS-PCM*, Singapore, Dec. 2003.

Appendix A

Examples of Jointly-Designed Code for 4 Transmitting Antennas

This appendix presents the examples of the proposed jointly-designed linear code with $M_t = 4$, $N = L = 4$ and $K = 16$ for $E_b/N_0 = 10$dB, which is one set of the many sets of codes used to obtain the results for a range of values plotted in Fig. 5.5 and Fig. 5.6. The kth codeword of the first code $\mathcal{C}(0)$ can be expressed as

$$\mathbf{C}_k^{(0)} = s_1^{(k)}\mathbf{A}_1^{(0)} + s_2^{(k)}\mathbf{A}_2^{(0)} + s_3^{(k)}\mathbf{A}_3^{(0)} + s_4^{(k)}\mathbf{A}_4^{(0)}. \tag{A.1}$$

ρ are set to 0 and 0.95 and $b = 6$ bits. Similar to Section 5.5, only the codewords of the first code $\mathcal{C}(0)$ are explicitly displayed in the following tables. It constitutes all the required codes in the case of no feedback CSI ($\rho = 0$). In the case of $\rho = 0.95$, the remaining codes $\mathcal{C}(p), p = 1, 2, \ldots, 63$ are obtained through the relation $\mathbf{C}_k^{(p)} = \mathbf{\Theta}_p\mathbf{C}_k^{(0)}$, where $\mathbf{\Theta}_p$ is 4×4 dimensional diagonal matrix as follows,

$$\mathbf{\Theta}_p = \begin{bmatrix} 1 & 0 & 0 & 0 \\ 0 & \exp\left[j\frac{\pi}{2}\tau_0(p)\right] & 0 & 0 \\ 0 & 0 & \exp\left[j\frac{\pi}{2}\tau_1(p)\right] & 0 \\ 0 & 0 & 0 & \exp\left[j\frac{\pi}{2}\tau_2(p)\right] \end{bmatrix}. \tag{A.2}$$

It is known from Section 5.2.2.2 that $p = \tau_0(p) + 4\tau_1(p) + 16\tau_2(p)$, where $\tau_\nu(p) \in \{0, 1, 2, 3\}$, $\nu = 0, 1, 2$. Here, $\tau_\nu(p)$ is obtained through the following calculation,

$$\tau_2(p) = \left\lfloor \frac{p}{16} \right\rfloor, \quad \tau_1(p) = \left\lfloor \frac{p - 16\tau_2(p)}{4} \right\rfloor, \quad \tau_1(p) = p - 4\tau_1(p) - 16\tau_2(p) \tag{A.3}$$

where $\lfloor \cdot \rfloor$ denotes the floor function.

$\mathbf{s}^{(1)}$ or $\mathbf{s}^{(16)}$, $\rho = 0$			
$\mathbf{A}_1^{(0)}$			
$+1.2512 + j2.5799$	$+1.1422 - j0.0775$	$+0.6526 + j0.7506$	$-2.4717 - j2.8312$
$-1.6721 + j0.2681$	$-0.9626 - j1.4958$	$+1.9543 + j2.6559$	$+1.7307 + j2.1537$
$+1.3492 + j0.6173$	$+2.8313 + j1.9610$	$+0.1316 - j0.6754$	$+0.9865 - j2.7013$
$+2.2396 - j2.4526$	$+0.0006 - j0.3982$	$-1.9531 + j0.4203$	$+2.0857 - j0.4227$
$\mathbf{A}_2^{(0)}$			
$-2.8268 + j2.0418$	$+1.1238 - j2.0020$	$+1.5858 - j1.0957$	$+2.0330 + j2.6385$
$-0.0374 + j1.1061$	$-0.7018 - j0.3540$	$-2.5161 - j1.6933$	$+0.6108 - j1.1944$
$-1.5463 + j2.0421$	$-2.0239 - j1.7474$	$+1.1410 + j1.3460$	$+0.7645 + j0.5369$
$-2.3115 + j1.1239$	$+0.2740 + j0.3119$	$+0.1750 + j1.4095$	$+0.7093 - j0.6075$
$\mathbf{A}_3^{(0)}$			
$+0.2833 - j2.4936$	$-1.2363 + j0.4541$	$+0.5455 + j2.5174$	$+0.2764 + j2.1565$
$+2.3481 - j1.8097$	$-1.3825 + j2.4636$	$-0.2239 - j1.7811$	$-0.7412 + j0.1153$
$-0.5514 - j1.0378$	$-2.0571 + j0.7040$	$-2.0728 - j0.0097$	$+1.4392 + j2.4353$
$+0.4825 + j2.3004$	$+1.2140 + j1.4125$	$-1.3451 - j2.3529$	$-1.3500 + j0.9990$
$\mathbf{A}_4^{(0)}$			
$+1.9788 - j2.0713$	$-1.2008 + j1.4900$	$-2.1324 - j2.3208$	$+0.2976 - j1.8515$
$-0.9416 + j0.1389$	$+2.8312 - j0.1794$	$+1.2394 + j1.0047$	$-2.0627 - j0.7132$
$+0.5405 - j1.3689$	$+0.4495 - j0.7596$	$+0.7153 - j0.6512$	$-2.7248 - j0.2100$
$-0.0911 - j1.3411$	$-1.3430 - j1.1518$	$+2.8308 + j0.9913$	$-1.0380 + j0.5206$

$\mathbf{s}^{(1)}$ or $\mathbf{s}^{(16)}$, $\rho = 0.95$			
$\mathbf{A}_1^{(0)}$			
$+0.8561 - j0.3132$	$+0.4059 - j0.4000$	$+1.3889 - j0.6000$	$-1.1444 + j1.1319$
$-1.1990 + j0.6598$	$+0.3564 + j0.8511$	$-0.5054 - j1.2517$	$-0.2407 - j0.8656$
$+1.3933 + j1.1821$	$-1.3608 + j0.4376$	$-1.3025 - j0.9692$	$-0.5511 - j0.5148$
$+0.2779 - j0.6944$	$+0.5313 - j0.1833$	$-0.9807 + j0.6373$	$-0.7224 - j1.0593$
$\mathbf{A}_2^{(0)}$			
$-0.4889 + j0.1225$	$-0.4919 - j0.9497$	$-0.0772 + j0.1303$	$-0.4953 - j0.2075$
$+0.1433 + j0.6142$	$-0.9832 - j0.7522$	$+0.7544 + j0.8552$	$-0.2383 + j1.1180$
$-1.3086 - j1.3300$	$+0.3864 - j1.2826$	$+1.2529 + j1.3906$	$-0.3531 - j0.1410$
$+1.3735 - j0.1772$	$-0.8784 - j0.5271$	$+0.6084 + j0.9933$	$-0.7327 + j0.7893$
$\mathbf{A}_3^{(0)}$			
$-0.7109 - j0.4748$	$-0.9427 + j0.7384$	$-0.8523 - j0.5509$	$+0.7987 - j0.6184$
$+0.6336 - j1.2279$	$-0.4077 - j0.8314$	$-0.7382 + j0.1779$	$+0.3507 + j0.8469$
$-0.2751 - j0.4392$	$+0.5935 - j0.1180$	$-1.0898 - j1.2684$	$-0.3492 - j1.0246$
$-1.0098 - j0.3583$	$-0.7327 + j0.4096$	$-1.0742 + j0.0183$	$+1.0109 - j1.1111$
$\mathbf{A}_4^{(0)}$			
$+0.0525 + j0.2227$	$+0.6980 + j1.2776$	$-0.2972 + j1.1175$	$+0.5674 - j0.2325$
$-0.1426 - j0.2688$	$+0.7247 + j1.0507$	$+0.6115 + j0.8762$	$+0.1832 - j1.0752$
$-0.4368 + j0.1769$	$+0.2628 + j1.0791$	$+1.2917 + j0.9222$	$+0.6907 + j1.3933$
$-0.6840 + j1.0939$	$+1.0876 + j0.8817$	$+1.3812 - j1.1075$	$-0.1389 + j1.2363$

$\mathbf{s}^{(2)}$ or $\mathbf{s}^{(15)}$, $\rho = 0$			
$\mathbf{A}_1^{(0)}$			
$-0.2610 + j1.4372$	$+1.4532 - j2.2342$	$-2.3318 + j0.1887$	$+1.9382 - j0.0560$
$-2.0043 - j0.6649$	$+2.0035 + j2.1676$	$-0.3204 - j0.5466$	$+1.3769 - j2.3037$
$-0.8974 + j0.8677$	$-1.4913 - j1.9407$	$-1.3861 - j0.9520$	$+0.3305 - j1.7337$
$+2.3322 - j0.4547$	$-1.1959 - j1.3393$	$+0.9996 + j0.0923$	$+0.4682 + j2.1478$
$\mathbf{A}_2^{(0)}$			
$+0.3268 + j0.5923$	$+1.7607 + j0.4647$	$-0.9209 - j1.1334$	$-1.7210 - j0.8880$
$+2.0822 - j0.5010$	$-1.0726 - j1.5841$	$-0.9721 + j1.9770$	$+0.9125 + j0.7400$
$-0.6989 - j1.0842$	$-0.6255 - j1.0050$	$+0.9508 + j1.1363$	$-2.2769 + j2.2118$
$-1.8314 + j1.2321$	$+0.5543 + j2.3317$	$-1.6953 + j0.6485$	$-0.7010 + j2.1297$
$\mathbf{A}_3^{(0)}$			
$+1.7036 - j1.6784$	$-1.3536 + j1.3577$	$+1.6513 + j2.1717$	$+1.8618 - j0.7799$
$-1.9472 + j1.0079$	$+1.7834 + j0.6130$	$+0.2734 - j0.8761$	$-1.7708 + j0.8564$
$+0.4139 - j1.5533$	$+1.0384 + j0.8421$	$+0.8415 - j2.3069$	$+0.6170 + j0.8810$
$-1.5956 - j1.8300$	$+2.1002 - j1.8403$	$-1.6139 + j1.4546$	$-0.8947 - j1.7151$
$\mathbf{A}_4^{(0)}$			
$+2.1858 + j0.1070$	$+1.6859 - j0.6447$	$-1.7663 + j1.8526$	$+1.5703 - j1.7949$
$-2.0543 - j0.1813$	$+2.1500 + j1.2518$	$-1.4288 + j0.0785$	$+0.0655 - j0.4987$
$-0.8426 - j1.1342$	$-0.8806 - j2.2258$	$+0.6902 - j2.2470$	$-1.6779 + j1.8169$
$-0.7159 - j1.3170$	$+1.7313 - j0.1658$	$-2.1959 + j1.9154$	$-1.4429 + j2.3254$
$\mathbf{s}^{(2)}$ or $\mathbf{s}^{(15)}$, $\rho = 0.95$			
$\mathbf{A}_1^{(0)}$			
$+1.0955 - j0.2299$	$+0.7467 + j0.5789$	$-1.2539 + j1.1098$	$+0.3460 - j1.0595$
$-0.5120 - j0.4564$	$-0.1433 + j0.2992$	$-1.1815 - j0.8297$	$+0.9664 - j0.1192$
$+0.7491 - j1.2514$	$-0.3356 + j0.9318$	$-0.6158 - j0.4491$	$-0.1360 + j0.8872$
$+1.3040 - j1.3903$	$+1.2845 + j0.1476$	$+0.1490 + j0.8977$	$+1.0004 - j0.8574$
$\mathbf{A}_2^{(0)}$			
$+0.2034 + j0.9895$	$-0.8294 - j1.2408$	$-0.9407 - j1.1172$	$+0.6271 - j0.0295$
$+0.4645 + j0.3358$	$-0.8351 + j0.6803$	$+0.7885 + j0.2036$	$+0.2655 + j1.2053$
$-0.6014 + j0.4828$	$-0.9639 - j0.3417$	$-0.7898 + j0.7235$	$-0.1848 + j0.7050$
$+1.3204 + j1.1754$	$-0.3705 + j0.1088$	$-1.1591 - j0.8445$	$-0.2910 + j0.5505$
$\mathbf{A}_3^{(0)}$			
$-1.1782 - j0.6175$	$-0.4006 + j0.2113$	$+0.7812 + j0.7002$	$-0.6026 + j0.9678$
$-0.9962 - j0.4223$	$+1.0316 - j1.4579$	$-0.9085 + j0.4486$	$-1.1096 - j0.8625$
$-0.7509 - j0.6301$	$+0.8667 + j0.2547$	$+0.5064 - j1.4474$	$+1.1455 - j0.0438$
$-1.2186 - j0.4818$	$-1.3708 - j0.6823$	$-0.3553 - j0.9410$	$+0.4474 - j0.3791$
$\mathbf{A}_4^{(0)}$			
$+0.2748 - j0.0004$	$-0.3417 - j1.2033$	$-1.0212 + j0.8054$	$+0.2755 + j0.2590$
$-0.9710 - j0.3467$	$+0.2666 - j1.0283$	$-0.6937 + j0.0916$	$+0.5490 + j0.2031$
$-0.5020 - j1.4108$	$-0.5759 - j0.0049$	$-0.9416 - j0.6681$	$+0.8132 + j1.4632$
$+0.8656 - j0.8881$	$-0.2793 - j1.0979$	$-0.9622 - j0.7528$	$+1.0076 - j0.7246$

$\mathbf{s}^{(3)}$ or $\mathbf{s}^{(14)}$, $\rho = 0$			
$\mathbf{A}_1^{(0)}$			
$-2.3812 - j1.6626$	$+1.1482 - j0.3059$	$-2.3259 - j1.3607$	$-0.0259 + j0.4973$
$+0.3678 + j2.4783$	$-0.8819 + j0.5788$	$+0.0285 + j1.0243$	$+1.7140 - j2.0780$
$+0.5692 + j2.7163$	$+0.1526 + j2.1230$	$+0.4948 - j1.4727$	$-2.7535 + j0.6831$
$-1.8697 + j1.8615$	$-1.0931 - j1.8837$	$+1.6778 - j1.4775$	$-2.7866 - j2.1217$
$\mathbf{A}_2^{(0)}$			
$-1.4015 + j0.1469$	$-1.1466 - j0.4706$	$+0.9363 - j1.4600$	$-2.5948 - j0.2518$
$+0.8486 - j2.5472$	$+0.3926 + j0.1779$	$+0.9626 - j0.4974$	$-2.1450 + j2.6988$
$-0.3806 - j1.6122$	$-1.0756 - j1.7102$	$+2.6723 + j0.9116$	$+1.1683 + j1.1362$
$+1.9759 + j0.9353$	$+2.4274 + j2.5172$	$-0.6013 - j2.1586$	$+1.5621 - j0.2262$
$\mathbf{A}_3^{(0)}$			
$-2.7867 - j1.7428$	$+2.1635 - j2.3106$	$-1.3836 + j0.0637$	$-2.4750 - j1.6747$
$+1.7862 - j0.7947$	$-2.5459 - j1.4321$	$-1.5563 + j0.9937$	$+1.4124 - j0.0431$
$+0.9245 + j2.7029$	$-2.1400 + j0.5397$	$+0.3339 - j2.1344$	$+0.5418 + j0.0743$
$-0.5075 + j0.7082$	$-0.5336 + j0.3419$	$-1.3336 - j1.9824$	$-0.8395 - j2.6279$
$\mathbf{A}_4^{(0)}$			
$+0.6553 - j0.7133$	$+2.1777 - j1.3522$	$+0.3911 + j2.3567$	$-0.2810 - j1.9993$
$+0.5858 - j0.5125$	$-1.1433 - j2.1072$	$-2.2695 + j0.4770$	$+1.9277 - j0.8328$
$+1.3738 + j1.5011$	$-1.1737 + j0.3396$	$-2.7779 - j2.0642$	$+2.3922 - j1.2753$
$-0.9090 - j1.7757$	$-2.1363 - j0.3702$	$-2.0669 + j1.2885$	$+1.0322 - j0.5403$
$\mathbf{s}^{(3)}$ or $\mathbf{s}^{(14)}$, $\rho = 0.95$			
$\mathbf{A}_1^{(0)}$			
$+1.3168 + j0.7601$	$+1.1660 - j0.2580$	$-0.8166 - j1.2182$	$-1.3340 - j0.7586$
$+1.1378 - j1.0660$	$-0.8158 - j1.1681$	$+0.6279 - j0.9768$	$+0.4064 - j0.2527$
$+0.9751 - j0.4554$	$+0.3555 - j0.9835$	$+0.0537 + j0.6952$	$-0.3354 - j1.3362$
$+0.7714 - j0.9459$	$-0.5658 - j0.4294$	$-0.4900 + j0.9459$	$+1.1560 - j1.1736$
$\mathbf{A}_2^{(0)}$			
$+0.2502 - j1.3219$	$-0.4810 - j0.4606$	$+0.8845 + j0.8084$	$+0.9588 - j0.2467$
$-0.8429 + j0.1468$	$+1.0105 + j0.6449$	$-0.6346 + j0.5012$	$-0.3412 - j1.3711$
$+1.1929 + j1.3652$	$-1.0431 + j0.8110$	$+1.0091 - j0.3883$	$-0.7819 - j0.2402$
$+0.6931 - j0.2473$	$+0.6604 + j1.2304$	$+0.9494 - j1.0644$	$+0.4687 - j0.8273$
$\mathbf{A}_3^{(0)}$			
$+0.4599 - j0.9791$	$+0.7978 - j1.3486$	$-1.0827 + j0.6829$	$-0.2371 - j0.2518$
$-0.1730 + j0.0563$	$+0.0345 - j1.3786$	$-1.0725 - j0.6691$	$+1.1054 - j0.4745$
$+0.6305 + j1.0133$	$-0.3759 - j1.3237$	$+0.6723 + j0.7155$	$+0.0314 - j0.6831$
$+0.6364 - j1.1702$	$-1.2224 + j0.3417$	$-0.4955 + j0.1671$	$+1.3036 - j0.2317$
$\mathbf{A}_4^{(0)}$			
$-1.1590 - j0.8394$	$-0.3180 - j0.9864$	$-1.0720 + j0.6688$	$+0.3034 + j0.2600$
$-0.7466 + j0.3406$	$-0.0394 - j0.8619$	$-0.9283 - j0.8593$	$+1.1746 + j0.9471$
$-1.1889 - j0.4464$	$+0.0942 - j1.2869$	$-0.8556 - j0.0757$	$+1.3648 + j0.7208$
$-0.6738 - j0.5182$	$-1.2975 - j0.9472$	$-0.9574 - j0.0515$	$-0.7640 + j1.3797$

$\mathbf{s}^{(4)}$ or $\mathbf{s}^{(13)}$, $\rho = 0$			
$\mathbf{A}_1^{(0)}$			
$+1.3054 - j1.8983$	$-2.3593 + j0.5669$	$+1.4560 + j0.7205$	$+1.2398 + j0.7786$
$+0.9353 - j0.1407$	$-1.5880 + j0.5502$	$-0.8222 + j2.1776$	$-0.6522 - j1.6372$
$-0.5622 + j2.4073$	$+0.8801 - j1.5291$	$+0.6425 - j2.2504$	$-0.8057 + j1.6890$
$-1.4489 - j0.5399$	$-2.1564 + j0.8951$	$-2.1967 + j1.8279$	$-0.5405 + j1.7893$
$\mathbf{A}_2^{(0)}$			
$-2.0090 + j1.1795$	$+0.7536 - j1.8447$	$-0.1060 + j0.6593$	$-1.3873 + j0.7099$
$-1.6528 - j1.4971$	$-1.3832 - j1.4293$	$+1.2365 - j2.0399$	$+1.8834 + j0.2969$
$+2.4029 - j2.1209$	$-1.7166 + j2.1066$	$+0.6292 - j1.2688$	$-1.9713 + j0.8079$
$-0.9949 + j0.1316$	$+1.6837 - j0.8505$	$+0.6268 - j2.4268$	$+0.7744 - j2.0550$
$\mathbf{A}_3^{(0)}$			
$-0.2526 + j1.8543$	$-2.1112 - j1.6336$	$+0.3806 + j0.5958$	$-0.7242 - j0.2362$
$+1.7030 + j0.0653$	$-1.0223 + j1.5952$	$-1.0366 - j2.3296$	$-1.5748 - j1.9221$
$+0.4501 - j0.3108$	$+0.6472 + j1.4933$	$+0.6762 - j1.0534$	$-2.0844 + j1.3634$
$+0.6037 - j1.9994$	$-1.3583 + j2.0397$	$-0.0084 + j1.4708$	$+0.7655 - j1.6734$
$\mathbf{A}_4^{(0)}$			
$-0.4944 - j2.3933$	$+0.7306 + j0.0972$	$+0.9749 - j0.1240$	$+0.6562 + j1.8562$
$-2.2516 - j2.1758$	$-1.6925 - j2.3482$	$+1.2306 + j2.4290$	$+2.2748 + j1.1592$
$+1.6620 + j0.9610$	$-0.7244 - j0.6107$	$+0.4105 - j2.2888$	$-0.4521 + j1.1098$
$-2.3868 + j1.8607$	$+0.5249 - j2.0210$	$-1.3197 - j2.0360$	$-0.3018 + j1.9064$

$\mathbf{s}^{(4)}$ or $\mathbf{s}^{(13)}$, $\rho = 0.95$			
$\mathbf{A}_1^{(0)}$			
$+0.7868 + j1.0149$	$+0.8665 + j0.3992$	$-0.5231 + j0.1905$	$-0.9163 + j0.9128$
$+0.9006 + j0.8024$	$-0.0047 - j0.6220$	$-0.8401 - j0.2098$	$-1.0400 - j1.0179$
$+1.0149 + j0.6252$	$+1.0886 + j0.2185$	$-0.7587 - j0.8466$	$-0.1970 - j0.2818$
$+0.7866 - j0.3282$	$+0.7815 + j0.3120$	$-0.7880 - j0.3117$	$-0.4463 + j0.7412$
$\mathbf{A}_2^{(0)}$			
$-1.1653 - j0.6343$	$+0.3854 - j0.7829$	$+0.1037 + j0.1310$	$-1.0793 + j0.4212$
$-1.1692 - j0.6295$	$-0.8595 + j0.4766$	$+0.2420 - j0.5444$	$-0.3672 - j0.2624$
$+0.0650 - j0.8075$	$-0.2616 - j0.4496$	$-0.9929 + j0.5568$	$-0.8854 + j0.6837$
$-0.6040 - j0.7815$	$-0.7669 - j1.0810$	$-0.2592 + j0.0682$	$+0.3548 - j0.5323$
$\mathbf{A}_3^{(0)}$			
$-0.9511 + j0.5994$	$+0.8375 + j0.8137$	$-0.0460 + j0.3262$	$-1.1517 + j0.4082$
$-0.8306 - j0.5035$	$+0.4113 + j1.0339$	$-0.9302 - j0.4936$	$-0.2997 - j0.6472$
$+0.0496 - j0.6955$	$+1.1748 - j0.6199$	$-1.0072 + j0.0695$	$-0.4041 - j0.9442$
$-0.9986 - j1.0473$	$+0.0820 + j0.5832$	$-0.1111 + j0.6335$	$-0.5407 + j0.9499$
$\mathbf{A}_4^{(0)}$			
$+0.3795 - j0.1498$	$+0.6892 - j1.0536$	$+0.0986 - j0.4799$	$-0.5422 + j0.4031$
$+0.7936 + j0.6294$	$-0.9821 - j0.8694$	$+0.6843 - j1.0235$	$-0.8478 - j0.5630$
$+0.7409 - j0.0071$	$-0.4118 + j0.4434$	$-0.2566 - j0.9494$	$-0.7163 + j1.0856$
$+1.0948 - j0.3214$	$+0.4118 - j0.7219$	$-0.6595 - j1.1128$	$+0.3428 - j1.1541$

$\mathbf{s}^{(5)}$ or $\mathbf{s}^{(12)}$, $\rho = 0$			
$\mathbf{A}_1^{(0)}$			
$+0.4209 + j2.1457$	$+1.0105 - j1.9181$	$-1.3742 - j1.5810$	$+1.1489 - j0.9528$
$-1.6463 - j1.5592$	$-0.1578 - j1.2974$	$+0.6904 - j1.9475$	$-0.2821 - j0.9796$
$-0.1459 + j0.3420$	$-0.1613 + j1.1499$	$-1.5376 - j1.1990$	$+0.5532 - j1.8380$
$-0.9043 - j0.6876$	$+1.4682 + j1.9610$	$-2.1528 + j0.0311$	$-0.7782 - j0.2308$
$\mathbf{A}_2^{(0)}$			
$+0.0061 + j1.6301$	$+1.6290 + j1.4593$	$+0.1361 + j1.3036$	$+2.0271 - j1.7048$
$-0.1623 + j1.0853$	$-0.6337 - j2.0435$	$+0.4357 + j1.7092$	$+1.0279 + j0.7079$
$+0.5896 - j1.7265$	$-0.6317 - j0.8907$	$-1.1793 - j1.9861$	$-1.5886 - j0.8230$
$+0.3615 + j1.6472$	$-1.8316 + j1.0630$	$-1.5428 - j1.2761$	$-1.8647 + j0.0640$
$\mathbf{A}_3^{(0)}$			
$-0.8827 - j0.973i$	$-1.2936 + j2.1817$	$+0.3833 + j2.1560$	$+0.4424 - j0.1318$
$+2.0530 + j0.8337$	$-1.7597 - j0.6789$	$+0.9897 + j1.9472$	$-1.3382 + j1.4044$
$-1.2496 - j1.6224$	$-0.0980 + j0.0217$	$+0.6969 - j1.3487$	$-2.1963 - j1.0609$
$-1.3677 + j1.0074$	$-1.7345 - j0.7580$	$+0.7750 + j1.2196$	$-1.5406 + j1.9687$
$\mathbf{A}_4^{(0)}$			
$+0.5907 - j0.2256$	$+1.3980 + j1.1166$	$+1.5509 + j0.9579$	$+0.4199 - j0.4952$
$-0.6219 + j2.0223$	$+0.5835 + j0.0143$	$-1.6535 + j1.5857$	$+2.1309 + j0.2156$
$+2.0847 - j0.6469$	$-0.6232 - j2.0534$	$-0.9150 + j0.4230$	$+0.7818 + j2.1508$
$+2.0505 + j1.0435$	$-1.3598 - j0.4974$	$-0.5466 - j2.2300$	$+0.2471 - j1.3088$
$\mathbf{s}^{(5)}$ or $\mathbf{s}^{(12)}$, $\rho = 0.95$			
$\mathbf{A}_1^{(0)}$			
$-0.7838 - j1.1501$	$-0.7332 - j1.0014$	$+1.0939 - j0.9939$	$+1.2448 + j0.8499$
$+0.8077 + j0.5391$	$+0.5522 - j0.0781$	$+1.2447 + j0.8709$	$+0.1586 - j0.9490$
$-0.7447 + j0.6089$	$-0.5910 + j0.7777$	$+1.0306 - j0.6976$	$+0.9385 + j0.6185$
$+0.6310 - j0.3580$	$-0.2602 + j0.9936$	$+0.5877 - j0.4147$	$+0.5598 - j0.4384$
$\mathbf{A}_2^{(0)}$			
$+0.4500 + j0.3264$	$-0.1451 - j0.6125$	$+1.1694 + j0.7448$	$+0.9788 + j0.8133$
$+0.5339 - j0.3718$	$+0.3893 + j1.1043$	$+0.6862 + j0.4304$	$-0.0700 - j0.9873$
$-0.0383 + j0.3515$	$-1.0812 + j1.1942$	$+0.8883 + j0.0180$	$-0.0048 + j1.0653$
$-1.1413 + j0.0644$	$-0.9887 + j0.8641$	$+0.7111 + j0.5800$	$-0.7403 + j1.1600$
$\mathbf{A}_3^{(0)}$			
$-0.4029 - j0.0734$	$+0.7910 + j0.8167$	$-0.7837 + j1.1250$	$+0.0389 - j1.0129$
$-0.8863 - j0.2510$	$-0.6180 + j0.8264$	$-0.7455 + j0.1110$	$+1.0818 + j0.3615$
$+0.4217 - j0.0725$	$+1.1694 + j0.6827$	$+0.5848 + j1.1972$	$-0.4315 + j0.8971$
$-0.8677 + j0.3199$	$+0.0714 - j0.1242$	$-1.0897 + j0.1316$	$-0.2102 + j1.2148$
$\mathbf{A}_4^{(0)}$			
$+1.2335 + j1.1666$	$+0.1783 - j0.4169$	$+0.7539 + j0.0449$	$-0.6772 + j1.1273$
$+0.3022 - j0.9586$	$+1.1898 + j0.5177$	$+0.2060 - j0.9338$	$-1.0073 - j0.2383$
$-0.0519 + j0.0536$	$-0.9812 + j0.0114$	$-0.6899 - j0.7819$	$-0.9791 - j0.4590$
$-0.9972 + j0.1851$	$-0.5772 + j0.2430$	$+1.0003 - j0.0552$	$-1.1126 + j0.3906$

$\mathbf{s}^{(6)}$ or $\mathbf{s}^{(11)}$, $\rho = 0$			
$\mathbf{A}_1^{(0)}$			
$-1.0420 + j0.5348$	$-1.6458 - j1.6433$	$+0.5460 - j2.2651$	$+1.7992 + j1.0676$
$+1.6797 + j0.1718$	$+0.6191 - j2.1944$	$-0.7132 + j0.8729$	$+1.8494 - j1.2910$
$+0.5749 - j1.1098$	$-0.4297 - j1.2677$	$-2.0123 + j2.2398$	$-0.3568 - j1.9002$
$+2.2666 - j1.7780$	$-0.1279 + j0.2749$	$+2.4385 + j1.6408$	$-1.9742 + j1.7380$
$\mathbf{A}_2^{(0)}$			
$-1.1657 + j0.1642$	$-2.2592 + j0.5313$	$-0.2112 - j1.6410$	$-1.5011 - j1.2493$
$+2.1555 + j2.1890$	$+0.1258 - j1.6742$	$+0.0748 + j2.1270$	$+0.9168 - j1.1057$
$-0.5172 + j1.4836$	$-0.8929 + j0.4328$	$-2.5336 + j0.4934$	$-0.7918 - j1.4100$
$+1.6651 - j1.9757$	$+1.2807 + j1.6355$	$+2.4686 + j2.4109$	$-1.4837 - j0.5721$
$\mathbf{A}_3^{(0)}$			
$-2.4247 - j1.5732$	$+0.8238 - j0.3967$	$+0.7779 - j0.4353$	$-1.5978 - j0.9949$
$-1.5134 + j2.0218$	$-0.2395 + j0.2780$	$-0.4401 + j2.0600$	$+1.3484 - j0.3891$
$+0.9474 + j1.2719$	$-1.0525 + j0.3664$	$+0.8374 - j0.8029$	$-1.3016 - j1.7295$
$-0.6134 - j1.3996$	$+2.4261 - j0.1596$	$-0.6892 - j0.6888$	$-1.4550 - j1.3217$
$\mathbf{A}_4^{(0)}$			
$-2.2996 - j1.6276$	$+1.8216 - j2.0637$	$+2.0497 - j1.4055$	$+1.7579 + j1.1587$
$-2.3512 + j0.0077$	$-0.2020 + j0.2571$	$-1.6691 + j0.5710$	$+2.4329 - j0.9485$
$+2.1671 - j1.8740$	$-0.6673 - j1.1221$	$+0.9625 + j0.9291$	$-1.2456 - j1.6476$
$+0.5488 - j0.9737$	$+1.2669 - j1.3640$	$-1.0707 - j1.7520$	$-1.3964 + j1.1738$
$\mathbf{s}^{(6)}$ or $\mathbf{s}^{(11)}$, $\rho = 0.95$			
$\mathbf{A}_1^{(0)}$			
$-1.2385 + j0.6927$	$+0.2141 + j0.3344$	$+1.5609 - j1.5967$	$+0.9062 - j0.0395$
$-0.4407 + j1.5623$	$+0.5903 + j0.6462$	$+1.4141 + j0.1689$	$+0.0287 + j0.4741$
$+0.6243 - j0.3366$	$-1.1743 + j1.1467$	$-0.0237 - j1.4796$	$+0.5861 + j0.3664$
$-1.2083 - j0.7170$	$+0.9892 - j0.5637$	$+0.7174 + j1.1663$	$+0.8765 + j0.1257$
$\mathbf{A}_2^{(0)}$			
$+0.1426 - j0.4037$	$+0.3316 + j0.9758$	$+0.7460 - j0.0277$	$+0.9659 + j0.8231$
$+1.5138 + j0.5554$	$-0.9609 - j0.4827$	$+1.4838 - j1.0448$	$+1.6170 - j1.5901$
$+1.2919 - j1.4296$	$-0.0728 + j1.6170$	$+0.7977 + j0.2083$	$+0.6386 - j0.2321$
$-1.5115 - j0.7774$	$+0.4041 - j0.1390$	$+1.0313 + j1.2895$	$+1.4294 - j1.3905$
$\mathbf{A}_3^{(0)}$			
$+0.7471 - j1.5939$	$-0.0790 - j0.5249$	$-1.1040 + j0.4264$	$-1.6120 - j0.2979$
$-0.0000 - j1.1160$	$-1.5365 - j1.5966$	$+0.4694 + j0.0530$	$+0.9488 - j0.4880$
$+0.4160 - j0.4784$	$-0.2947 - j0.9633$	$+1.3694 + j1.5213$	$+0.7158 - j1.1777$
$-1.2935 + j0.0242$	$-0.0944 + j0.3160$	$-0.6473 + j0.2464$	$-0.7226 - j0.3396$
$\mathbf{A}_4^{(0)}$			
$+0.1469 - j0.7453$	$-0.2968 - j1.4227$	$-0.1698 - j1.5078$	$-1.4640 - j1.0454$
$-1.4944 - j0.2784$	$+0.0571 - j0.6744$	$+0.5134 + j0.5197$	$-1.0362 + j1.5228$
$+0.5559 + j0.5080$	$-1.0778 - j1.5266$	$+0.2164 - j0.3635$	$+0.6611 - j0.8861$
$-0.5251 - j0.3159$	$+1.0732 - j0.1292$	$-0.7921 - j0.2876$	$-1.0903 + j1.4378$

$\mathbf{s}^{(7)}$ or $\mathbf{s}^{(10)}$, $\rho = 0$			
$\mathbf{A}_1^{(0)}$			
$+1.8790 + j1.7756$	$-0.6582 + j1.5396$	$-1.8324 - j2.3719$	$-0.5138 - j1.4703$
$-1.1318 - j0.6413$	$-1.2322 - j1.2398$	$+0.2167 - j1.7895$	$+1.5470 - j1.0882$
$-0.9050 + j1.4306$	$-1.1612 + j2.2329$	$+0.0138 - j0.3143$	$-0.5443 + j0.3248$
$+2.0735 + j0.5176$	$+1.2183 - j0.4637$	$-0.5352 + j2.6161$	$+1.4082 - j1.8690$
$\mathbf{A}_2^{(0)}$			
$+0.7463 - j0.0230$	$-2.0316 - j0.1017$	$-2.0810 - j1.0977$	$-0.7380 + j1.7712$
$-0.5906 - j2.0771$	$+0.6355 + j1.4608$	$-0.5458 - j0.4105$	$-2.1798 + j1.8413$
$-1.5171 + j1.7849$	$+1.6756 + j1.4894$	$-1.1017 + j0.1788$	$+1.3004 + j0.0903$
$+0.2095 + j1.9211$	$-0.4128 + j2.4224$	$-1.7826 + j1.9603$	$+0.6745 + j0.3075$
$\mathbf{A}_3^{(0)}$			
$+1.3514 + j1.4672$	$+1.8920 + j0.9674$	$+1.8034 - j2.1098$	$+0.1024 - j1.3220$
$+0.2000 - j0.4851$	$-0.5929 - j2.5546$	$-1.0273 - j1.8930$	$+1.3438 - j2.0730$
$+2.0744 + j1.7514$	$-1.5394 - j2.3099$	$-0.0908 + j0.5085$	$-2.0887 + j0.8353$
$+2.0402 + j0.4685$	$-0.4063 - j0.5762$	$+1.3077 + j2.4731$	$-1.4403 - j1.9110$
$\mathbf{A}_4^{(0)}$			
$+0.0367 - j0.7333$	$-0.2008 - j0.9280$	$+1.5744 - j0.6933$	$-0.1181 + j1.4697$
$-0.0129 - j2.1132$	$+1.3068 + j0.0046$	$-2.0707 - j0.6596$	$-2.1188 + j1.3068$
$+1.5089 + j1.8394$	$+1.5090 - j2.6002$	$-1.6754 + j0.6763$	$+0.0813 + j0.1047$
$-0.0370 + j2.1552$	$-1.9415 + j1.9394$	$+0.2441 + j1.0960$	$-2.4235 - j0.0680$
$\mathbf{s}^{(7)}$ or $\mathbf{s}^{(10)}$, $\rho = 0.95$			
$\mathbf{A}_1^{(0)}$			
$+0.6834 + j0.9278$	$-0.6783 + j1.3602$	$-0.7992 + j0.1590$	$+0.8243 - j1.4089$
$-1.1160 + j0.1255$	$+0.4470 + j0.9419$	$+1.2094 + j0.1420$	$-0.2548 - j0.6572$
$-1.3840 - j0.9985$	$+0.1432 + j0.9751$	$-0.0595 - j0.0109$	$-0.5930 - j0.2638$
$+1.0699 - j0.1974$	$-1.2125 + j0.5302$	$+0.4371 + j0.0456$	$-0.9583 - j0.1413$
$\mathbf{A}_2^{(0)}$			
$+1.1824 + j0.3614$	$-0.1836 + j0.7545$	$-0.4062 + j0.0111$	$-0.6450 + j0.6259$
$-1.0428 - j0.1241$	$-0.3520 + j1.3182$	$+1.1175 - j0.1900$	$-1.2300 - j0.3735$
$+0.7048 - j1.1319$	$+0.1985 + j0.9982$	$-0.7542 - j1.0890$	$-1.2153 + j1.2485$
$+0.3038 + j0.2262$	$-0.5230 + j0.3236$	$-0.4266 + j0.0452$	$-0.8861 + j1.0944$
$\mathbf{A}_3^{(0)}$			
$-1.1087 + j0.6938$	$+0.2942 + j0.5225$	$+0.4861 + j0.8471$	$+0.1769 - j1.4063$
$-0.6156 + j0.6066$	$-0.8056 + j0.2762$	$+0.1430 + j0.8880$	$-0.0155 + j0.8203$
$-1.3309 + j0.2250$	$-1.2736 - j0.9174$	$+0.9581 + j0.0618$	$-0.7042 - j0.7056$
$-0.4482 + j0.2239$	$-0.7125 - j0.9661$	$+0.7293 + j0.3017$	$+1.1750 + j0.0333$
$\mathbf{A}_4^{(0)}$			
$-0.0319 + j0.1230$	$+1.1932 - j0.0316$	$+0.7281 + j1.3472$	$-1.3640 + j0.6832$
$+0.3889 + j0.5507$	$-1.4222 + j0.7550$	$+0.2588 + j0.6669$	$-0.9342 + j1.0120$
$+1.1875 - j0.0066$	$-0.8238 - j0.5041$	$+0.2357 - j0.6349$	$-0.7378 + j0.9572$
$-0.8699 + j0.6981$	$+0.6739 - j0.7136$	$+0.0947 + j0.5343$	$+0.9860 + j1.4215$

$\mathbf{s}^{(8)}$ or $\mathbf{s}^{(9)}$, $\rho = 0$			
$\mathbf{A}_1^{(0)}$			
$+2.0557 + j1.3292$	$-0.6231 + j1.8802$	$+0.3644 - j0.0087$	$-1.1581 + j2.2817$
$-0.2295 + j1.7046$	$-2.6377 - j1.9866$	$+2.4533 + j0.3037$	$+1.9540 - j1.9483$
$+1.3660 - j2.3638$	$-0.0496 - j0.1118$	$-0.6145 + j1.7446$	$+2.4634 - j0.6670$
$+1.5972 + j1.3873$	$+2.3202 + j1.7121$	$-0.3524 + j1.9891$	$-2.2682 + j1.9716$
$\mathbf{A}_2^{(0)}$			
$-0.0241 + j0.5004$	$-1.3821 + j1.4353$	$-0.0410 - j0.9524$	$+1.3071 + j0.0670$
$-0.3418 - j1.6405$	$-0.7684 - j2.6161$	$-1.3280 + j0.8370$	$+1.7998 + j0.1405$
$-1.6635 - j1.1110$	$-1.6226 - j1.9282$	$-2.6455 - j1.7482$	$+1.9658 + j2.0089$
$-0.6752 + j0.0674$	$-2.2480 - j1.3119$	$-0.8855 + j2.0492$	$-1.6357 + j0.8483$
$\mathbf{A}_3^{(0)}$			
$-0.2139 + j1.7165$	$-1.2222 + j1.0492$	$+1.1469 + j2.1746$	$-2.6629 + j2.6473$
$+0.1931 + j0.7008$	$-0.7965 + j1.1649$	$+1.8132 - j1.6138$	$+0.8818 - j2.2376$
$+2.4187 - j0.4149$	$+1.5509 + j0.9034$	$+0.9861 + j1.6174$	$-0.4278 - j1.7127$
$+0.4316 + j2.2006$	$+1.9778 + j2.1635$	$+0.2627 + j0.3198$	$+1.3948 + j2.4544$
$\mathbf{A}_4^{(0)}$			
$+2.4266 - j1.1266$	$+2.4472 - j0.7872$	$-0.2127 - j1.0349$	$+0.7945 - j0.4548$
$-0.6693 + j2.4724$	$-0.7892 - j0.6797$	$+1.7966 + j0.6966$	$-0.6323 + j0.7287$
$+0.4342 - j0.7086$	$+0.5098 + j1.5475$	$+0.8652 + j1.6340$	$+1.0509 - j1.4173$
$+1.7273 - j0.1820$	$+2.6453 + j0.9271$	$+0.8919 - j0.5512$	$-2.2312 - j1.1462$
$\mathbf{s}^{(8)}$ or $\mathbf{s}^{(9)}$, $\rho = 0.95$			
$\mathbf{A}_1^{(0)}$			
$+1.0729 - j0.6360$	$+0.3216 + j1.1767$	$-0.4294 + j0.6788$	$+0.7069 + j1.0339$
$-0.0308 + j0.5080$	$-0.0597 - j1.0421$	$+0.7311 - j0.1883$	$+0.6501 + j1.0083$
$+0.6475 - j1.2551$	$-0.1130 + j0.7982$	$+0.9773 - j1.0044$	$+0.2462 + j0.6884$
$+0.3779 + j0.6108$	$+1.0364 + j1.0911$	$+0.4770 + j0.8617$	$+1.2159 + j0.9196$
$\mathbf{A}_2^{(0)}$			
$-0.2989 - j0.5575$	$-0.5729 + j0.5920$	$-0.3083 - j0.3966$	$+0.9257 + j0.0251$
$-0.2358 - j0.8615$	$-0.2759 - j1.2247$	$-0.7237 + j0.3652$	$+0.8493 + j0.1718$
$-0.7915 - j0.7353$	$-0.7232 - j0.3501$	$+0.9755 - j0.8308$	$+0.9710 + j0.8979$
$-0.2462 + j0.7193$	$-1.0368 - j0.6456$	$-0.0313 + j0.6400$	$+1.1525 + j0.2649$
$\mathbf{A}_3^{(0)}$			
$-0.1588 + j0.7897$	$-0.3807 + j0.5317$	$+0.3163 + j1.0518$	$-0.6990 + j1.2507$
$+0.0751 + j0.3100$	$-0.9478 + j0.4312$	$+1.0333 - j0.6250$	$+0.3823 - j0.5365$
$+0.7735 - j0.1594$	$+0.6630 + j0.8172$	$+0.3804 + j0.7593$	$-1.1449 - j0.8500$
$+0.3604 + j1.1165$	$+0.6575 + j1.0456$	$+0.1410 + j1.1268$	$+0.5976 + j1.1757$
$\mathbf{A}_4^{(0)}$			
$+1.1952 - j0.7379$	$+1.2135 - j0.3653$	$+0.2068 - j0.4499$	$+0.5373 - j0.2142$
$-0.4191 + j1.1550$	$+1.2335 - j0.2042$	$+0.8604 - j0.2990$	$-0.1204 + j0.9779$
$+0.5209 - j0.3261$	$-0.5293 + j0.3909$	$+0.3865 - j1.1685$	$+0.2970 + j0.3126$
$-0.5908 - j1.1204$	$+1.1028 + j0.5218$	$+0.6650 - j1.0647$	$-0.7188 - j0.5068$

Bibliography

[1] "Physical Layer Procedures," 3rd Generation Partnership Project (3GPP), Tech. Rep. 3GPP TS 25.214 V3.10.0, 2002.

[2] Nokia, "An extension of closed-loop Tx diversity mode 1 for multiple Tx antennas," Temporary document R1-00-0712, 3GPP TSG RAN WG1,2000.

[3] Motorola, "Closed-loop transmit diversity mode 2 with reduced states for 4 elements," Temporary document R1-00-1132, 3GPP TSG RAN WG1, Aug. 2000.

[4] S. M. Alamouti, "A simple transmit diversity technique for wireless communications," *IEEE J. Select. Areas Commun.*, Vol. 16, No. 8, pp. 1451-1458, Oct. 1998.

[5] M. S. Bazaraa and H. D. Sherali, *Nonlinear Programming: Theory and Algorithms.* 2nd ed., New York, Wiley Press, 1993.

[6] A. O. Berthet and B. S. Unal and R. Visoz, "Iterative decoding of convolutionally encoded signals over multipath Rayleigh fading channels," *IEEE J. Select. Areas Commun.*, Vol. 19, No. 9, pp. 1729-1743, Sep. 2001.

[7] S. Bhashyam, A. Sabharwal and B. Aazhang, "Feedback gain in multiple antenna systems," *IEEE Trans. Commun.*, Vol. 50, No. 5, pp. 785-798, May 2002.

[8] E. Biglieri, G. Caire, G. Taricco and J. Ventura, "Simple method for evaluating error probabilities," *IEE Electron. Lett.*, Vol. 32, No. 3, pp. 191-192, Feb. 1996.

[9] J. K. Cavers, "Optimized use of diversity modes in transmitter diversity systems," in *Proc. IEEE VTC*, Vol. 3, 1999, pp. 1768-1773.

[10] J. K. Cavers, "Single-user and multiuser adaptive maximal ratio transmission for Rayleigh channels," *IEEE Trans. Veh. Technol.*, Vol. 49, No. 6, pp. 2043-2050, Nov. 2000.

[11] E. Chiavaccini and G. M. Vitetta, "MAP symbol estimation on frequency-flat Rayleigh fading channels via a Bayesian EM algorithm," *IEEE Trans. Commun.*, Vol. 49, No. 11, pp. 1869-1872, Nov. 2001.

[12] M. Coupechoux and V. Braun, "Space-time coding for the EDGE mobile radio system," in *Proc. IEEE Int. Conf. Personal Wireless Commun.*, Hyderabad, India, 2000, pp. 28-32.

[13] C. Cozzo and B. L. Hughes, "Joint detection and estimation in space-time coding and modulation," in *Proc. IEEE Conference Record of the Thirty-Third Asilomar Conference on Signals, Systems, and Computers*, Vol. 1, 1999, pp. 613 -617.

[14] R. T. Derryberry, S. D. Gray, D. M. Ionescu, G. Mandyam and B. Raghothaman, "Transmit diversity in 3G CDMA systems," *IEEE Commun. Mag.*, Vol. 40, No. 4, pp. 68-75, Apr. 2002.

[15] N. Farvardin and V. Vaishampayan, "On the performance and complexity of channel-optimized vector quantizers," *IEEE Trans. Inform. Theory*, Vol. 37, No. 1, pp. 155-160, Jan. 1991.

[16] G. J. Foschini and M. J. Gans, "On limits of wireless communications in a fading environment when using multiple antennas," *Wireless Personal Commun.*, Vol. 6, No. 3, pp. 311-335, Mar. 1998.

[17] G. Ganesan and P. Stoica, *Signal Processing Advances in Wireless and Mobile Communications: Trends in Single-User and Multi-User Systems.* Englewood Cliffs, NJ: Prentice-Hall, 2000, ch.2.

[18] G. Ganesan and P. Stoica, "Space-time diversity using orthogonal and amicable orthogonal designs," *Wireless Personal Commun.*, Vol. 18, No. 2, pp. 165-178, Aug. 2001.

[19] C. N. Georghiades and J. C. Han, "Sequence estimation in the presence of random parameters via the EM algorithm," *IEEE Trans. Commun.*, Vol. 45, No. 3, pp. 300-308, Mar. 1997.

[20] D. Gerlach and A. Paulraj, "Adaptive transmitting antenna arrays with feedback," *IEEE Signal Processing Lett.*, Vol. 1, No. 10, pp. 150-152, Oct. 1994.

[21] D. Gerlach and A. Paulraj, "Base station transmitting antenna arrays for multipath environments," *EURASIP J. Signal Processing*, Vol. 54, No. 1, pp. 59-73, Oct. 1996.

[22] G. B. Giannakis and S. Zhou, "Optimal transmit-diversity precoders for random fading channels," in *Proc. GLOBECOM*, Vol. 3, San Francisco, CA, 2000, pp. 1839-1843.

[23] D. E. Goldberg, *Genetic Algorithms in Search, Optimization and Machine Learning.* Addison Wesley Publishing Company, Jan. 1989.

[24] I. S. Gradshteyn and I. M. Ryzhik, *Table of Integrals, Series, and products.* Corrected and enlarged, 4th ed., Academic Press, 1980.

[25] J. C. Guey, M. P. Fitz, M. R. Bell and W. Y. Kuo, "Signal design for transmitter diversity wireless communication systems over Rayleigh fading channels," *IEEE Trans. Commun.*, Vol. 47, No. 4, pp. 527-537, Apr. 1999.

[26] L. Hanzo, T. H. Liew and B. L. Yeap, *Turbo Coding, Turbo Equalisation and Space-time Coding.* John Wiley and Sons, 2002.

[27] B. Hassibi and B. M. Hochwald, "High-rate codes that are linear in space and time," *IEEE Trans. Inform. Theory*, Vol. 48, No. 7, pp. 1804-1824, Jul. 2002.

[28] R. W. Heath Jr and A. J. Paulraj, "A simple scheme for transmit diversity using partial channel feedback," in *Proc. 32nd Asilomar Conf. Signals, Systems and Computers*, Pacific Grove, CA, Nov. 1998, pp. 1073-1078.

[29] R. W. Heath Jr and A. J. Paulraj, "A simple scheme for transmit diversity using partial channel feedback," in *Proc. 32nd Asilomar Conf. Signals, Systems and Computers*, Pacific Grove, CA, Nov. 1998, pp. 1073-1078.

[30] R. W. Heath, Jr. and A. J. Paulraj, "Linear despersion codes for MIMO systems based on frame theory," *IEEE Trans. Signal Processing*, Vol. 50, No. 10, pp. 2429-2441, Oct. 2002.

[31] R. W. Heath, Jr. and A. J. Paulraj, "Linear despersion codes for MIMO systems based on frame theory," *IEEE Trans. Signal Processing*, Vol. 50, No. 10, pp. 2429-2441, Oct. 2002.

[32] B. Hochwald, T. L. Marzetta and C. B. Papadias, "A transmitter diversity scheme for wideband CDMA systems based on space-time spreading," *IEEE J. Select. Areas Commun.*, Vol. 19, No. 1, pp. 48-60, Jan. 2001.

[33] R. A. Horn and C. R. Johnson, *Matrix Analysis*, Cambridge, U.K.: Cambridge University Press, 1990.

[34] R. A. Horn and C. R. Johnson, *Topics in Matrix Analysis*, Cambridge, U.K.: Cambridge University Press, 1991.

[35] A. Hottinen and R. Wichman, "Transmit diversity by antenna selection in CDMA downlink," in *Proc. IEEE Int. Symp. Spr. Spect. Tech. Appl.*, Sun City, South Africa, Vol. 3, Sep. 1998, pp. 767-770.

[36] A. Hottinen, O. Tirkkonen and R. Wichman, "Closed-loop transmit diversity techniques for multi-element transceivers," in *Proc. IEEE VTC* , Vol. 1, 2000, pp. 70-73.

[37] A. Hottinen, O. Tirkkonen and R. Wichman, *Multi-Antenna Transceiver Techniques for 3G and Beyond.* John Wiley and Sons, 2003.

[38] S. Jafar and A. Goldsmith, "On optimality of beamforming for multiple antenna systems with imperfect feedback," in *Proc. IEEE Int. Symp. Inform. Theory*, Washington, DC, Jun. 2001, pp. 321.

[39] S. Jafar, S. Vishwanath and A. Goldsmith, "Channel capacity and beamforming for multiple transmit and multiple receive antennas with covariance feedback," in *Proc. IEEE Int. Conf. Commun.*, Vol. 7, Helsinki, Finland, Jun. 2001, pp. 2266-2270.

[40] H. Jafarkhani, "A quasi-orthogonal space-time block code," *IEEE Trans. Commun.*, Vol. 49, No. 1, pp. 1-4, Jan. 2001.

[41] W. C. Jakes, *Mobile Microwave Communication.* New York, Wiley Press, 1974.

[42] J. Jalden, C. Martin and B. Ottersten, "Semidefinite programming for detection in linear systems: Optimality conditions and space-time decoding," in *Proc. IEEE Int. Conf. Acoustics, Speech, Signal Processing*, Vol. IV, Apr. 2003, pp. 9-12.

[43] G. Jongren, M. Skoglund and B. Ottersten, "Combining transmit beamforming and orthogonal space-time block codes by utilizing side information," in *Proc. IEEE 1st Sensor Array and Multichannel Signal Processing Workshop*, Mar. 2000.

[44] G. Jongren and M. Skoglund, "Improving orthogonal space-time block codes by utilizing quantized feedback information," in *Proc. ISIT2001*, Washington, DC, Jun. 2001, pp. 220.

[45] G. Jongren, M. Skoglund and B. Ottersten, "Combining beamforming and orthogonal space-time block coding," *IEEE Trans. Inform. Theory*, Vol. 48, No. 3, pp. 611-627, Mar. 2002.

[46] G. Jongren, M. Skoglund and B. Ottersten, "Utilizing partial channel information in the design of space-time block codes," in *Proc. 5th Int. Symp. Wireless Personal Multimedia Communications (WPMC2002)*, Oct. 2002, pp. 681-685.

[47] G. Jongren, "Design of near-orthogonal LD space-time codes," in *Proc. IEEE Int. Zurich Seminar on Communications (IZS)*, Feb. 2004, pp. 10-13.

[48] G. Jongren, M. Skoglund and B. Ottersten, "Design of channel-estimate-dependent space-time block codes," *IEEE Trans. Commun.*, Vol. 52, No. 7, pp. 1191-1203, Jul. 2004.

[49] G. Jongren, M. Skoglund, "Quantized feedback information in orthogonal space-time block coding," *IEEE Trans. Inform. Theory*, Vol. 50, No. 10, pp. 2473-2482, Oct. 2004.

[50] E. Jorswieck and H. Boche, "On transmit diversity with imperfect channel state information," in *Proc. IEEE Int. Conf. Acoustics, Speech and Signal Processing*, 2002, pp. 2181-2184.

[51] S. M. Kay, *Fundamentals of Statistical Signal Processing: Estimation Theory.* Englewoods Cliffs, NJ: Prentice-Hall, 1993.

[52] E. G. Larsson and P. Stoica, *Space-Time Block Coding for Wireless Communications.* Cambridge University Press, 2003.

[53] Y. Li and C. N. Georghiades and G. Huang, "Iterative maximum-likelihood sequence estimation for space-time coded systems", *IEEE Trans. Commun.*, Vol. 49, No. 6, pp. 948-951, Jun. 2001.

[54] T. H. Liew and L. Hanzo, "Space-time codes and concatenated channel codes for wireless communications," in *Proceedings of the IEEE*, Vol. 90, No. 2, pp. 187-219, 2002.

[55] E. Lindskog and A. Paulraj, "A transmit diversity scheme for channels with intersymbol interference," in *Proc. IEEE Int. Conf. Commun.*, New Orleans, LA, Vol. 1, 2000, pp. 307-311.

[56] J. Liu and E. Gunawan, "Combining ideal beamforming and Alamouti space-time block codes," *IEE Electronics Lett.*, Vol. 39, No. 17, pp. 1258 -1259, Aug. 2003.

[57] J. Liu and E. Gunawan, "Exact bit-error rate analysis for the combined system of beamforming and Alamouti's space-time block code," *IEEE Microwave and Wireless Components Lett.*, Vol. 14, No. 8, pp. 398-400, Aug. 2004.

[58] J. Liu and E. Gunawan, "Combining beamforming and Alamouti's space-time block codes," *IEEE Trans. Commun.*, submitted in Sep. 2004.

[59] Z. Liu, G. B. Giannakis, S. Zhou and B. Muquet, "Space-time coding for broadband wireless communications," *Wireless Communications and Mobile Computing*, Vol. 1, No. 1, pp. 35-53, 2001.

[60] T. K. Y. Lo, "Maximum ratio transmission," *IEEE Trans. Commun.*, Vol. 47, No. 10, Oct. 1999.

[61] D. J. Love, R. W. Heath, Jr., W. Santipach and M. L. Honig, "What is the value of limited feedback for MIMO channels?" *IEEE Commun. Mag.*, Vol. 42, No. 10, pp. 54-59, Oct. 2004.

[62] B. Lu and X. D. Wang and Y. Li, "Iterative receivers for space-time block-coded OFDM systems in dispersive fading channels", *IEEE Trans. wireless Commun.*, Vol. 1, No. 2, pp. 213-225, Apr. 2002.

[63] G. J. McLachlan and T. Krishnan, *The EM Algorithm and Extensions*, New York: Wiley, 1997.

[64] T. K. Moon, "The expectation-maximization algorithm", *IEEE Signal Processing Mag.*,

[65] A. L. Moustakas and S. H. Simon, "Optimizing multi-transmitter-single-receiver (MISO) antenna systems with partial channel knowledge," *Bell Laboratories Technical Memorandum*, 2002.

[66] K. K. Mukkavilli, A. Sabharwal and B. Aazhang, "Design of multiple antenna coding schemes with channel feedback," in *Proc. of Asilomar Conference on Signals, Systems and Computers*, Pacific Grove, CA, 2001, pp. 1009-1013.

[67] A. F. Naguib, V. Tarokh, N. Seshadri and A. R. Calderbank, "A space-time coding Modem for high-data-rate wireless communications," *IEEE J. Select. Areas Commun.*, Vol. 16, No. 8, pp. 1459-1478, Oct. 1998.

[68] A. F. Naguib, N. Seshadri and A. R. Calderbank, "Increasing data rate over wireless channels: Space-time coding and signal processing for high data rate wireless communications," *IEEE Signal Processing Mag.*, Vol. 17, No. 3, pp. 76-92, May, 2000.

[69] A. Narula, M. J. Lopez, M. D. Trott and G. W. Wornell, "Efficient use of side information in multiple-antenna data transmission over fading channels," *IEEE J. Select. Areas Commun.*, Vol. 16, No. 8, pp. 1423-1436, Oct. 1998.

[70] A. Narula, M. D. Trott and G. W. Wornell, "Performance limits of coded diversity methods for transmitter antenna arrays," *IEEE Trans. Inform. Theory*, Vol. 45, pp. 2418-2433, Nov. 1999.

[71] R. Negi, A. M. Tehrani, and J. Cioffi, "Adaptive antennas for space-time coding over block-time invariant multi-path fading channels," in *Proc. IEEE VTC*, May 1999, pp. 70-74.

[72] Nokia, "Downlink transmit diversity," Temporary document, ETSI SMG1 contribution, Bocholt, Germany, 18-20 May 1998.

[73] K. Park and J. W. Modestino, "An EM-based procedure for iterative maximum-likelihood decoding and simultaneous channel state estimation on slow-fading channels", in *Proc. IEEE Int. Symp. Inform. Theory*, 1994, pp. 27.

[74] C. Papadias and G. Foschini, "A space-time coding approach for systems employing four transmit antennas," in *Proc. IEEE ICASSP*, Vol. 4, Salt Lake City, UT, 2001, pp. 2481-2484.

[75] A. Paulraj and T. Kailath, "Increasing capacity in wireless broadcast systems using distributed transmission/directional reception," U.S. Patent No. 5,345,599., 1993.

[76] A. Paulraj, R. Nabar and D. Gore, *Introduction to Space-Time Wireless Communications*. Cambridge University Press, 2003.

[77] A. Paulraj and C. B. Papadias, "Space-time processing for wirelss communications," *IEEE Signal Processing Mag.*, Vol. 14, No. 6, pp. 49-83, 1997.

[78] J. G. Proakis, *Digital Communications.* 4th ed., McGraw-Hill, Inc., 2001.

[79] G. G. Raleigh and J. M. Cioffi, "Spatio-temporal coding for wireless communications," *IEEE Trans. Commun.*, Vol. 46, No. 3, pp. 357-366, Mar. 1998.

[80] H. Sampath and A. Paulraj, "Linear precoding for space-time coded systems with known fading correlations," *IEEE Commun. Letters*, Vol. 6, No. 6, pp. 239-241, 2002.

[81] S. Sandhu, R. Heath and A. Paulraj, "Space-time block codes versus space-time trellis codes," in *Proc. IEEE ICC*, Vol. 4, Helsinki, Finland, Jun. 2001, pp. 1132-1136.

[82] S. Sandhu, A. Paulraj and K. Pandit, "On nonlinear space-time block codes," in *Proc. Int. Conf. Acoustics, Speech and Signal Processing (ICASSP)*, Vol. 3, Orlando, FL, 2002, pp. 2417-2420.

[83] N. Sharma and C. Papadias, "Improved quasi-orthogonal codes through constellation rotation, in *Proc. IEEE ICASSP*, Vol. 4, Orlando, FL, May, 2002, pp. 3968-3971.

[84] S. H. Simon and A. L. Moustakas, "Optimizing MIMO antenna systems with channel covariance feedback," *Bell Laboratories Technical Memorandum*, 2002.

[85] M. K. Simon, *Probability Distributions Involving Gaussian Random Variables.* Kluwer Academic Publishers, 2002.

[86] G. Taricco and E. Biglieri, "Exact pairwise error probability of space-time codes," *IEEE Trans. Inform. Theory*, Vol. 48, No. 2, pp. 510-513, Feb. 2002.

[87] V. Tarokh, N. Seshadri and A. R. Calderbank, "Space-time codes for high data rate wireless communication: Performance criterion and code construction," *IEEE Trans. Inform. Theory*, Vol. 44, No. 2, pp. 744-765, Mar. 1998.

[88] V. Tarokh, H. Jafarkhani and A. R. Calderbank, "Space-time block coding for wireless communications: performance results," *IEEE J. Select. Areas Commun.*, Vol. 17, No. 3, pp. 451-460, Mar. 1999.

[89] V. Tarokh, H. Jafarkhani and A. R. Calderbank, "Space-time block codes from orthogonal designs," *IEEE Trans. Inform. Theory*, Vol. 45, No. 5, pp. 1456-1467, Jul. 1999.

[90] I. E. Telatar, "Capacity of multi-antenna Gaussian channels," *Eur. Trans. Telecomm.*, Vol. 10, No. 6, pp. 585-595, Nov./Dec. 1999, based on AT and T Bell Laboratories, Internal Tech. Memo., Jun. 1995.

[91] O. Tirkkonen and A. Hottinen, "Complex space-time block codes for four tx antennas," in *Proc. IEEE GLOBECOM*, Vol. 2, Nov. 2000, pp. 1005-1009.

[92] H. Vikalo and B. Hassibi, "Maximum-likelihood sequence detection of multiple-antenna systems over dispersive channels via sphere decoding," *EURASIP J. Appl. Signal Processing*, Vol. 2002, No. 5, pp. 525-531, May 2002.

[93] E. Visotsky and U. Madhow, "Space-time transmit precoding with imperfect feedback," *IEEE Trans. Inform. Theory*, Vol. 47, No. 6, pp. 2632-2639, Sep. 2001.

[94] B. Vucetic and J. Yuan, *Space-Time Coding*. John Wiley and Sons, 2003.

[95] J. Winters, "Switched diversity with feedback for DPSK mobile radio," *IEEE Trans. Veh. Tech.*, Vol. 32, pp. 134-150, Feb. 1983.

[96] A. Wittneben, "Optimal predictive TX combining diversity in correlated fading for microcellular mobile radio applications," in *Proc. IEEE GLOBECOM*, Singapore, Nov. 1995, pp. 48-54.

[97] S. Zhou and G. B. Giannakis, "Optimal transmitter eigen-beamforming and space-time block coding based on channel mean feedback," *IEEE Trans. Signal Processing*, Vol. 50, No. 10, pp. 2599-2613, Oct. 2002.

[98] S. Zhou and G. B. Giannakis, "Optimal transmitter eigen-beamforming and space-time block coding based on channel correlations," *IEEE Trans. Inform. Theory*, Vol. 49, No. 7, pp. 1673-1690, Jul. 2003.